

6
RADC-TR-83-261
AD A140026

RADC-TR-83-261, Vol II (of two)

Interim Report
December 1983



ACROSS ELEVEN (ACTIVE CONTROL OF SPACE STRUCTURES)

The Charles Stark Draper Laboratory, Inc.

Sponsored by
Defense Advanced Research Projects Agency (DOD)
ARPA Order No. 3655

APPROVED FOR PUBLIC RELEASE; DISTRIBUTION UNLIMITED

The views and conclusions contained in this document are those of the authors and should not be interpreted as necessarily representing the official policies, either expressed or implied, of the Defense Advanced Research Projects Agency or the U.S. Government.

FILE COPY

ROME AIR DEVELOPMENT CENTER
Air Force Systems Command
Griffiss Air Force Base, NY 13441

DTIC ELECTED
APR 11 1984
S D

This report has been reviewed by the RADC Public Affairs Office (PA) and is releasable to the National Technical Information Service (NTIS). At NTIS it will be releasable to the general public, including foreign nations.

RADC-TR-83-261, Vol II (of two) has been reviewed and is approved for publication.

APPROVED:



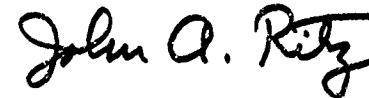
RICHARD W. CARMAN
Project Engineer

APPROVED:



FRANK J. REHM
Technical Director
Surveillance Division

FOR THE COMMANDER:



JOHN A. RITZ
Acting Chief, Plans Office

If your address has changed or if you wish to be removed from the RADC mailing list, or if the addressee is no longer employed by your organization, please notify RADC (OCSE) Griffiss AFB NY 13441. This will assist us in maintaining a current mailing list.

Do not return copies of this report unless contractual obligations or notices on a specific document requires that it be returned.

Accession For	
NTIS GRA&I	<input checked="" type="checkbox"/>
DTIC TAB	<input type="checkbox"/>
Unannounced	<input type="checkbox"/>
Justification	
ACOSS ELEVEN (ACTIVE CONTROL OF SPACE STRUCTURES)	
Vol II	
By	
Distribution	
Available	
Dist	Specia
A/1	



ACOSS ELEVEN (ACTIVE CONTROL OF SPACE STRUCTURES)

Vol II

Thomas H. Brooks
Virendran Mahajan
Daniel R. Hegg

Glen J. Kissel
Harris N. McClamroch
James D. Turner

Contractor: The Charles Stark Draper Laboratory, Inc.
Contract Number: F30602-81-C-0180
Effective Date of Contract: 27 April 1981
Contract Expiration Date: 27 April 1984
Short Title of Work: ACOSS Eleven (Active Control of Space Structures)

Program Code Number: 1E20

Period of Work Covered: Nov 82 - May 83

Principal Investigator: Dr. Keto Soosaar
Phone: (617) 258-2575

Project Engineer: Richard W. Carman
Phone: (315) 330-3148

Approved for public release; distribution unlimited

This research was supported by the Defense Advanced Research Projects Agency of the Department of Defense and was monitored by Richard W. Carman (OCSE), Griffiss AFB NY 13441, under contract F30602-81-C-0180.

UNCLASSIFIED

AD-A140026

SECURITY CLASSIFICATION OF THIS PAGE (When Data Entered)

REPORT DOCUMENTATION PAGE		READ INSTRUCTIONS BEFORE COMPLETING FORM
1. REPORT NUMBER	2. GOVT ACCESSION NO.	3. RECIPIENT'S CATALOG NUMBER
RADC-TR-83-261, Vol II (of two)		
4. TITLE (and Subtitle) ACOSS ELEVEN (ACTIVE CONTROL OF SPACE STRUCTURES)		5. TYPE OF REPORT & PERIOD COVERED Interim Report Nov 82 - Apr 83
7. AUTHOR(s) Thomas H. Brooks Glen J. Kissel Virendran Mahajan Harris N. McClamroch Daniel R. Hegg James D. Turner		6. PERFORMING ORG. REPORT NUMBER CSDL-R-1648
9. PERFORMING ORGANIZATION NAME AND ADDRESS The Charles Stark Draper Laboratory, Inc. 555 Technology Square Cambridge MA 02139		10. PROGRAM ELEMENT, PROJECT, TASK AREA & WORK UNIT NUMBERS 62301E C6550104
11. CONTROLLING OFFICE NAME AND ADDRESS Defense Advanced Research Projects Agency 1400 Wilson Blvd Arlington VA 22209		12. REPORT DATE December 1983
14. MONITORING AGENCY NAME & ADDRESS (if different from Controlling Office)		13. NUMBER OF PAGES 126
Rome Air Development Center (OCSE) Griffiss AFB NY 13441		15. SECURITY CLASS. (of this report) UNCLASSIFIED
		16a. DECLASSIFICATION/DOWNGRADING SCHEDULE N/A
16. DISTRIBUTION STATEMENT (of this Report) Approved for public release; distribution unlimited		
17. DISTRIBUTION STATEMENT (of the abstract entered in Block 20, if different from Report) Same		
18. SUPPLEMENTARY NOTES RADC Project Engineer: Richard W. Carman (OCSE)		
19. KEY WORDS (Continue on reverse side if necessary and identify by block number) Large Flexible Space Structures Reduced-order Model Active Control Synthesis Interlaced Model Broadband Disturbance Accommodation Contiguous Model Power Spectral Density Active Transducer Selection Scientific Experiment Design Flexibility (over)		
20. ABSTRACT (Continue on reverse side if necessary and identify by block number) Volume 2 presents theoretical advances and demonstrations in vibration control against broadband disturbances and in large-angle linear tracking control for flexible optical support structures. Stability results for discrete-time vibration control are also given. The importance of active transducer selection for broadband disturbance accommodation is emphasized. An algorithm for systematically selecting actuators with high influence on the regulated variables is described, together with its theoretical (over)		

UNCLASSIFIED

SECURITY CLASSIFICATION OF THIS PAGE (When Data Entered)

cont

foundation. The algorithm is demonstrated on the ACOSS Model No. 2 structure, obtaining minimal selections with substantially fewer actuators than controlled modes. Disturbance-rejection control designs based on these selections exhibit stability in the presence of residual modes over a frequency range well beyond that of the design model. Sampled-data control for flexible structures is examined using second-order difference equations. A sufficient condition for geometric stability with velocity output feedback requiring non-colocation of actuators and sensors is obtained. Non-colocation reduces to colocation as the sampling period converges to zero. Optimal large-angle slew for linear tracking and terminal convergence is considered. Explicit solutions as a function of matrices satisfying linear algebraic equations are obtained. Demonstrations on a rotating rigid hub with four flexible appendages exhibit the computational efficiency of the solution techniques.

Item 19 (Cont'd)

Full-rank Factorization

QR-decomposition

Gram-Schmidt Orthogonalization

Householder Triangularization

Diagonal Dominance

Least-squares Approximation

Moore-Penrose Inverse

Normal Equations

Residual Vector

Generalized Node Shapes

Elimination Lattice

Richness

Level of Reduction

Riccati Differential Equation

Prefilter Equation

Minimal Selection

Linear-Quadratic-Gaussian Control

Disturbance-Rejection Control

Optimal State Estimation

ACOSS Model No. 2

Sampled-data Control

Second-order Difference Equations

Constant-Gain Velocity Feedback

Bilinear Transformation

Geometric Stability

Non-colocated Velocity Feedback

Large-angle Slewing Maneuvers

Optimal Linear Tracking

Control-rate Penalty

Optimal Terminal Tracking

UNCLASSIFIED

SECURITY CLASSIFICATION OF THIS PAGE (When Data Entered)

ACKNOWLEDGEMENT

This report was prepared by The Charles Stark Draper Laboratory, Inc., under Contract F30602-81-C-0180. This research was supported by the Advanced Research Projects Agency of the Department of Defense and monitored by the Rome Air Development Center.

The program manager is Dr. Keto Soosaar and the project leader for Active Control of Space Structures (ACOSS) is Mr. Robert R. Strunce. The authors of Volume 2 of this report are: Dr. Daniel R. Hegg (Sections 1,2), Mr. Glen J. Kissel (Section 3), Dr. N. Harris McClamroch (Section 4), and Dr. James D. Turner (Section 5). Assistance from Mr. Timothy C. Henderson, Dr. Eliezer Fogel, Dr. I. Gary Rosen, and Mr. Patrick Battstone (Section 2) is gratefully acknowledged. Ms. Lisa E. Kern did the typing.

Publication of this report does not constitute approval by the Defense Advanced Research Projects Agency or the United States Government of the findings or conclusions contained herein. It is published for the exchange and stimulation of ideas.

VOLUME 2

TABLE OF CONTENTS

<u>Section</u>		<u>Page</u>
1	INTRODUCTION	1-1
1.1	Scope	1-1
1.1.1	Vibration Control	1-1
1.1.2	Large-Angle Slew Control	1-3
1.2	Limitations	1-4
2	PROGRESS ON SYNTHESIS OF ACTIVE CONTROL FOR BROADBAND DISTURBANCE ACCOMMODATION - PART 1: ACTIVE TRANSDUCER SELECTION	2-1
2.1	Background	2-1
2.2	Theory: A Selection Algorithm	2-3
2.2.1	Fundamental Concepts	2-4
2.2.2	Algorithm Formulation	2-13
2.3	Applications with ACOSS Model No. 2	2-24
2.3.1	Specifications for Design Examples	2-26
2.3.2	Selection Results	2-28
2.4	Summary	2-30
2.5	Appendix	2-31
	List of References	2-34

TABLE OF CONTENTS (CONT.)

<u>Section</u>		<u>Page</u>
3	PROGRESS ON SYNTHESIS OF ACTIVE CONTROL FOR BROADBAND DISTURBANCE ACCOMMODATION - PART 2: CONTROL SYSTEM DESIGN AND EVALUATION	3-1
3.1	Introduction	3-1
3.2	Control System Design Philosophy	3-1
3.3	Controller Results	3-5
3.4	Future Controller Designs	3-6
3.5	Conclusion	3-7
	List of References	3-7
4	SAMPLED DATA CONTROL OF FLEXIBLE STRUCTURES USING NON-COLOCATED VELOCITY FEEDBACK	4-1
4.1	Overview	4-1
4.2	Models for Sampled Data Controlled Flexible Structures	4-1
4.3	Constant Gain Velocity Feedback	4-4
4.4	Colocated Velocity Feedback	4-5
4.5	Non-colocated Velocity Feedback	4-7
4.6	An Example	4-8
4.7	Conclusions	4-9
	List of References	4-10
5	OPTIMAL TRACKING AND TERMINAL TRACKING MANEUVERS FOR FLEXIBLE SPACECRAFT	5-1
5.1	Introduction	5-1
5.2	Closed Form Solution for the Linear Tracking Problem	5-2
5.2.1	Optimal Linear Tracking Problem	5-3
5.2.2	Necessary Conditions for the Linear Tracking Problem	5-5
5.2.3	Closed Form Solution for the Time-Varying Riccati Equation	5-5

TABLE OF CONTENTS (CONT.)

<u>Section</u>	<u>Page</u>
5.2.4 Closed Form Solution for the Prefilter Equation	5-6
5.2.5 Illustrative Examples	5-11
5.3 Closed Form Solution for the Terminal Tracking Problem	5-14
5.3.1 Optimal Terminal Controller	5-15
5.3.2 Closed Form Solution for the Time-Varying Riccati Equation	5-17
5.3.3 Closed Form Solution for $S(t)$	5-17
5.3.4 Closed Form Solution for $G(t)$	5-18
5.3.5 Calculation of the Optimal Control	5-18
5.3.6 Example Maneuvers	5-19
5.4 An Analytic Solution for the State Trajectories of a Feedback Control System	5-21
5.4.1 Optimal Control Problem	5-22
5.4.2 Change of Variables for $x(t)$	5-23
5.4.3 Recursion Relationship for Evaluating the State at Discrete Times	5-25
5.4.4 Conclusions	5-25
List of References	5-26

SECTION 1

INTRODUCTION

1.1 Scope

Volume 2 of the present report gives an account of theoretical advances and associated demonstrations made during the reporting period relating to the synthesis of active controllers for large flexible structures. Particular applications discussed include the quenching of vibrations in support structures for optical pointing systems and the efficient generation of closed-loop large-angle slewing maneuvers for linear tracking. Certain aspects of discrete-time dynamic modeling for structural vibration control are also treated in depth. The vehicles for the demonstration examples are the ACOSS Model No. 2 representation of an optical pointing system (for vibration control) and a rotating rigid hub with four flexible appendages (for large-angle slew control). A concise summary of the principal results contained in the present volume is given in the remainder of Section 1.

1.1.1 Vibration Control

Effective accommodation of disturbances is fundamental to closed-loop regulation, being especially vital for the quenching of vibrations in large flexible optical pointing systems. Accommodation of a (small) finite number of periodic disturbances at fixed known frequencies poses only mild difficulty. Substantially more difficult is the problem of accommodating an aperiodic disturbance having nonnegligible power spectral density across a broad range of frequencies. In the preceding

reporting period, a scientific experiment was conceived to examine the question of active control synthesis for broadband disturbance accommodation in which the selection of reduced-order models and of active transducers were to be given substantial consideration.

Sections 2 and 3 of the present volume taken together constitute an initial account of progress in the study of broadband disturbance accommodation for large flexible optical pointing systems. The disturbance to be neutralized has a constant nonzero power spectral density over the frequency range between 0 and 5 Hz. In the first part (Section 2), attention is focused primarily upon the selection of active transducers, both by functional type and by location. The theoretical basis of a recently-developed selection algorithm is fully described; the principal elements are full-rank matrix factorizations -- in particular, the QR-decomposition -- and their employment in the representation of solutions to least-squares approximation problems. The algorithm is designed to select a relatively small number of actuators that have a relatively high influence on the variables to be regulated (in this case, optical system pointing errors). Results of four examples with ACOSS Model No. 2 demonstrate that selections are readily achievable that are substantially fewer in number than the number of controlled modes, and yet give promise of effective performance. In the second part (Section 3), attention is shifted to the design and evaluation of controllers for ACOSS Model No. 2 associated with the four active transducer selections described in Section 2. The controller feedback structure is generated using a textbook disturbance-rejection control design. Attempts at stability-enhancing adjustments beyond meeting the specifications on the optical pointing error are deliberately postponed in order to isolate the influence upon the overall synthesis process of the selection of reduced-order models and of active transducers, including their mutual interaction. In each example, the effect of unmodeled modes upon control system stability and performance is examined using an expanding family of reduced-order evaluation models. In the evaluations, closed-loop

stability over a range of frequencies substantially beyond that of the design model is demonstrated.

In the modeling of dynamic systems, state space representation provides a unified framework which abstracts certain system-theoretic characteristics common to a wide variety of physical systems. The resulting separation of dynamic characteristics from specific physical processes provides beneficial clarification. However, it has the disadvantage of masking the physics of the problem. The sharpened understanding that follows from taking into account the unique characteristics of a specific physical process usually increases the performance achievable from a process controller. In this spirit, a fresh approach to sampled-data control for flexible structures is taken in Section 4 in which second-order difference equations provide the dynamic model. For the problem of velocity output feedback, explicit sufficient conditions for stability in terms of the feedback gain matrix and the sampling rate are given. Surprisingly, these conditions require non-colocation of actuators and sensors as a function of the sampling rate. The non-colocation property collapses to the familiar colocation property for analog systems as the sampling period converges to zero.

1.1.2 Large-Angle Slew Control

Large-angle slewing maneuvers for flexible spacecraft generally require the consideration of nonlinear structural dynamics. However certain problems of substantial interest for applications require only the consideration of linear autonomous structural dynamics. Several such problems are formulated and solved in Section 5; namely, the problem of optimally tracking a known trajectory (without hard terminal constraints), and the problem of optimal linear slew in which the terminal values of some or all of the state variables at a fixed finite terminal time are prescribed. The emphasis is upon obtaining explicit expressions for solutions of the necessary conditions for optimality in terms of matrix parameters which are solutions of linear algebraic

equations. The problem of computing solutions is thereby reduced from one of numerical calculus (i.e., integration) to one of numerical linear algebra. Significant increases in computational efficiency resulting from this approach are demonstrated with a variety of examples on a rotating rigid hub with four flexible appendages. The method of obtaining explicit solution expressions is also shown to have direct application to the efficient generation of feedback control solutions to the general unconstrained fixed time linear optimal control problem.

1.2 Limitations

The scientific experiment relating to active control synthesis for broadband disturbance accommodation is incomplete. Projected work includes:

- (1) Expansion of the class of candidates from which active transducers are selected;
- (2) Examination of the interaction between the selection of reduced-order models and of active transducers; and
- (3) Modifications of the controller feedback structure to ensure an acceptable compromise between the requirement to neutralize the effects of disturbances, and the limitations imposed by an incomplete knowledge of structural and disturbance characteristics.

SECTION 2

PROGRESS ON SYNTHESIS OF ACTIVE CONTROL FOR BROADBAND DISTURBANCE ACCOMMODATION

PART 1: ACTIVE TRANSDUCER SELECTION

2.1 Background

In the automatic control of dynamic systems, the achievement of stability and a specified level of performance, in spite of anticipated disturbances, is fundamental. When the object of control has substantial inherent flexibility, the problem of accommodating disturbances is aggravated by the tendency of the disturbances to excite structural vibrations. Even with flexible structures, the effects of a few periodic disturbances at known frequencies are relatively easy to accommodate. However, when the frequency of periodic disturbances is unknown or variable, or when the disturbances are aperiodic, disturbance accommodation is much more difficult. Relatively little has been written regarding accommodation of the latter class of disturbances in the context of large flexible structures. One careful study treating unknown-frequency periodic disturbances [Ref. 2-1] has reported moderate success. It is notable that the treatment reported gave careful attention to the placement of active transducers (i.e., actuators and sensors). The only study available to date on accommodation of aperiodic disturbances with a continuum frequency spectrum ("broadband") in the context of large flexible structures [Ref. 2-2] also reports moderate success, without however, giving any attention to the selection of active

transducers beyond the analysis developed for accommodating periodic disturbances of known frequencies [Ref. 2-3].

The presence of a broadband disturbance escalates the importance of giving careful attention to the selection of reduced-order models, the selection of active transducers, and the interdependence of these two selections. In Reference 2-4, we outlined a scientific experiment (not in hardware) for the purpose of systematically investigating the impact upon the performance of active broadband disturbance accommodation of various assumptions relating to the selection of reduced-order models and of active transducers. This experiment is not a single design attempt, but rather a process involving a sequence of many variously-constrained designs, in order to converge on an appropriate overall algorithm for broadband disturbance accommodation with large flexible structures.

Sections 2 and 3 of the present report constitute the initial report of progress in the conduct of the aforementioned experiment. Section 2 focuses principally on the theory and application of the active transducer selection strategy being employed, while Section 3 focuses on the related matters of controller design and evaluation. Two very encouraging trends have emerged from the results reported herein:

- (1) Under appropriate assumptions, substantial reductions in the number of active transducer pairs below the number of controlled modes are feasible, which implies substantial design flexibility may be available; and
- (2) Using an expanding family of evaluation models, stability of reduced-order controllers over a frequency range well beyond the range of the design model has been demonstrated.

The significance of item (2) is that sophisticated adjustments of the controller design have been deliberately postponed; this result reflects principally the reward of careful attention to active transducer selection.

The remainder of Section 2 is briefly summarized. The active transducer selection strategy being employed in the scientific experiment was briefly outlined in a previous report [Ref. 2-5, Sec. 3]. In Section 2.2, a complete account of the theory that underlies this strategy is given. In addition, all phases of the strategy are fully discussed in the light of the theoretical building blocks. In Section 2.3, a number of applications of the selection strategy to ACOSS Model No. 2, under varying assumptions, is presented. In Section 2.4, some principal observations on the results are made. An appendix, Section 2.5, contains the proof of some technical matters that arise in Section 2.2.

2.2 Theory: A Selection Algorithm

Most strategies for active transducer selection reported in the literature use appropriately-defined indices of controllability and observability to evaluate alternatives. The selection strategy proposed and briefly outlined previously [Ref. 2-5, Sec. 3] approaches the selection problem from a different direction. Linear combinations of the modal influence vectors associated with each actuator are sought which best approximate the modal coefficient vectors of variables to be regulated (e.g., line-of-sight errors in an optical system). The principal theoretical building blocks of this strategy are the special properties of full-rank matrix factorizations (in particular, the QR-decomposition) and the representation theory for solutions of least squares approximation problems. In what follows, a complete though concise account of this underlying theory is necessary to enable a proper description of the construction and operation of the selection algorithm.

2.2.1 Fundamental Concepts

As will be seen shortly, least-squares approximation problems lead naturally and directly to the Moore-Penrose generalized inverse. This construction exists for arbitrary rectangular matrices $A: n \times m$, but is not quite so direct in the case that the inequality

$$k \triangleq \text{rank}(A) \leq \min \{n, m\} \quad (2-1)$$

becomes strict. In that case, the ability to decompose A into factors is extremely helpful. A decomposition of the form

$$A = BC \quad (2-2)$$

where $B: n \times k$ and $C: k \times m$ satisfy

$$\text{rank}(B) = k = \text{rank}(C)$$

with k defined by Eq. (2-1), is called a full-rank factorization of A . It is well known that every matrix has such a factorization [Ref. 2-6]. Although such factorizations are not unique, the class of all such factorizations is generated from a known factorization by the relations

$$B_1 = BY, \quad C_1 = Y^{-1}C$$

for some nonsingular matrix Y [Ref. 2-7]. Full-rank factorizations assume great importance in numerical linear algebra [Ref. 2-8]. Essential to the selection algorithm to be described later is the QR-decomposition [Ref. 2-9], which always has embedded within it a full-rank factorization.

2.2.1.1 The QR-Decomposition

The classical Gram-Schmidt orthogonalization [Ref. 2-10, pp. 127-128] is a constructive process of transforming a set of linearly independent vectors in an inner-product space into an orthonormal set. The matrix representation of the result is the QR-decomposition. It follows that every matrix has a QR-decomposition, whose specific structure depends on the rank of the matrix. Since the results are thoroughly discussed in the literature [e.g., Ref. 2-11], the parts relevant here are simply quoted.

Theorem 2-1 (Existence of QR-Decomposition). Assume that the matrix $A: n \times m$ has rank $k = \min\{n, m\}$. Then there exists a (nonsingular) column permutation matrix $P: m \times m$, a unitary matrix $Q: n \times n$, and a matrix $R: n \times m$ containing an upper triangular submatrix $R_1: k \times k$ with positive diagonal elements, such that

$$AP = QR \quad (2-3)$$

The structure of the R matrix is

$$\begin{bmatrix} R_1 \end{bmatrix} \quad (2-4a)$$

$$\begin{bmatrix} R_1 \\ \vdots \\ 0 \end{bmatrix} \quad (2-4b)$$

or

$$\begin{bmatrix} R_1 : S \end{bmatrix} \quad (2-4c)$$

according as A is determinate ($k = n = m$), overdetermined ($k = m < n$), or underdetermined ($k = n < m$), respectively. \square

The word "unitary" refers, in the complex case, to a matrix allowing complex entries whose columns are orthogonal relative to the complex inner product; the corresponding property in the real case refers to a matrix restricted to real entries whose columns are orthogonal relative to the real inner product ("orthogonal").

Theorem 2-1 has an obvious extension to the rank-deficient case that $k < \min\{n, m\}$. The extended result is used only in the proof of Proposition 2-8 in the Appendix (Section 2.5). The decomposition of Eq. (2-3) is a full-rank factorization (cf. Eq. (2-2)) except in the over-determined case (cf. Eq. (2-4b)). In that case, Eq. (2-3) is equivalent to the full-rank factorization

$$AP = Q_1 R_1$$

where Q_1 is the partition of Q compatible with R_1 .

For the intended application, stronger properties of the nonsingular submatrix R_1 are required than are evident in the Gram-Schmidt interpretation as reflected in Theorem 2-1. A powerful tool for accomplishing this is the following triangularization lemma of Householder [Ref. 2-12].

Lemma 2-2. Assume that n -vectors $a \neq 0$ and v are specified. Then there exists a unit vector $w: n \times 1$ such that

$$H(a) \triangleq (I_n - 2 w w^*)a = \|a\|v \quad \square \quad (2-5)$$

In Eq. (2-5), I_n is the $n \times n$ identity matrix, the asterisk (*) denotes the complex conjugate transpose operation, and the double bars denote the vector norm generated by the inner product:

$$\|a\|^2 \triangleq (a, a) = a^* a$$

Successive application of Householder transformations, each having the form defined in Eq. (2-5), to columns of the A matrix, including appropriate rearrangement (pivoting) of the columns at each step, leads to the desired triangularization. Reliable and widely available software for computing a QR-decomposition uses the Householder lemma [Ref. 2-13]. The stronger property that results is the following.

Theorem 2-3. In Theorem 2-1, elements of the matrix $R_1 \in [r_{ij}]$ may be taken to have the diagonal dominance property:

$$r_{\ell\ell}^2 \geq \sum_{i=\ell}^j r_{ij}^2, \quad j=\ell, \dots, k; \quad \ell=1, \dots, k \quad (2-6)$$

In particular, this implies the (weaker) property that the diagonal elements form a nonincreasing sequence:

$$r_{\ell\ell} \geq r_{\ell+1, \ell+1} > 0, \quad \ell=1, \dots, k-1 \quad \square \quad (2-7)$$

The subtle distinction between the two theorems above should be carefully noted. The results of Theorem 2-1 describe every QR-decomposition; the sharper results of Theorem 2-3 describe only those QR-decompositions generated by the use of Householder transformations.

2.2.1.2 Solutions to Least-Squares Problems

Least-squares problems for finite-dimensional linear systems of the form

$$Ax = b$$

(2-8)

with $A: n \times m$ become significant in the overdetermined case ($n > m$) in which there are too many equations for a solution to exist (in general). Instead, one attempts to minimize a positive-definite quadratic function of the difference, such as

$$J(x; A, b) \triangleq (b - Ax)^* (b - Ax) \quad (2-9)$$

or, more generally (apparently),

$$J_W(x; A, b) \triangleq (b - Ax)^* W (b - Ax) \quad (2-10)$$

where $W: n \times n$ is Hermitian (i.e., $W^* = W$) and positive definite. Being positive definite however, W can be written in the factored form

$$W = L^* L$$

with $L: n \times n$ nonsingular [Ref. 2-10, pp. 139-140]. This enables Eq. (2-10) to be written as

$$J_W(x; A, b) \simeq (\tilde{b} - \tilde{A}x)^* (\tilde{b} - \tilde{A}x) = J(x; \tilde{A}, \tilde{b}) \quad (2-11)$$

where $\tilde{b} \triangleq Lb$, $\tilde{A} \triangleq LA$, so that the least-squares problems associated with Eq. (2-10) and Eq. (2-9), respectively, are in fact equivalent under a simple scaling. It is therefore sufficient to discuss the relevant parts of the least-squares theory using Eq. (2-9), even though the selection algorithm is formulated using Eq. (2-10). Only the unconstrained minimization of Eq. (2-9) is discussed. Full details, including treatment of constrained minimization, can be found in Reference 2-11.

The minima of Eq. (2-9) are precisely the set of solutions to the normal equations

$$A^*(b - Ax) = 0 \quad (2-12)$$

It is worth noting that this result is a consequence of the geometric structure of inner-product spaces [Ref. 2-7] and does not follow from the methods of calculus (the operation $x \rightarrow \bar{x}$ of complex conjugation being nowhere differentiable). In addition, Eq. (2-12) provides a useful geometric insight: at any least-squares minimum, the residual vector

$$r \triangleq b - Ax$$

associated with the linear system Eq. (2-8) is orthogonal to the range space (i.e., the subspace spanned by the columns) of A , denoted by $\text{col}(A)$.

The solutions of the normal equations form an affine space of dimension $m-k$, where m and k are defined by Eq. (2-1). Written explicitly, they are:

$$x = A^t b + (I_m - A^t A)w, \quad w: n \times 1 \text{ arbitrary} \quad (2-13)$$

where the superscript (t) represents the Moore-Penrose inverse [Refs. 2-14, 2-15]. The basic properties of this generalized inverse will be used without elaboration, as they are thoroughly documented [Ref. 2-16] and have been discussed previously in a related context [Refs. 2-17, 2-18]. It follows from these properties that the two terms in Eq. (2-13) are orthogonal and, therefore, that the particular least-squares solution

$$x^0 \triangleq A^t b$$

has (uniquely) the smallest norm of all the solutions Eq. (2-13).

Each least-squares solution gives the minimum value

$$J_{\min} \triangleq \|(I_n - AA^{\dagger})b\|^2 \quad (2-14)$$

for the functional Eq. (2-9). Geometrically, this represents the length (squared) of the projection of b onto $\text{col}(A)^{\perp}$, the orthogonal complement of the range space of A . In particular, it follows that the minimum value is zero if and only if

$$b \in \text{col}(A) \quad (2-15)$$

i.e., that Eq. (2-8) has an exact solution.

The representation of least-squares solutions can be sharpened substantially if the Moore-Penrose inverse is displayed using the QR-decomposition of A . Two cases are distinguished:

- (I) $k = n \leq m$, for which Eq. (2-15) is true; and
- (II) $k = m < n$, for which Eq. (2-15) is false.

Theorem 2-4 (Case I). Assume that A has the decomposition of Eq. (2-3) with $k = n \leq m$. Then the minima of Eq. (2-9) are given by:

$$(P^{-1}x) = R^{\dagger}Q^*b + (I_m - R^{\dagger}R)\omega, \quad \omega: nx1 \text{ arbitrary} \quad (2-16)$$

If $n=m$, the set of Eq. (2-16) collapses to the unique solution

$$(P^{-1}x) = R^{-1}Q^*b \quad (2-17)$$

In both instances, the minimum value in Eq. (2-14) is zero. \square

This result is used in the initial stages of the selection algorithm.

An even richer structure develops in the next case.

Theorem 2-5 (Case II). Assume that A has the decomposition of Eq. (2-3) with $k = m < n$. Denote by $Q \equiv [Q_1 : Q_2]$ the partition of Q compatible with the partition of R in Eq. (2-4b). Then the minimum of Eq. (2-9) is given (uniquely) by:

$$(P^{-1}x) = R_1^{-1} Q_1^* b \quad (2-18)$$

and the minimum value in Eq. (2-14) is

$$J_{\min} = \|Q_2^* b\|^2 \quad \square \quad (2-19)$$

The significance of Theorem 2-5 arises from the rich structure of the mappings associated with the matrices $Q_1: n \times k$ and $Q_2: n \times (n-k)$, which are briefly summarized next. They all follow from viewing Eq. (2-3) in the equivalent form

$$Q^*(AP) = R \quad (2-20)$$

which exhibits the final result of the Householder construction (cf. Lemma 2-2). It follows immediately that Eq. (2-20) embodies the two equations:

$$Q_1^*(AP) = R_1 \quad (2-21)$$

and

$$Q_2^* (AP) = 0 \quad (2-22)$$

From Eqs. (2-21) and (2-22) it follows quite directly that Q_1 and Q_2 are orthogonal:

$$Q_1^* Q_2 = 0, \quad Q_2^* Q_1 = 0 \quad (2-23a)$$

$$Q_1^* Q_1 = I_k, \quad Q_2^* Q_2 = I_{n-k} \quad (2-23b)$$

and have range spaces

$$\text{col}(Q_1) = \text{col}(AP), \quad \text{col}(Q_2) = \text{col}(AP)^\perp \quad (2-24)$$

respectively. Furthermore the product mappings

$$Q_1 Q_1^* = I_n - Q_2 Q_2^* \quad (2-25)$$

and

$$Q_2 Q_2^* = I_n - Q_1 Q_1^* \quad (2-26)$$

are orthogonal projections, respectively (cf. Eqs. (2-23), onto the range spaces listed in Eq. (2-24). Note that Eq. (2-26) provides the link between Eq. (2-14) and the result in Eq. (2-19). Theorem 2-5 forms the principal basis for the selection algorithm.

The behavior of the minimum value in Eq. (2-14) as a function of A , and in particular as columns are removed from A , is of considerable interest for the active transducer selection problem. Roughly, one expects that the minimum value does not change if columns of A are simply rearranged, and that it does not decrease if a column of A is removed.

Theorem 2-6. Let p be an integer, $1 \leq p \leq m$, and denote by $A_{i_1 \dots i_p}$ an arbitrary p -column submatrix of A . Then

$$\min_{x \in E^m} J(x; A, b) \leq \min_{y \in E^p} J(y; i_{i_1 \dots i_p}, b) \quad (2-27)$$

where E^a denotes the appropriate a -dimensional inner product space. \square

The proof of this result is deferred to the Appendix (Section 2.5).

2.2.2 Algorithm Formulation

It is now possible to give a precise formulation of the active transducer selection algorithm. It is assumed in what follows that:

- (1) A reduced-order structural model has been chosen; and
- (2) Sensors are to be colocated with actuators.

The focus is on determining an appropriate, and relatively small, selection of actuators from a prespecified collection of candidates.

Dynamic equations in modal coordinates for the reduced-order model to be considered have the general form:

$$\ddot{\eta} + 2\zeta\dot{\eta} + \Omega^2\eta = (\phi^T B_A)u_A + (\phi^T B_D)u_D \quad (2-28)$$

$$y = (\phi^T C_p^T)^T \eta + (\phi^T C_v^T)^T \dot{\eta} \quad (2-29)$$

$$z = (\phi^T D^T)^T \eta \quad (2-30)$$

where $\eta \equiv (\eta_1, \dots, \eta_n)^T$ is the vector of modal coordinates retained in the reduced-order model; $\Omega \equiv \text{diag}(\omega_i)$: $n \times n$ is the matrix of characteristic frequencies; Φ : $v \times n$ is the truncation of the principal-axis matrix of transformation defining the modal coordinates (mode shapes of the reduced-order model), v being the number of physical generalized coordinates; $Z \equiv \text{diag}(\zeta_1, \dots, \zeta_n)$: $n \times n$ is the matrix of assumed modal damping ratios representing inherent structural damping; $u_A \equiv (u_1, \dots, u_m)^T$ is the vector of inputs to the actuators; $u_D \equiv (w_1, \dots, w_r)^T$ is the vector of disturbance inputs; $y \equiv (y_1, \dots, y_\ell)^T$ is the vector of outputs from the sensors; $z \equiv (z_1, \dots, z_s)^T$ is the vector of variables to be regulated; and B_A : $v \times m$, B_D : $v \times r$, C_p : $\ell \times v$, C_y : $\ell \times v$, D : $s \times v$ are the influence matrices associated with the actuators, disturbances, displacement sensors, rate sensors, and regulated variables, respectively. The superscript (T) denotes matrix transpose. Equations (2-28) through (2-30) are written in a form that highlights the presence of generalized node shapes (modal influence vectors) of the form $\Phi^T x$.

The selection problem is defined in terms of two sets of parameters:

- (1) A collection \mathcal{A} of actuator candidates, consisting of the generalized node shapes $\Phi^T b_A^j$, where b_A^j is the j -th column of the matrix B_A in Eq. (2-28); and
- (2) A collection \mathcal{B} of regulation target vectors, consisting of the generalized node shapes $\Phi^T d_i^T$, where d_i^T is the i -th row of the matrix D in Eq. (2-30).

It is assumed that the designer has a relatively wide range of choices for actuators (in particular, having redundancy) both by functional type and location for inclusion in the candidate collection \mathcal{A} . The idea behind collection \mathcal{B} is as follows: actuators are to be selected from the collection \mathcal{A} which have a relatively strong influence on each of the vectors in collection \mathcal{B} , thereby enhancing the prospects of achieving

the desired regulation of the vector z in Eq. (2-30). In order to clarify ideas and simplify the notation, the remaining discussion identifies the regulated variable z with the two-vector $(\epsilon_{\text{LOSX}}, \epsilon_{\text{LOSY}})$ that is of interest in the applications of Section 2.3 and which represents line-of-sight (LOS) error parameters for an optical system. The collection \mathcal{B} then consists of the two elements:

$$b^{\text{LOSX}} \triangleq \phi^T d_{\text{LOSX}}, \quad b^{\text{LOSY}} \triangleq \phi^T d_{\text{LOSY}} \quad (2-31)$$

where d_{LOSX}^T and d_{LOSY}^T are the rows of D corresponding to the regulated variables ϵ_{LOSX} and ϵ_{LOSY} in Eq. (2-30).

Using the parameters from collections \mathcal{A} and \mathcal{B} , an ideal selection problem, and a least-squares approximation to it, are defined. Denote by

$$A \triangleq [\mathcal{A}] \triangleq [a^1 : \dots : a^{\mu}] : n \times \mu \quad (2-32)$$

the matrix formed from elements of the actuator candidate collection \mathcal{A} . (The type of correspondence defined by Eq. (2-32) is used repeatedly in what follows.) It is assumed that the collection \mathcal{A} is rich enough to span the space E^n of modal coordinates; i.e.,

$$\text{sp}(\mathcal{A}) \triangleq \text{col}(A) = E^n \quad (2-33)$$

Then there exist coefficient vectors $x \triangleq (x_1, \dots, x_n)^T$, $y \triangleq (y_1, \dots, y_n)^T$ such that

$$b^{\text{LOSX}} = Ax \triangleq \sum_{j=1}^{\mu} a^j x_j$$

and

$$b^{\text{LOSY}} = Ay \equiv \sum_{j=1}^{\mu} a^j y_j$$

Ideal Selection Problem: Find a minimal subcollection \mathcal{A}' of \mathcal{A} and real coefficient vectors $x' \equiv (x_j)$, $y' \equiv (y_j)$, $j \in I(\mathcal{A}')$, such that

$$b^{\text{LOSX}} = A'x' \equiv \sum_{j \in I(\mathcal{A}')} a^j x'_j$$

and

$$b^{\text{LOSY}} = A'y' \equiv \sum_{j \in I(\mathcal{A}')} a^j y'_j$$

where the index set $I(\mathcal{A}')$ is the subset of $\{1, \dots, \mu\}$ that identifies which elements of \mathcal{A} are retained in \mathcal{A}' , and $A' \triangleq [\mathcal{A}']$.

As a more feasible alternative to the ideal selection problem, the following least-squares approximation is formulated.

Approximate Selection Problem: Find a subcollection \mathcal{A}' of \mathcal{A} and corresponding coefficient vectors $x' \equiv (x_j)$, $y' \equiv (y_j)$, $j \in I(\mathcal{A}')$ such that

$$(1) J_W(x'; A', b^{\text{LOSX}}) \triangleq (b^{\text{LOSX}} - A'x')^T W (b^{\text{LOSX}} - A'x') \text{ and } \quad (2-34)$$

$$J_W(y'; A', b^{\text{LOSY}}) \triangleq (b^{\text{LOSY}} - A'y')^T W (b^{\text{LOSY}} - A'y') \quad (2-35)$$

are minimized, where $A' \triangleq [\mathcal{A}']$; and

(2) the subcollection \mathcal{A}' is minimal with respect to acceptable increases in the minimum values:

$$J_{\min}(A', b^{\text{LOSX}}) \triangleq \min_{x'} J_W(x'; A', b^{\text{LOSX}}) \quad (2-36)$$

$$J_{\min}(A', b^{\text{LOSY}}) \triangleq \min_{y'} J_W(y'; A', b^{\text{LOSY}}) \quad (2-37)$$

In the above, the matrix $W: nxn$ is chosen to be real, symmetric, and positive definite. However, in view of the equivalence, under appropriate scaling, conveyed by Eq. (2-11), the discussion below omits explicit reference to the weighting matrix W . Note that, although the correspondence

$$\mathcal{A}' + [\mathcal{A}'] \equiv A'$$

defined by Eq. (2-32) does not distinguish between distinct column rearrangements, Proposition 2-7 (Section 2.5) shows that such distinguishability is inessential for its intended usage. Thus, the approximate selection problem is well-defined.

A brief overview of the algorithm for the solution of the approximate selection problem is as follows. A sequence of eliminations from the actuator candidate collection \mathcal{A} is generated on the basis of information from least-squares solutions corresponding to Eqs. (2-34) and (2-35) at each step. These solutions are displayed using the appropriate QR-decomposition. Note that each elimination also leads to a reduction in dimension of the inner-product space in which the least-squares minimization is done. No matter what elimination sequence develops, Theorem 2-6 guarantees a sequence of least-squares approximations that is steadily deteriorating in quality in the sense that the sequence of norms for the residual vector at each least-squares solution is nondecreasing. When \mathcal{A} has been reduced by elimination to a collection \mathcal{A}' for which further elimination (say to \mathcal{A}'') leads to the condition that either of the minimum values Eq. (2-36) or (2-37) (corresponding to \mathcal{A}'' rather than to \mathcal{A}') exceeds a specified tolerance τ_0 , the elimination sequence is

terminated, and \mathcal{A}' is taken to be a minimal subcollection. Next, details of the elimination sequence are outlined.

2.2.2.1 Criteria for Elimination

In view of Theorem 2-4, the search for a minimal subcollection in the sense of the approximate selection problem eventually requires criteria for intelligently eliminating a column from a determinate or overdetermined matrix. Two such criteria are discussed prior to describing the elimination sequence. Consider a stage of the sequence at which the matrix $A \in [\mathcal{A}(\ell)]$ of the remaining actuator candidates is (say) overdetermined with $\ell < n$ columns. The QR-decomposition of A has the form of Eq. (2-3) with R having the form of Eq. (2-4b). Denote by x and y , respectively the unique solutions (cf. Eq. (2-18)) to the least-squares problems associated with Eqs. (2-34) and (2-35). The criteria for elimination of actuator candidates from A are defined in terms of the matrices R , x , and y ; in particular:

- (I) the relative magnitude of the smallest diagonal element $r_{\ell\ell}$ of R_1 ; and
- (II) the relative magnitude of the products $r_{1i}x_i$, $i=1, \dots, \ell$, and $r_{jj}y_j$, $j=1, \dots, \ell$, respectively.

The rationale for each criterion is briefly discussed.

Criterion I. The scalar equations for the QR-decomposition of A have the triangular structure:

$$a^j = q^1 r_{1j} + q^2 r_{2j} + \dots + q^j r_{jj}, \quad j=1, \dots, \ell \quad (2-38)$$

where the diagonal elements r_{jj} of R_1 form a nonincreasing sequence (cf. Eq. (2-7)). Denote by $S_{\ell-1}$ the $(\ell-1)$ -dimensional subspace spanned by the vectors $\{q^1, \dots, q^{\ell-1}\}$. Since the vector $a^{\ell} - q^{\ell} r_{\ell\ell}$ is in $S_{\ell-1}$, $r_{\ell\ell}$ is an upper bound for the Euclidean distance between a^{ℓ} and $S_{\ell-1}$:

$$d(a^\ell, S_{\ell-1}) = \inf\{\|a^\ell - s\|: s \in S_{\ell-1}\} \leq r_{\ell\ell} \quad (2-39)$$

Because of the triangular structure of Eqs. (2-38), $S_{\ell-1}$ is also the linear span of $\{a^1, \dots, a^{\ell-1}\}$. Therefore, Eq. (2-39) is a measure of the near-dependence of a^ℓ upon the preceding column vectors a_i , $i=1, \dots, \ell-1$. Sufficiently small values of $r_{\ell\ell}$ relative to $r_{\ell-1, \ell-1}$ suggest that a^ℓ might be eliminated without an unacceptable increase in the resulting minimum value Eq. (2-36) and (2-37) associated with the truncated matrix.

Criterion II. Eliminations in accordance with Criterion I are made only on the basis of the QR-decomposition of A , and without regard for the least-squares solutions that determine the quality of the desired approximation. Criterion II takes those solutions into account. In comparing the numbers $|r_{ii}x_i|$, $i=1, \dots, \ell$, suppose that the minimum occurs at some index $\sigma < \ell$; i.e.,

$$|r_{\sigma\sigma}x_\sigma| = \min_{i=1, \dots, \ell} \{|r_{ii}x_i|\} \quad (2-40)$$

Recalling the nonincreasing property Eq. (2-7) of the diagonal elements r_{ii} , it follows from Eq. (2-40) that

$$|x_\sigma| = \min_{i=\sigma, \dots, \ell} \{|x_i|\} \quad (2-41)$$

Equation (2-41) is an indication that column a^σ is less important to the least-squares approximation than the succeeding columns a_j , $j=\sigma+1, \dots, \ell$. Sufficiently small values of the minimum in Eq. (2-40) relative to the other $|r_{ii}x_i|$ values suggest that a^σ might be eliminated from A . Similar considerations relating to the numbers

$|r_{jj}y_j|$, $j=1, \dots, \ell$, suggest the elimination of a (possibly different) column a_j from A . Taken together, Criteria I and II may suggest up to three distinct candidates for elimination from A .

2.2.2.2 The Elimination Sequence

Having specified the following parameters:

- (1) an actuator candidate collection \mathcal{A} ;
- (2) a regulation target collection \mathcal{B} (e.g., $\{b^{\text{LOSX}}, b^{\text{LOSY}}\}$);
- (3) a least-squares weighting matrix W (notational references suppressed); and
- (4) a least-squares minimum tolerance parameter $\tau_0 > 0$;

the elimination sequence can be defined.

Step 1: Initial Factorization. Set $A^{(0)} \triangleq A \in [\mathcal{A}]$ and compute a QR-decomposition of $A^{(0)}$. [Because of the assumption Eq. (2-33), the R-matrix in the decomposition (cf. Eq. (2-3))

$$A^{(0)} P^{(1)} = Q^{(1)} R^{(1)} \quad (2-42)$$

has the structure of Eq. (2-4c).]

Step 2: Initial Least-Squares Solutions. Denote $A^{(1)} \triangleq A^{(0)} P^{(1)}$ and solve the least-squares problems of the form Eqs. (2-34) and (2-35), respectively, for $A^{(1)}$. [It follows from Theorem 2-4 that there are infinitely many least-squares solutions (cf. Eq. (2-16)), but all give zero for the minimum values Eqs. (2-36) and (2-37) corresponding to $A^{(1)}$.]

Step 3: Initial Elimination. Truncate $A^{(1)}$ by retaining only its first n columns; denote the result by $A^{(2)}$; i.e.,

$$A^{(2)} = [a^{p_1(1)} : \dots : a^{p_1(n)}] : n \times n$$

where p_1 is the permutation mapping of the indices $\{1, \dots, \mu\}$ induced by the column permutation matrix $P^{(1)}$ of Step 2. [Because of the assumption Eq. (2-33) and the structure of the matrix $R^{(1)}$, the first n columns of $A^{(1)}$ are linearly independent. Moreover, $A^{(2)}$ inherits the QR-decomposition

$$A^{(2)} = Q^{(1)} R_1^{(1)}$$

from Eq. (2-42) in which the R-matrix has the form of Eq. (2-4a). There are unique solutions $x^{(2)}$ and $y^{(2)}$ to the least-squares problems of the form Eqs. (2-34) and (2-35), respectively, for $A^{(2)}$ (cf. Eq. (2-17)), and the corresponding minimum values Eqs. (2-36) and (2-37) are again zero.]

Step 4: Secondary Elimination. Examine the numbers $r_{nn}^{(1)}$, $r_{ii}^{(1)} x_i^{(2)}$, $i=1, \dots, n$; and $r_{jj}^{(1)} y_j^{(2)}$, $j=1, \dots, n$, associated with $A^{(2)}$, $x^{(2)}$, and $y^{(2)}$. Using either Criterion I or II, select a column, say the σ -th, of $A^{(2)}$ for elimination. Truncate $A^{(2)}$ by removing the σ -th column. [When the criteria suggest more than one column of $A^{(2)}$ for elimination, all eliminations may be done in parallel. The result is a (generally expanding) lattice of alternatives for elimination.]

Step 5: Secondary Factorization. Denote

$$A^{(3)} \triangleq [a^{p_1(1)} : \dots : a^{p_1(\sigma)-1} : a^{p_1(\sigma)+1} : \dots : a^n] : (n-1) \times n$$

and compute a QR-decomposition of $A^{(3)}$. [The columns of $A^{(3)}$ are linearly independent, having been inherited from $A^{(2)}$. The QR-decomposition

$$A^{(3)} P^{(2)} = Q^{(2)} R^{(2)}$$

has an R-matrix with the structure of Eq. (2-4b).]

Step 6: Secondary Least-Squares Solutions. Denote $A^{(4)} \triangleq A^{(3)} P^{(2)}$ and solve the least-squares problems of the form Eqs. (2-34) and (2-35), respectively, for $A^{(4)}$. [It follows from Theorem 2-5 that each of the two least-squares problems has a unique solution (cf. Eq. (2-18)), and the minimum values corresponding to Eqs. (2-36) and (2-37), respectively, are generally nonzero (cf. Eq. (2-19)).]

Step 7: Subsequent Eliminations. Repeat Steps 4 through 6, successively, applying Step 4 of the current cycle to the results of Step 6 for the preceding cycle.

Step 8: Termination. Assume that the preceding eliminations have reduced the initial collection \mathcal{A} to the subcollection \mathcal{A}' and that each elimination (say to \mathcal{A}'') from \mathcal{A}' via the application of Steps 4 through 6 leads to corresponding minimum values (cf. Eqs. (2-36), (2-37)) such that either

$$J_{\min} (A'', b^{\text{LOSX}}) > \tau_0 \quad (2-43)$$

or

$$J_{\min} (A'', b^{\text{LOSY}}) > \tau_0 \quad (2-44)$$

where $A'' \triangleq [\mathcal{A}'']$. Terminate the elimination sequence; \mathcal{A}' is a minimal selection.

The actual numerical implementation of the termination tests Eqs. (2-43) and (2-44) is modified slightly when very small residual vectors in the least-squares solutions are required, as in the applications to be presented subsequently. The test Eq. (2-43) has the form

$$\sum_{i=1}^n |\rho_i|^2 > \tau_0. \quad (2-45)$$

where $\rho = (\rho_1, \dots, \rho_n)^T$ is the residual vector $b^T A^{-1} x^*$ at a least-squares solution x^* corresponding to A^T . The actual computation of the squares of small numbers in Eq. (2-45) is undesirable. In view of the equivalence of all norms on \mathbb{E}^n , and in particular, from Jensen's inequality [Ref. 2-19]:

$$M \triangleq \max_{i=1, \dots, n} |\rho_i| \leq \left(\sum_{i=1}^n |\rho_i|^2 \right)^{1/2} \leq \sum_{i=1}^n |\rho_i| \leq n M$$

the test Eq. (2-45) is equivalent to the condition

$$\|\rho\|_\infty \equiv \max_{i=1, \dots, n} |\rho_i| > \tau_1 \quad (2-46)$$

for appropriately chosen τ_1 . Similar remarks apply to the test Eq. (2-44). In addition to being simpler and subject to less computational error, Eq. (2-46) also provides information (not provided by Eq. (2-45)) as to which of the modal coordinates is associated with the unacceptable approximation.

It should be observed that the elimination sequence has embedded within it a considerable degree of design flexibility that goes far beyond the choice of the parameters \mathcal{A} , \mathcal{B} , W , and τ_0 . Step 3 accomplishes a (generally quite large) reduction in the number of actuator candidates from μ (cf. Eq. (2-32)) to n . The candidates that are retained in Step 3 are determined by the column permutation $p^{(1)}$ generated in Step 1. That permutation in turn is the result of successive applications of the Householder Lemma 2-2 that are performed in Step 1 in order to achieve the diagonal dominance property Eq. (2-6) in the factorization of Eq. (2-42). In general, $p^{(1)}$ is not unique in this regard. The implications of this lack of uniqueness have yet to be fully explored.

2.3 Applications with ACOSS Model No. 2

In the description of the scientific experiment for active control synthesis with generic structural models [Ref. 2-4], four principal elements of the synthesis process are identified as variables of the experiment:

- (1) Design of the basic structure to be controlled;
- (2) Selection of reduced-order models;
- (3) Selection of active transducers; and
- (4) Determination of the controller feedback structure.

For the work summarized in the present report, the first and last of these elements are fixed in order to focus on the other two, especially active transducer selection.

The first element, basic structural design, is a significant variable in relation to the generic structural models because of the many modifications to original designs. In particular, the original structural design for ACOSS Model No. 2 [Ref. 2-20] has undergone three major revisions [Ref. 2-21]. The choice of Revision 1 for the work reported here represents a compromise which retains improvements on the original design in the modeling of the attachments for certain rigid-body elements, while avoiding the extremes of very high inherent flexibility (Revision 3) or very high inherent stiffness (Revision 4).

The last element, controller feedback structure determination, is held fixed for the work reported here in order to avoid obscuring the view of whatever improvements in performance may be attributable to judicious selections of reduced-order models and of active transducers. The choice of the disturbance-rejection control feedback structure [Ref. 2-22; Sec. 3.6], which assumes full knowledge of the statistics of the disturbance, provides an upper bound for control system performance.

The disturbance to be accommodated is assumed to be an aperiodic disturbance with a constant power spectral density at frequencies from 0

to 5 Hz, applied in a fixed direction at nodes no. 37 and 46 of the structural model. Full details of the disturbance definition and relevant assumptions have been given previously [Ref. 2-5, Sec. 2].

To assist in the selection of reduced-order models, criteria for ranking the structural modes are commonly used [e.g., Ref. 2-2]. In the present context, ranking of modes is done by comparing open-loop modal responses of the regulated variable to the disturbance input; i.e., the root-mean-square (RMS) value of the response of the two-input, single-output system between the disturbance input and the contribution of each mode to the line-of-sight error (cf. Eqs. (2-28) and (2-30)). The precise formulation has been given previously [Ref. 2-5, Sec. 5]. The resultant ranking of flexible-body modes for the chosen structural model (Revision 1) is shown in Table 2-1. An inevitable feature of any such ranking procedure is that, in general, a selected group G of consecutively-ranked modes is not contiguous in frequency; i.e., there exist modes not in G which are interlaced in frequency with modes in G . For example, the first eleven modes according to the ranking of Table 2-1 are interlaced in frequency with seven modes (11, 15, 17-21) of considerably lower rank. The interlacing can be seen clearly in the frequency listing of Table 2-2. A reduced-order model having this property is said to be interlaced; otherwise it is called contiguous.

As indicated in the preceding section, the objective of the active transducer selection algorithm (roughly speaking) is to choose a relatively small number of those actuators that are expected to have relatively high effectiveness in achieving the desired regulation of line-of-sight error. It therefore seems desirable that the selection process lead to a rich lattice of alternatives (Step 4) for elimination from the initial class of actuator candidates. This qualitative property is termed richness. It is certainly desirable that upon termination of the elimination sequence, the number of retained actuators is substantially smaller than the number of modes to be controlled. Denoting by p the number of actuators retained in a minimal selection, the level of reduction

$$\Delta \equiv \Delta(\mathcal{A}, \tau_0) \triangleq n - p \quad (2-47)$$

is an important quantitative measure of the effectiveness of the selection algorithm. It is obvious that the level of reduction should depend on the tolerance parameter τ_0 ; it also turns out to be a very strong function of the class \mathcal{A} of actuator candidates chosen.

Principal observations with respect to the performance of the selection algorithm that have emerged from work to date are the following:

- (1) Level of reduction increases with augmented richness;
- (2) Richness is augmented when:
 - (a) Interlaced reduced-order-design models for which active transducer selection is tailored are made contiguous;
 - (b) The class of actuator candidates is enlarged;
 - (c) Suitable restrictions are imposed upon a sufficiently large actuator candidate class;
- (3) Minimal selections which realize the same level of reduction are not necessarily unique.

Four design examples with ACOSS Model No. 2 are described next. These examples demonstrate the observations noted and show in addition some of the design flexibility that is available when relatively high levels of reduction are achievable.

2.3.1 Specifications for Design Examples

Considerations which apply to each of the four examples are the following:

- (1) The basic structural design is Revision 1 of ACOSS Model No. 2 [Ref. 2-21] with $Z = \text{diag}(0.001)$ in Eq. (2-28);
- (2) A broadband disturbance [Ref. 2-5, Sec. 2] is applied to nodes no. 37 and 46 of the structure, assuming constant direction;

- (3) Selection of modes for inclusion in reduced-order models for controller design is assisted by the disturbance response ranking of Table 2-1;
- (4) The regulation target collection \mathcal{B} consists of the elements defined by Eq. (2-31) (whose dimension is that of the design model);
- (5) The least-squares weighting matrix W has the form:

$$W = \text{diag}(w_i) : n \times n \quad (2-48)$$

where w_i is the RMS LOS-error disturbance response associated with mode η_i of the reduced-order design model as listed in Table 2-1;

- (6) The least-squares minimum tolerance parameter is

$$\tau_0 \approx 10^{-6} \quad (2-49)$$

The four examples are distinguished by differing specifications on the reduced-order design model and actuator candidate class \mathcal{A} . The specifications are summarized in Table 2-3 and are discussed briefly below.

Reduced-order design model. In Example A, the reduced-order design model consists only of the modes ranked 1 through 11 in Table 2-1; it is interlaced. In all the succeeding examples, this design model is made contiguous by incorporating the formerly excluded modes between mode 7 and mode 24. However, mode 19 -- a solar panel torsion mode -- is excluded from the numerical implementation. The associated entry in the least-squares weighting matrix W (cf. Eq. (2-48)) is extremely small (10^{-22}) causing the resulting weighting matrix to be poorly conditioned numerically with respect to inversion. The small weighting is a

reflection of the very low influence of this mode (ranking at most 147 out of 156) on any of the modeled node-connecting elements.

Actuator candidate class. In Examples A and B, only axial member actuators (137 total) on node-connecting elements of the finite-element model are allowed. In Example C, the class of candidates is expanded to include translation actuators at all nodes, an aggregate of 311. In Example D, certain nodal translation actuators are disallowed; in particular, these are the z-translation actuators on equipment section nodes (6 total) and both y-translation and z-translation actuators on interior solar panel nodes (16 total).

2.3.2 Selection Results

Active transducer selection results with Examples A through D are summarized in Table 2-3; visual representations are given in Figures 2-7 through 2-9. The results are discussed briefly.

Example A yields somewhat unsatisfactory results from the viewpoint of design flexibility in actuator selection ($\Delta=1$). Only two alternatives are available (Step 4) for removing an actuator from the candidates remaining after completion of the initial elimination (Step 3). Both alternatives lead to least-squares solutions which exceed the specified termination tolerance (Eq. (2-49)). The least undesirable of the two elimination alternatives leads to the minimal selection shown in Fig. 2-1. It can be seen that the measure of the residual vector in Eq. (2-46) slightly exceeds the specified tolerance τ_0 in the required variable associated with b^{LOSX} (cf. Eq. (2-31)). Inclusion of the member connecting one solar panel (at node 52) to the equipment section (at node 43) is somewhat surprising, since in a static comparison of influence upon each of the modes in the design model (intra-row comparison of entries in the $\Phi^T B_A$ matrix of Eq. (2-28)), this member ranks no higher than 91st of all 137 members.

Example B yields a somewhat richer lattice of elimination alternatives and a substantial improvement of the level of reduction in the minimal selection. This is attributable entirely to having (minimally) augmented the reduced-order design model to make it contiguous, as Table 2-3 indicates. The minimal selection is shown in Fig. 2-2.

Example C yields only a slightly richer lattice of elimination alternatives, but a quite substantial improvement in the level of reduction in the minimal selection, in comparison to example B. This is attributable to having enlarged the class of actuator candidates \mathcal{A} to include translation actuators at nodes, as Table 2-3 indicates. This explains the presence of \mathcal{A} in Eq. (2-47). The minimal selection is shown in Figure 2-3. It is noteworthy, but not surprising, that no axial actuators appear in the minimal selection even though the candidate class includes them all. In fact, all axial candidates are removed in the initial elimination (Step 3).

Example D provides somewhat surprising and quite satisfying results. The lattice of elimination alternatives is extremely rich and leads to an even more substantial improvement in the level of reduction in minimal selections, of which there are two in this case. A portion of the branch of the elimination lattice that leads to the minimal selections is shown in Fig. 2-4. The label "TX-34" indicates the removal of the translational (T) actuation in the x-coordinate (X) body-axis direction at node 34, other labels having an analogous interpretation. Parentheses indicate eliminations along a portion of the branch that do not lead to one of the minimal selections. Preselections D-17, D-14, and D-11 are shown in Figs. 2-5 through 2-7, respectively, and minimal selections D-9A and D-9B are shown in Figs. 2-8 and 2-9, respectively. Taken together, Figs. 2-4 through 2-9 show quite clearly how the elimination sequence (beginning with Step 4) leads systematically to minimal selections. The steady increase in the measure of Eq. (2-46) for the residual vectors associated with b_{LOSX} and b_{LOSY} (Eq. (2-31)),

respectively, as the elimination sequence proceeds may be noted, consistent with the expectation of Theorem 2-6 (Eq. (2-27)). In this example, the number of actuators in a minimal selection is only half the number of controlled modes. This implies a very desirable degree of design flexibility is available (and may be beneficial) by employing intermediate (ancestral) selections such as D-14 or D-11 that lie along the path to a minimal selection. A full explanation of how the restriction imposed in proceeding to example D leads to the improvements observed is not yet available. However it does provide a substantiation of the design flexibility embedded within the elimination sequence that is mentioned at the end of Section 2.2.

Minimal selections from Examples B, C, and L are employed in the design of optimal linear-quadratic disturbance-rejection controllers as reported subsequently in Section 3. Each of the designs is evaluated in the presence of a family of contiguous reduced-order evaluation models (cf. Table 2-2) with increasing ranges of frequency. Stability well beyond the frequency range (5 Hz) of the design model is demonstrated in each case.

2.4 Summary

Work accomplished to date in connection with the scientific experiment for active control synthesis with broadband disturbances has led to substantial insight into a relatively new and systematic approach to active transducer selection. This process leads to selections which at the same time have relatively high influence upon variables to be regulated in the control problem and require substantially fewer actuators than controlled modes. The selection process itself, as well as the selections it produces, exhibit potentially beneficial design flexibility. Linear-quadratic disturbance-rejection controllers employing transducer selections generated by this process (cf. Sec. 3) demonstrate stability in the presence of residual modes over a frequency range substantially beyond that of the design modes. These

demonstrations are significant in that stability-enhancing adjustments of the controller feedback structure have been deliberately postponed in order to focus on the connections between the selection of reduced-order models and active transducers on the one hand and closed-loop stability and performance on the other hand.

Subsequent work in regard to active transducer selection will include:

- (1) Expansion of the actuator candidate class to include rotational actuators;
- (2) Deeper investigation of the design flexibility inherent in the selection process; and
- (3) Examination of the interaction between the selection of reduced-order models and the selection of active transducers.

2.5 Appendix

Theorem 2-6 is an immediate consequence of the following two results.

Proposition 2-7 (Column Rearrangements). The minimum value defined by Eq. (2-14) is unchanged by an arbitrary column permutation $P: m \times m$ of A ; i.e.,

$$\min_x J(P^{-1}x; AP, b) = \min_x J(x; A, b) \quad (2-50)$$

Proof. The identity

$$J(P^{-1}x; AP, b) = \|b - (AP)(P^{-1}x)\|^2 = J(x; A, b) \quad (2-51)$$

holds for all n -vectors x . It follows that for each minimum, say x_0 (cf. Eq. (2-13)), of $J(\cdot; A, b)$, $P^{-1}x_0$ is a minimum of $J(\cdot; AP, b)$, and conversely. The desired coincidence of minimum values Eq. (2-50) follows from Eq. (2-51) by this correspondence of minimum points. \square

Proposition 2-8 (Terminal Removals). Let p be an integer, $1 \leq p \leq m-1$. The minimum value defined by Eq. (2-14) does not decrease if columns $p+1, \dots, m$ are removed from A ; i.e.,

$$J_{\min} \triangleq \min_{x \in E^m} J(x; A, b) \leq \min_{y \in E^p} J(y; A_{1 \dots p}; b) \triangleq J_{\min}^p$$

where $A_{1 \dots p}$ denotes the submatrix consisting of the first p columns of A .

Proof. Integers k , m , and n are defined as in Eq. (2-1). In view of Proposition 2-7, there is no loss of generality in assuming that the leading k columns are linearly independent. Two cases are considered, depending on whether Eq. (2-1) represents an equality or a strict inequality.

Case A: $k = \min\{n, m\}$. If $n \leq m$, then the result is trivial: Eq. (2-15) is true, and therefore

$$J_{\min} = 0 \leq J_{\min}^p$$

Thus, consider that $m < n$. The QR-decomposition of A (cf. Theorem 2-1) has the structure

$$A = QR \equiv [Q_1 : Q_2] \begin{bmatrix} R_1 \\ \vdots \\ 0 \end{bmatrix} \quad (2-52)$$

where in this case the column permutation P is taken to be the identity matrix. The truncated matrix $A_{1\dots p}$ inherits a QR-decomposition from Eq. (2-52) by a corresponding truncation of R :

$$A_{1\dots p} = QR_{1\dots p} \equiv [\hat{Q}_1 : \hat{Q}_2] \begin{bmatrix} (R_1) \\ \hline \dots \\ \hline 0 \end{bmatrix}_{1\dots p}$$

where the matrix Q is the same as in Eq. (2-52) but is repartitioned to be compatible with $(R_1)_{1\dots p}$: $p \times p$. Denoting by q^j the j -th column of Q , it can be seen that

$$\hat{Q}_2 = [q^{p+1} : \dots : q^k : \hat{Q}_2].$$

Using Eq. (2-19) with both Q_2 and \hat{Q}_2 , it follows that:

$$J_{\min}^p = \|\hat{Q}_2^* b\|^2 = \sum_{j=p+1}^k |(q^j)^* b|^2 + \|\hat{Q}_2^* b\|^2 \geq J_{\min}$$

Case B: $k < \min \{n, m\}$. The proof for this case uses the same approach as in Case A, except that Eq. (2-52) is replaced by the decomposition for the rank-deficient case that is a simple extension of Theorem 2-1:

$$A = QR \equiv [Q_1 : Q_2] \begin{bmatrix} R_1 : S \\ \hline \dots \\ \hline 0 \end{bmatrix}$$

The details are omitted. \square

References

- 2-1. Barrett, M.F. and Enns, D.F., "ACOSS-Sixteen (Active Control of Space Structures," Report RADC-TR-82-225, Honeywell Systems and Research Center, Minneapolis, MN, October 1982.
- 2-2. Aubrun, J.N., "ACOSS-Twelve (Active Control of Space Structures)," Report RADC-TR-82-320, Lockheed Missiles and Space Company, Sunnyvale, CA, December 1982.
- 2-3. Aubrun, J.N., et. al., "ACOSS-Five (Active Control of Space Structures) Phase 1A," Report RADC-TR-82-21, Lockheed Missiles and Space Company, Sunnyvale, CA, March 1982.
- 2-4. Hegg, D.R., "A Controlled Experiment for ACOSS Design," ACOSS Eleven Third Interim Technical Report, Vol. 2, Report CSDL-R-1598, Charles Stark Draper Laboratory, Cambridge, MA, December 1982; Section 5.
- 2-5. Fogel, E. et. al., ACOSS Eleven Second Semiannual Technical Report, Vol. 2: Active Controller Designs, Report CSDL-R-1583, Charles Stark Draper Laboratory, Cambridge, MA, August 1982.
- 2-6. Greville, T.N.E., "Some Applications of the Pseudoinverse of a Matrix," SIAM Review, Vol. 2, No. 1, Jan. 1960, pp. 15-22.
- 2-7. Peters, G. and Wilkinson, J.H., "The Least-Squares Problem and Pseudo-Inverses," Computer J., Vol. 13, No. 3, Aug. 1970, pp. 309-316.
- 2-8. Wilkinson, J.H., The Algebraic Eigenvalue Problem, Oxford University Press, Oxford, England, 1965.
- 2-9. Francis, J.G.F., "The QR Transformation: A Unitary Analogue to the LR Transformation--Part 1," Computer J., Vol. 4, No. 3, Oct. 1961, pp. 265-271.
- 2-10. Halmos, P.R., Finite-Dimensional Vector Spaces, Second Edition, Van Nostrand, Princeton, NJ, 1958.

- 2-11. Lawson, C.L. and Hanson, R.J., Solving Least Squares Problems, Prentice-Hall, Englewood Cliffs, NJ, 1974.
- 2-12. Householder, A.S., "Unitary Triangularization of a Nonsymmetric Matrix," J. Assoc. Comput. Mach., Vol. 5, No. 4, 1958, pp. 339-342.
- 2-13. Dongarra, J.J., Moler, C.B., Bunch, J.R., and Stewart, G.W., LINPACK User's Guide, SIAM, Philadelphia, PA, 1979.
- 2-14. Moore, E.H., "On the Reciprocal of the General Algebraic Matrix," Amer. Math. Soc. Bull., Vol. 26, Jun. 1920, pp. 394-395.
- 2-15. Penrose, R., "A Generalized Inverse for Matrices," Proc. Cambridge Philos. Soc., Vol. 51, Jul. 1955, pp. 406-413.
- 2-16. Ben-Israel, A. and Greville, T.N.E., Generalized Inverses: Theory and Applications, Wiley, New York, NY, 1974.
- 2-17. Hegg, D.R., "Output Feedback," Actively Controlled Structures Theory Final Report, Vol. 1, Report R-1338, Charles Stark Draper Laboratory, Cambridge, MA, December 1979; Section 3.
- 2-18. Hegg, D.R., "Design Freedom and the Implementation of Suboptimal Feedback Control," ACOSS-Eleven Semiannual Technical Report, CSDL-R-1536, Charles Stark Draper Laboratory, Cambridge, MA, February 1982; Section 6.
- 2-19. Hardy, G.H., Littlewood, J.E., and Polya, G., Inequalities, Second Edition, Cambridge University Press, Cambridge, England, 1952.
- 2-20. Henderson, T., "Active Control of Space Structures (ACOSS) Model 2," Report C-5437, Charles Stark Draper Laboratory, Cambridge, MA, September 1981.
- 2-21. Henderson, T., "Modifications to ACOSS Model No. 2 Design; Technical Report, Data Base (Final)," Report R-1585, Charles Stark Draper Laboratory, Cambridge, MA, October 1982.
- 2-22. Kwakernaak, H. and Sivan, R., Linear Optimal Control Systems, Wiley, New York, NY, 1972.

Table 2-1. Ranking of modes: disturbance input to open-loop modal RMS LOS-error output; ACOS Model No. 2, Revision 1.

U1 AND U2 TO LOS RANK	HOPE	RHS LOS ERROR (fixed)	RANK	HOPE	RHS LOS ERROR (fixed)	RANK	HOPE	RHS LOS ERROR (fixed)	
7	7	600.974296	87	72	0.065123	107	97	0.000748	
8	6	455.765531	58	82	0.064655	108	140	0.000612	
9	23	105.885663	59	75	0.05773	109	111	0.000571	
10	23	92.645676	60	91	0.049028	119	114	0.000492	
11	22	77.035728	61	69	0.040689	111	126	0.000489	
12	12	72.428174	62	129	0.040623	112	116	0.000360	
13	16	32.469978	63	100	0.035467	113	125	0.000354	
14	14	15.914558	64	132	0.024779	114	32	0.000306	
15	10	12.940235	65	76	0.02838	115	124	0.000304	
16	8	12.220513	66	95	0.021058	116	46	0.000239	
17	9	5.053526	67	93	0.016075	117	122	0.000190	
18	39	5.012726	68	126	0.017055	118	106	0.000162	
19	40	4.267759	69	77	0.015698	119	141	0.000125	
20	55	3.267414	70	98	0.015241	120	134	0.000110	
21	52	3.204134	71	67	0.014756	121	136	0.000053	
22	37	2.521406	72	31	0.014260	122	144	0.000040	
23	34	2.323334	73	105	0.011677	123	44	0.000037	
24	47	2.300195	74	115	0.011131	124	120	0.000037	
25	38	1.933064	75	87	0.010266	125	68	0.000025	
26	62	1.053394	76	123	0.009782	126	137	0.000022	
27	42	1.563806	77	107	0.008331	127	120	0.000017	
28	15	0	1.447236	78	101	0.008063	128	43	0.000009
29	56	1.431284	79	99	0.007360	129	131	0.000007	
30	70	1.258158	80	86	0.007192	130	59	0.000004	
31	48	1.229866	81	74	0.006031	131	135	0.000003	
32	11	0	1.190130	82	68	0.005941	132	58	0.000002
33	30	1.150389	83	99	0.005709	133	57	0.000002	
34	29	1.112429	84	16	0	0.005293	134	145	0.000001
35	63	1.097339	85	121	0	0.005069	135	45	0.000000
36	61	1.060952	86	28	0.0046285	136	143	0.000000	
37	35	1.031477	87	92	0.004263	137	96	0.000000	
38	60	0.017339	88	76	0.004176	138	61	0.000000	
39	49	0.799112	89	133	0.003335	139	142	0.000000	
40	41	0.780077	90	139	0.002958	140	146	0.000000	
41	21	0.720893	91	89	0.002829	141	153	0.000000	
42	64	0.677221	92	104	0.002351	142	152	0.000000	
43	50	0.555752	93	102	0.002338	143	151	0.000000	
44	66	0.549964	94	113	0.002133	144	154	0.000000	
45	54	0.501721	95	136	0.002082	145	155	0.000000	
46	36	0.272236	96	109	0.002076	146	156	0.000000	
47	71	0.251211	97	115	0.002070	147	150	0.000000	
48	20	0.2466074	98	116	0.001752	148	148	0.000000	
49	73	0.230518	99	108	0.001614	149	51	0.000000	
50	65	0.195569	100	112	0.001536	150	27	0.000000	
51	63	0.163532	101	26	0.001427	151	19	0.000000	
52	65	0.117612	102	119	0.001043	152	25	0.000000	
53	17	0.091860	103	127	0.001018	153	80	0.000000	
54	64	0.090553	104	117	0.000954	154	149	0.000000	
55	33	0.065674	105	103	0.000792	155	147	0.000000	
56	79	0.078959	106	53	0.000764	156	94	0.000000	

Table 2-2. Reduced-order models in terms of open-loop undamped characteristic frequencies:

- Interlaced design
- Contiguous design
- Contiguous evaluation

MODE NO.	EIGENVALUE			REAL EIGENVALUES	
		ω_i^2	ω_i (rad/s)	ω_i (Hz)	
1		0.0	0.0	0.0	0.0
2		0.0	0.0	0.0	0.0
3		0.0	0.0	0.0	0.0
4		0.0	0.0	0.0	0.0
5		0.0	0.0	0.0	0.0
6		0.0	0.0	0.0	0.0
7	○	●	■ 8.650672E-01	9.300899E-01	1.480284E-01
8	○	●	■ 3.148905E+00	1.774515E+00	2.824228E-01
9	○	●	■ 4.009007E+00	2.002251E+00	3.186681E-01
10	○	●	■ 4.434997E+00	2.105943E+00	3.351712E-01
11		●	■ 8.638482E+00	2.939130E+00	4.677770E-01
12	○	●	■ 1.344033E+01	3.666106E+00	5.834789E-01
13	○	●	■ 1.424241E+01	3.773911E+00	6.006367E-01
14	○	●	■ 1.790326E+01	4.231224E+00	6.734203E-01
15		●	■ 3.639226E+01	6.032599E+00	9.601181E-01
16	○	●	■ 4.708934E+01	6.862167E+00	1.092148E+00
17		●	■ 1.334769E+02	1.155322E+01	1.838752E+00
18		●	■ 1.341718E+02	1.158326E+01	1.843533E+00
19		●	■ 1.408955E+02	1.186994E+01	1.889159E+00
20		●	■ 1.564057E+02	1.250623E+01	1.990426E+00
21		●	■ 1.675513E+02	1.294416E+01	2.060127E+00
22	○	●	■ 2.372882E+02	1.540416E+01	2.451648E+00
23	○	●	■ 2.412209E+02	1.553129E+01	2.471881E+00
24	○	●	■ 4.149673E+02	2.037074E+01	3.242105E+00
25		■	■ 1.051814E+03	3.243167E+01	5.161660E+00
26		■	■ 1.055404E+03	3.248690E+01	5.170464E+00
27		■	■ 2.449482E+03	4.949223E+01	7.876933E+00
28		■	■ 2.474952E+03	4.974889E+01	7.917781E+00
29		■	■ 3.037863E+03	5.511682E+01	8.772115E+00
30		■	■ 3.040462E+03	5.514038E+01	8.775864E+00
31		■	■ 3.083413E+03	5.552849E+01	8.837633E+00
32		■	■ 3.183598E+03	5.642339E+01	8.900061E+00
33		■	■ 3.653264E+03	6.044223E+01	9.619679E+00
34		■	■ 4.265980E+03	6.531447E+01	1.039512E+01
35		■	■ 5.379633E+03	7.334598E+01	1.167338E+01
36		■	■ 5.939781E+03	7.706998E+01	1.226607E+01
37		■	■ 7.075340E+03	8.411504E+01	1.338732E+01
38		■	■ 7.319027E+03	8.855132E+01	1.361592E+01
39		■	■ 8.614004E+03	9.281166E+01	1.477143E+01
40			1.065900E+04	1.032424E+02	1.643153E+01
41			1.713255E+04	1.308914E+02	2.083200E+01
42			1.874883E+04	1.369264E+02	2.179250E+01
43			1.883882E+04	1.372546E+02	2.184474E+01
44			1.884647E+04	1.372024E+02	2.184917E+01
45			1.884669E+04	1.372832E+02	2.184930E+01
46			1.889893E+04	1.374734E+02	2.187956E+01
47			2.227858E+04	1.492601E+02	2.375548E+01
48			2.364327E+04	1.537637E+02	2.447224E+01
49			2.455703E+04	1.567068E+02	2.494066E+01
50			2.643350E+04	1.625838E+02	2.587601E+01

Table 2-3. Active transducer selection: design example specifications and results.

Example	Design Model	Actuator Candidate Class (\mathcal{A})	Richness	Size of Minimal Selection (p)	Level of Reduction (Δ)
A	Rank 1-11 Interlaced (n = 11)	Axial only ($\mu = 137$)	Sparse	10	1
B	Rank 1-11 Contiguous* (n = 18)	Axial only ($\mu = 137$)	Moderate (-)	14	4
C	Rank 1-11 Contiguous* (n = 18)	Axial and Nodal Translation ($\mu = 311$)	Moderate (+)	12	6
D	Rank 1-11 Contiguous* (n = 18)	Axial and Restricted Nodal Translation ($\mu = 289$)	Very rich	9	9

*Mode 19 excluded from simulation

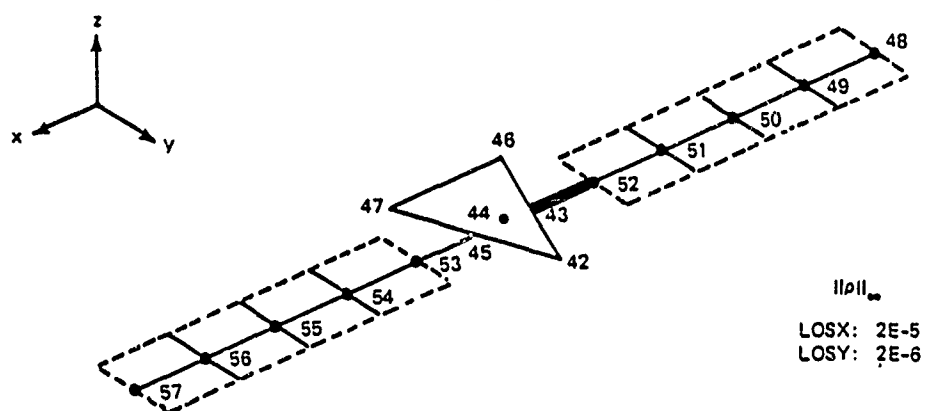
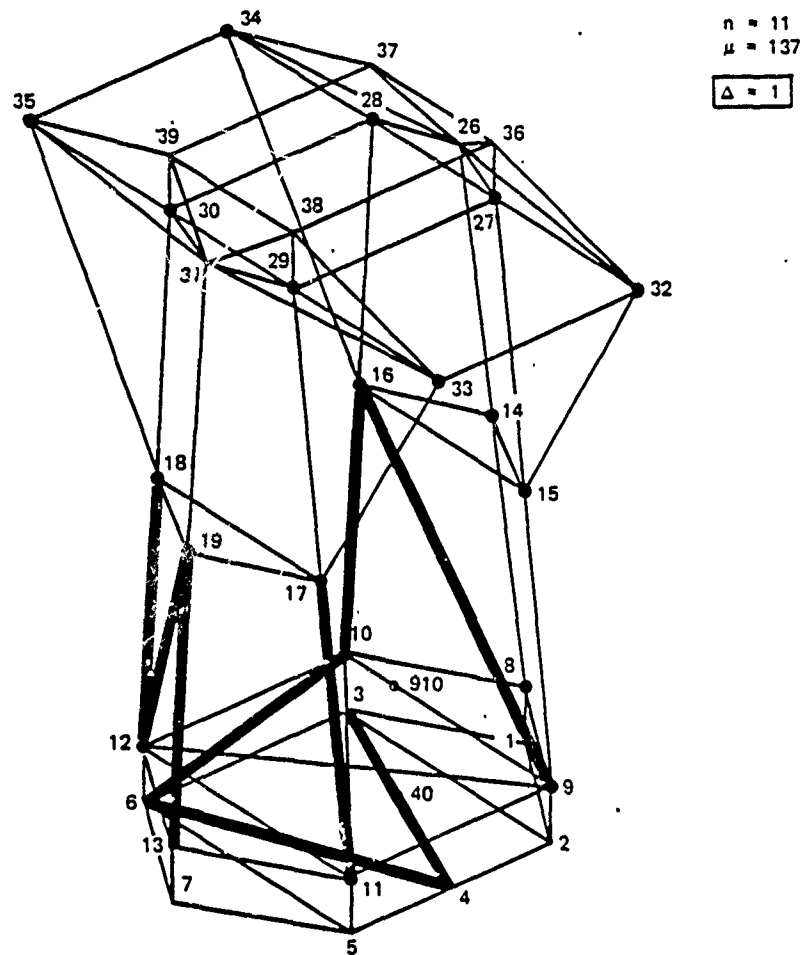


Figure 2-1. Minimal selection, example A.

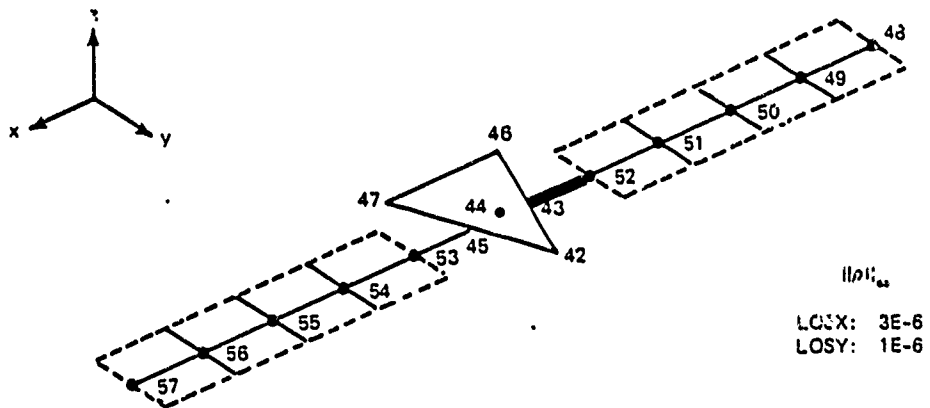
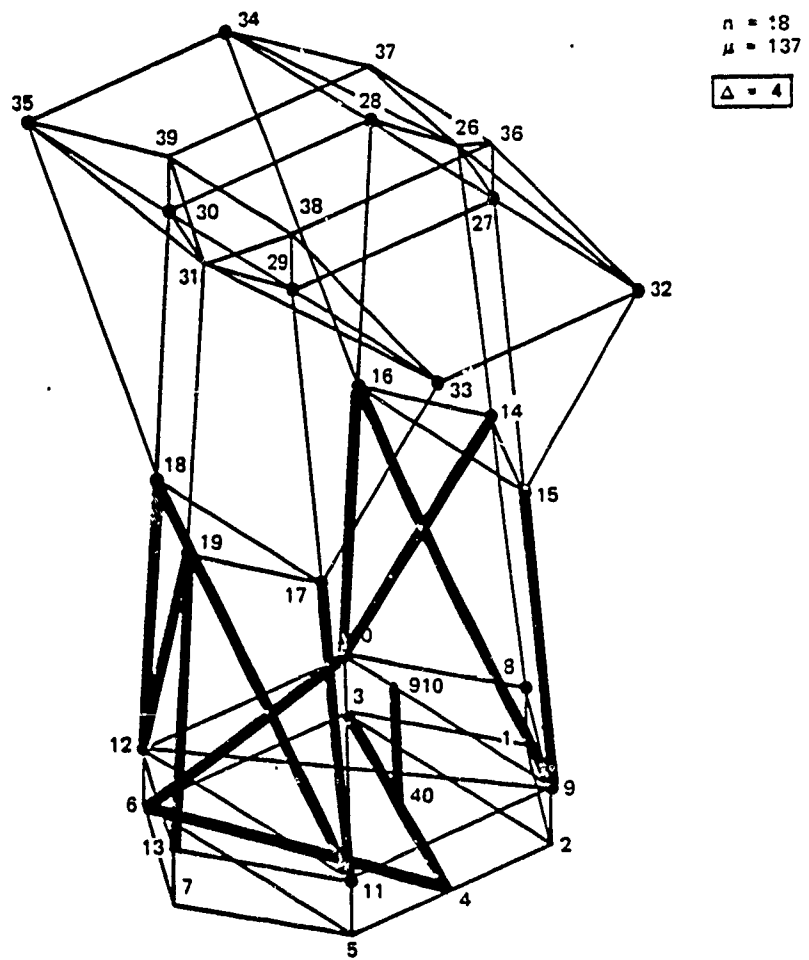


Figure 2-2. Minimal selection, example B.

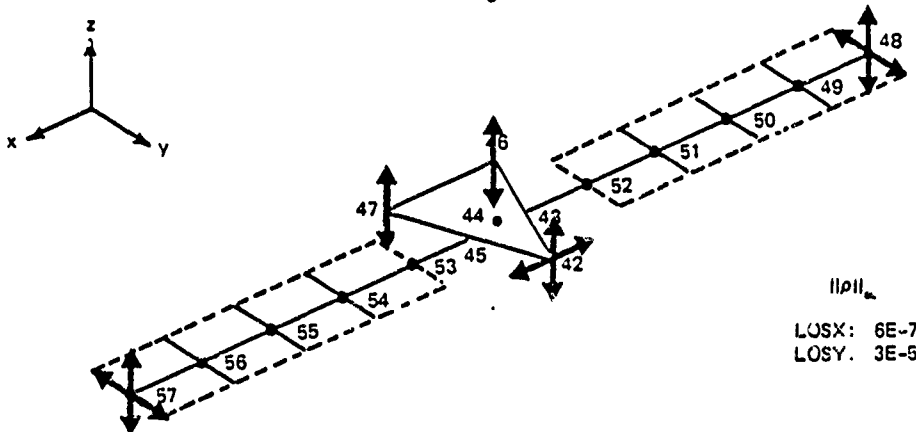
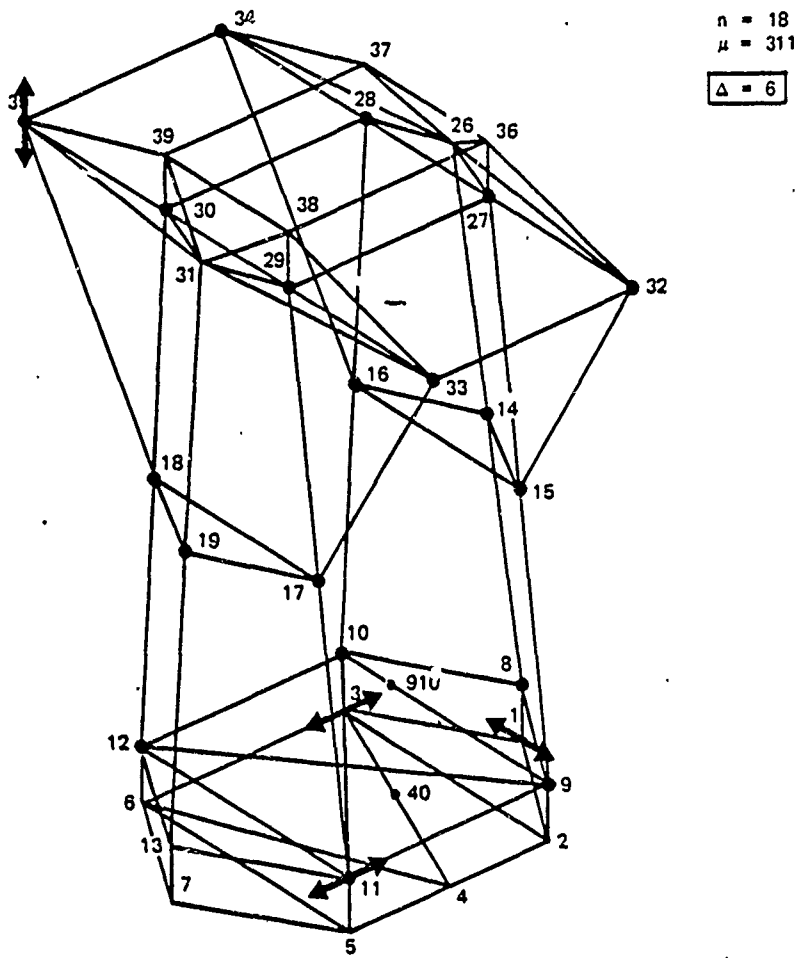


Figure 2-3. Minimal selection, example C.

NO. OF ACTUATORS

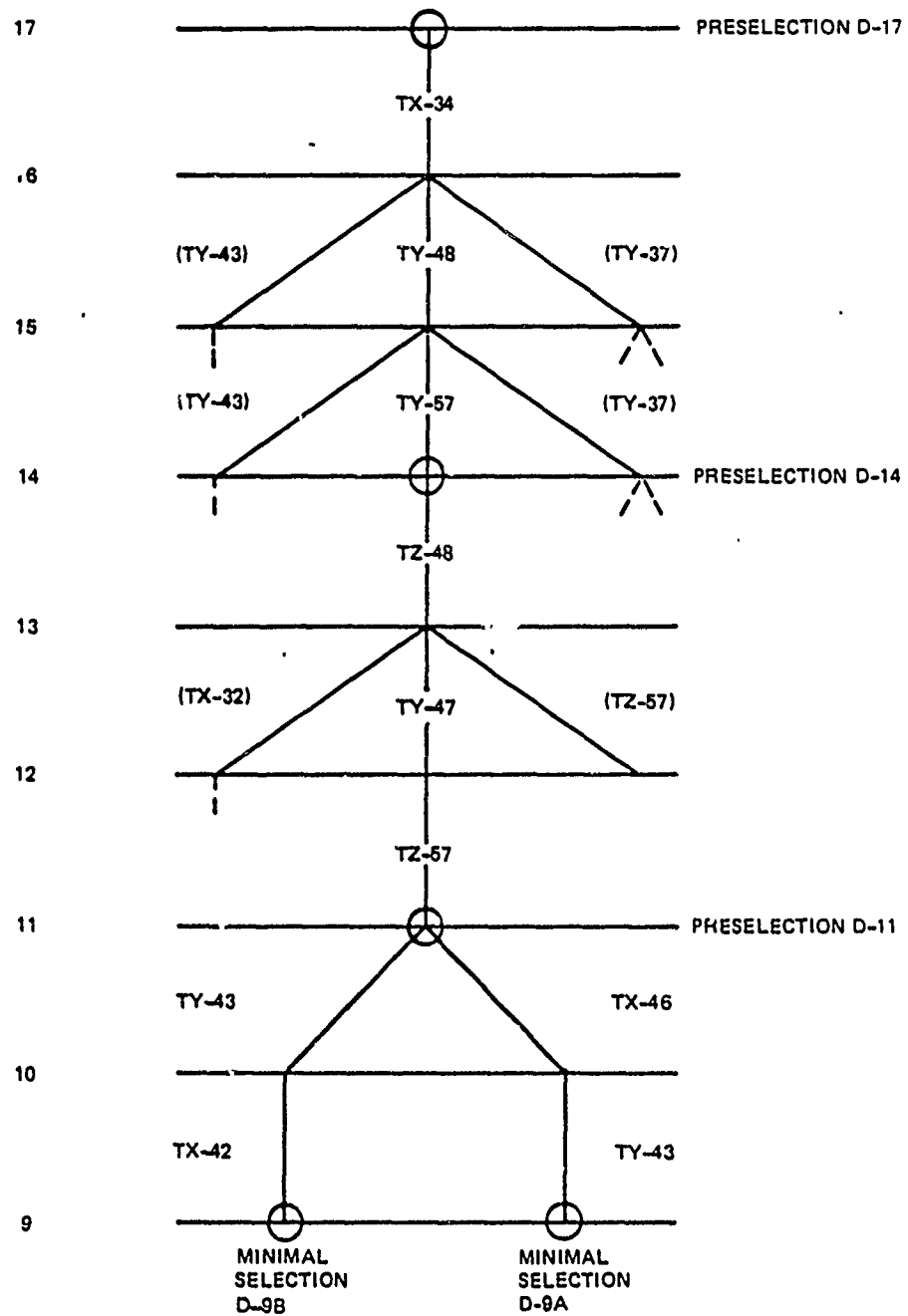


Figure 2-4. Branch of elimination lattice, example D.

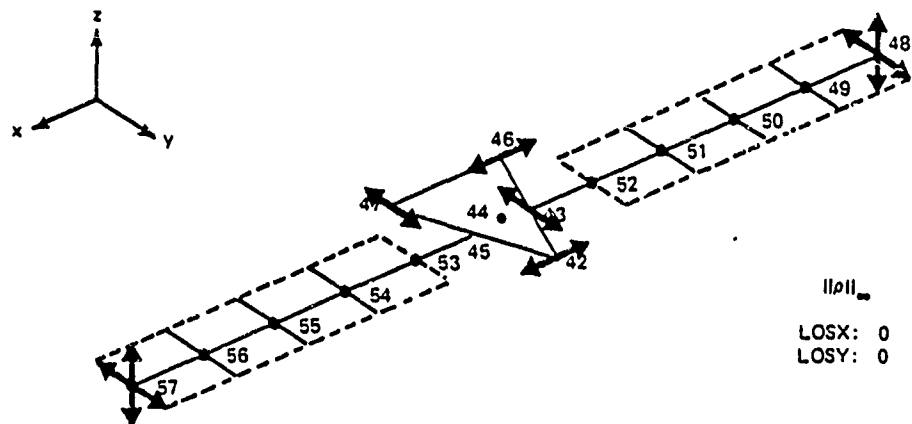
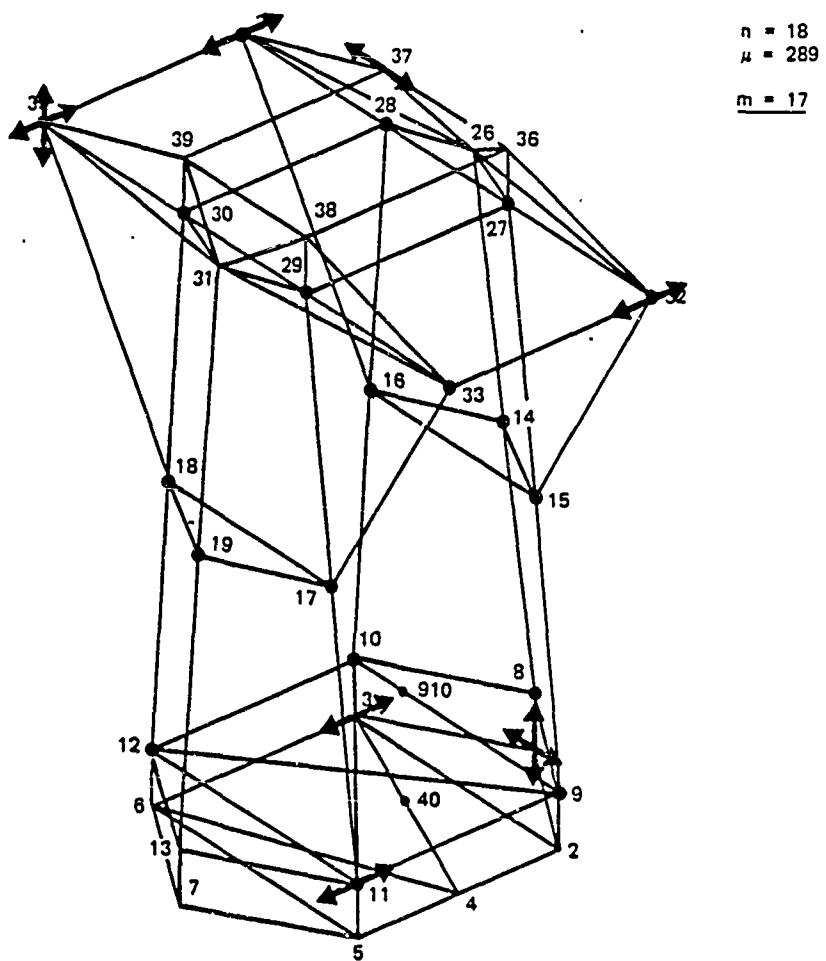


Figure 2-5. Preselection D-17, example D.

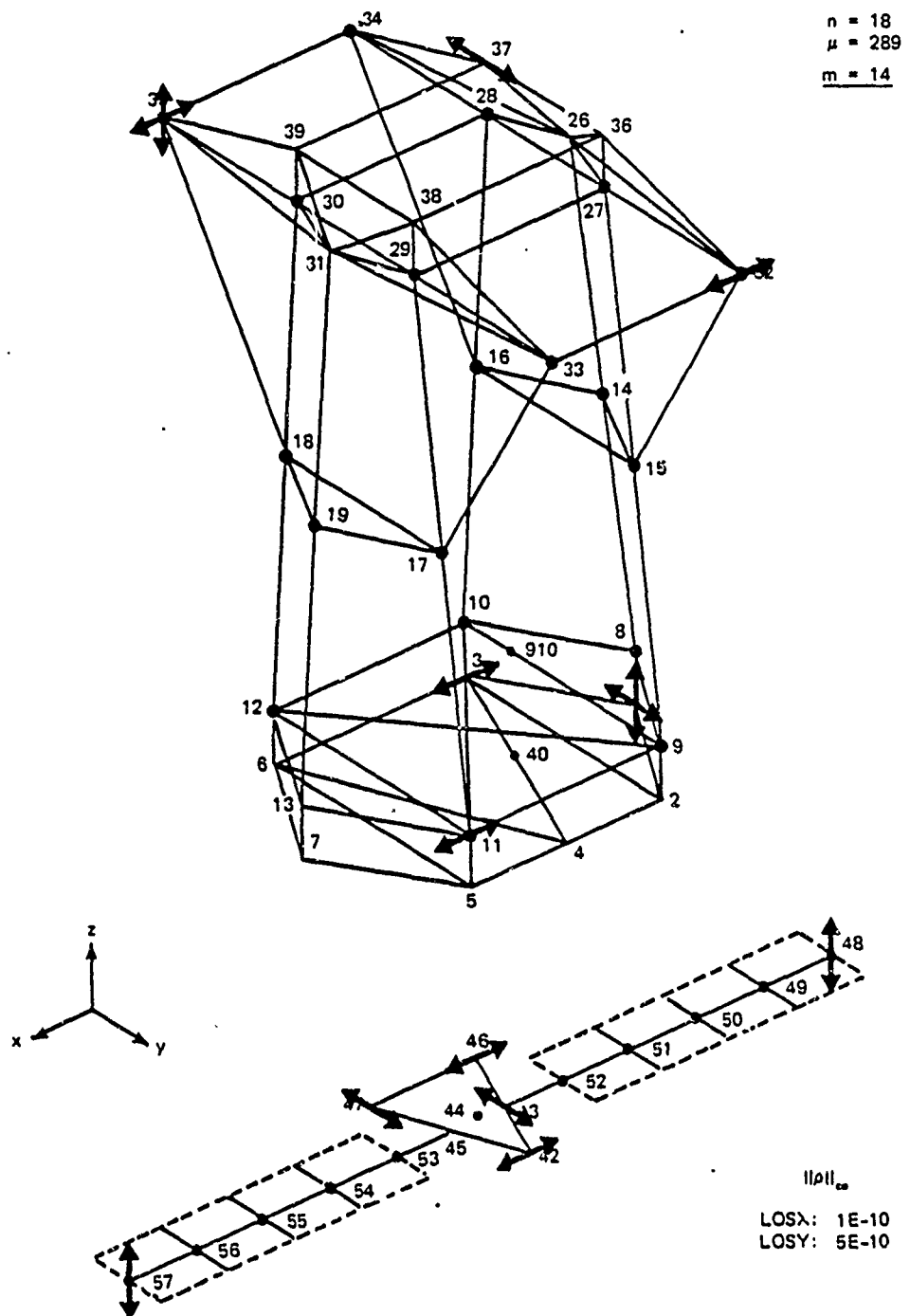


Figure 2-6. Preselection D-14, example D.

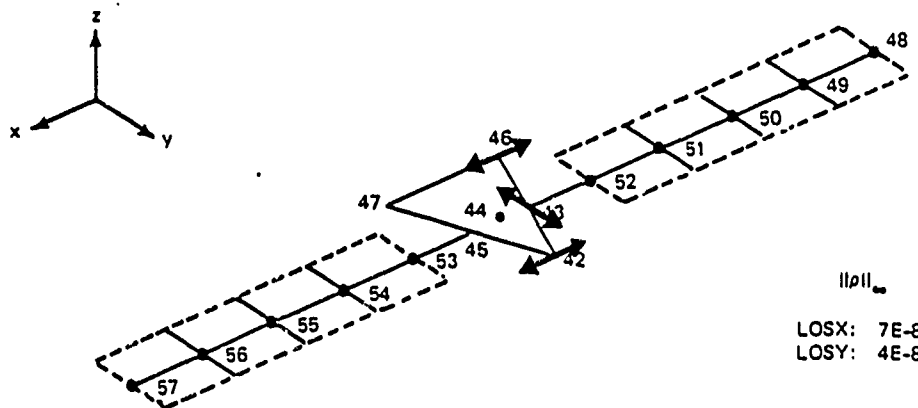
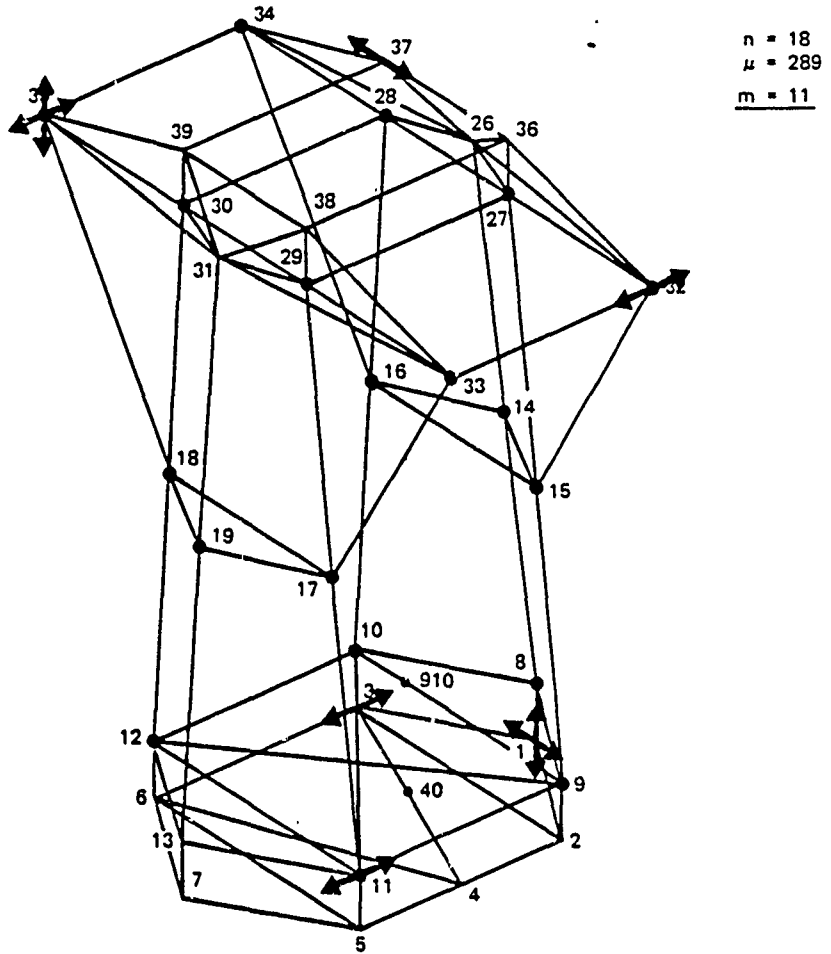


Figure 2-7. Preselection D-11, example D.

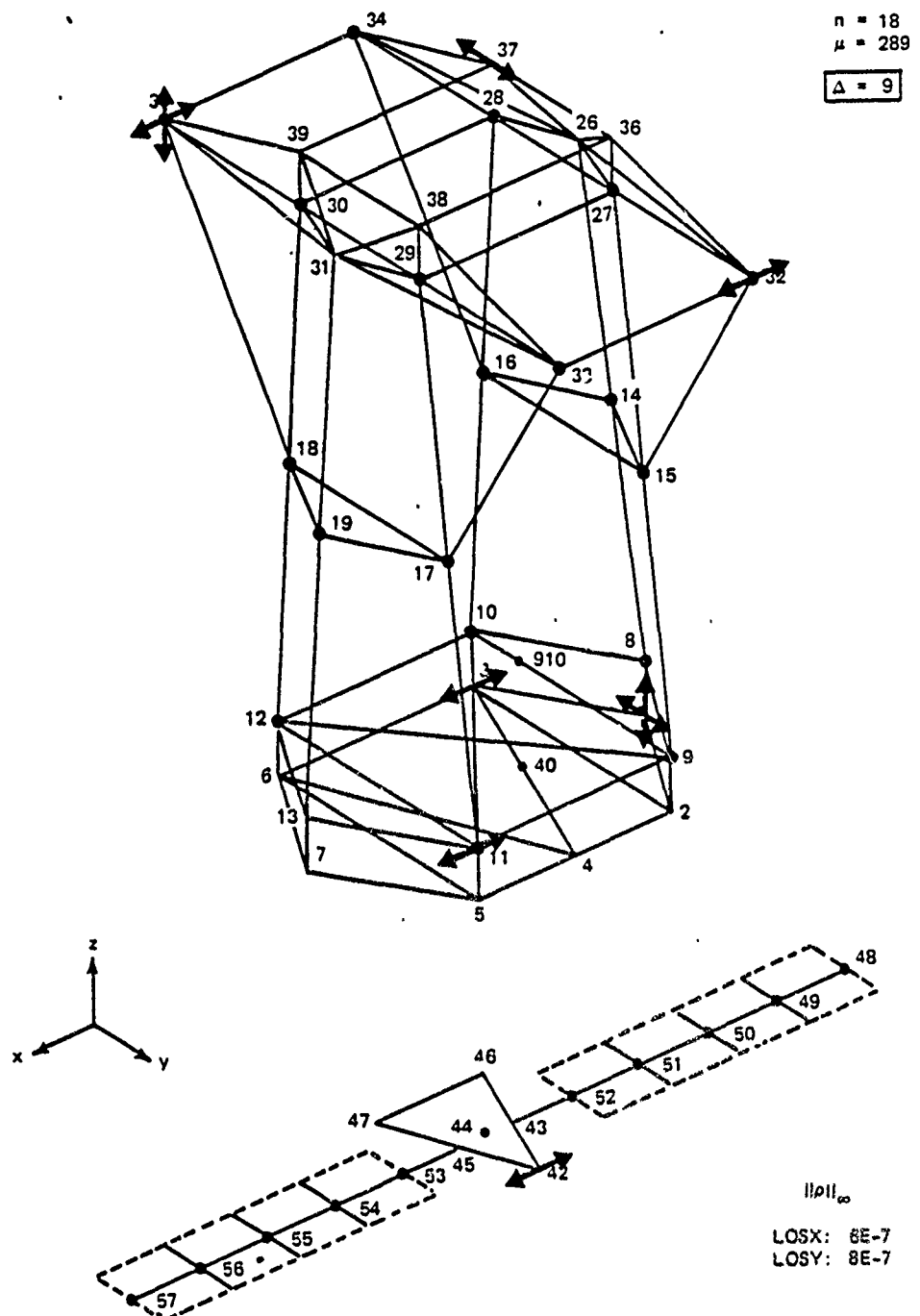


Figure 2-8. Minimal selection D-9A, example D.

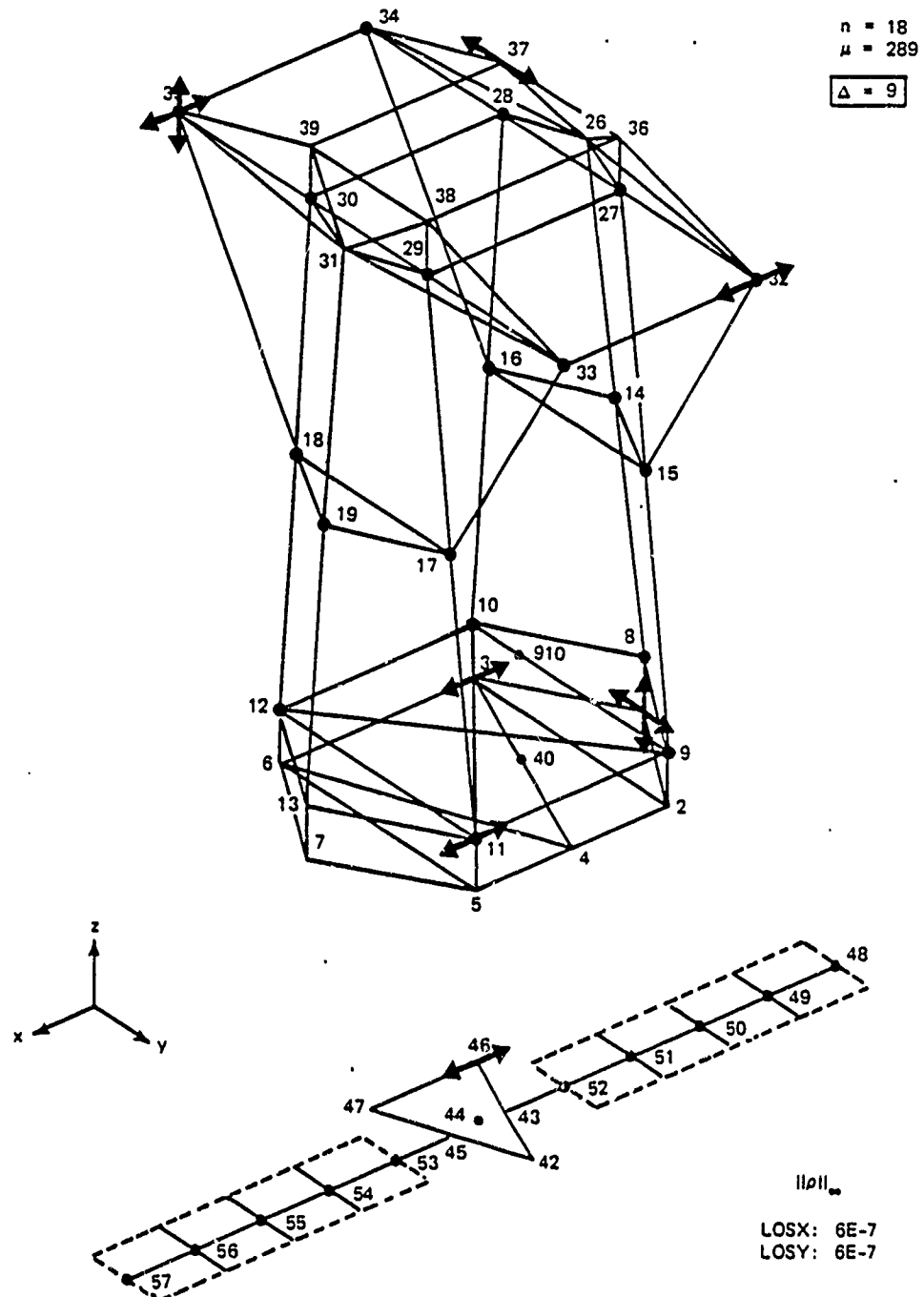


Figure 2-9. Minimal selection D-9B, example D.

SECTION 3

PROGRESS ON SYNTHESIS OF ACTIVE CONTROL FOR BROADBAND DISTURBANCE ACCOMMODATION

PART 2: CONTROL SYSTEM DESIGN AND EVALUATION

3.1 Introduction

The philosophy of our scientific experiment for active control design with ACOSS Model No. 2 was reviewed in the previous section. Now we make use of the 18 mode (modes 7-24) design model from Revision 1 of Model No. 2, and let the several actuator and sensor placements be variables in the experiment.

This section will review the control system design philosophy which remains fixed while working with the various actuator and sensor selections. After the design results are examined, some changes in the controller design will be suggested for the future part of the experiment.

3.2 Control System Design Philosophy

For these designs we have employed the Linear-Quadratic-Gaussian (LQG) methodology, where a model of the disturbance has been augmented with the state equations of the structure. Such a disturbance model uses knowledge of the point of application on the structure and power spectral density of the incoming disturbances. The resulting controller is frequently referred to as a disturbance rejection controller, and has been treated in References 3-1 (Section 4) and 3-2.

To clarify some of the values used here and in the designs of Reference 3-1, we examine the transfer function model for the power spectral density function corresponding to the incoming disturbances as given by Eq. (2-1) of Reference 3-1 (Section 2):

$$S_{xx}(s) = \frac{G \omega_c^2}{\omega_c^2 - s^2}$$

where

$$G = 40 \text{ N}^2 \text{ sec}$$

$$\omega_c = 2\pi f_c$$

$$f_c = 5 \text{ Hz}$$

The corresponding state space representation is (cf. Eq. (2-28))

$$v = B_D u_D$$

where u_D is the solution of

$$\dot{u}_D = A_D u_D + B_D w$$

In particular, v is the disturbance acting on the structure, and B_D , the influence matrix of the disturbances, has been discussed in Section 2 of Reference 3-1. Here

$$A_D = \begin{bmatrix} \lambda_1 & 0 \\ 0 & \lambda_2 \end{bmatrix}$$

where $\lambda_1 = \lambda_2 = -\omega_c = -31.4159$, and

$$B_{\omega} = \begin{bmatrix} b_{\omega 1} & 0 \\ 0 & b_{\omega 2} \end{bmatrix}$$

where $b_{\omega 1} = b_{\omega 2} = \sqrt{G} \omega_c = 198.692$. The above terms are discussed in Section 4 of Reference 3-1, but without noting the numerical values. Also the covariance matrix of the fictitious white noise input vector ω is

$$\text{Cov}(\omega \omega^T) = I_{2 \times 2}$$

Note that the power spectral density function has a bandwidth of 5 Hz and has a zero frequency value of $40 \text{ N}^2/\text{Hz}$ if it is considered to be a two-sided function of frequency, and has a zero frequency value of $80 \text{ N}^2/\text{Hz}$ if it is considered to be a one-sided function of frequency.

Among the controller designs presented in this section for the four actuator/sensor placements, the only parameters that have been altered are the diagonal terms of the 3×3 Q matrix in the performance index for the LQ regulator where,

$$Q = \begin{bmatrix} q_1 & 0 & 0 \\ 0 & q_2 & 0 \\ 0 & 0 & q_3 \end{bmatrix}$$

and q_1 weights the line-of-sight displacements in the x direction (LOSX), q_2 weights the line-of-sight displacements in the y direction (LOSY), and q_3 weights the defocus displacements (Z). In particular, the diagonal terms of the Q matrix are adjusted to ensure that the state feedback portion of each LQG design will meet the line-of-sight (LOS) specifications. These LOS specifications are taken to be:

$$LOSX = \left[\sum_{i=1}^m (U_i - Y_1) \right]^{1/2} \leq 0.05 \text{ } \mu\text{-radians}$$

$$LOSY = \left[\sum_{i=1}^m (U_i - Y_2) \right]^{1/2} \leq 0.05 \text{ } \mu\text{-radians}$$

$$Defocus = Z = \left[\sum_{i=1}^m (U_i - Y_3) \right]^{1/2} \leq 0.025 \times 10^{-3} \text{ meters}$$

where $U_i - Y_j$ represents the mean square value at one of the three line-of-sight outputs resulting from the i -th disturbance. For our designs there are two identical disturbances, one at node 37 and one at node 46 of the model, so m is two in the above LOS specifications.

For all designs the control weighting matrix, R , in the LQ performance index was an identity matrix of appropriate dimension and its scalar factor, ρ_R , was always 1×10^{-17} .

The design of the optimal state estimator is dual to that of the LQ regulator and the covariance of the sensor noise term, θ , was taken to be:

$$\text{Cov}(\theta \theta^T) = \rho_o I_{m \times m}$$

where $\rho_o = 1 \times 10^{-17}$, and m is the number of sensor outputs, as in the designs of Section 4 of Reference 3-1.

The state estimator is connected to the constant LQ gain to form a compensator which, when evaluated with the 18 mode design model of the structure, is guaranteed to yield a stable closed-loop system. Note that Model No. 2 has 132 elastic modes of higher frequency than the 18 modes

used in our design. One goal should be to have a control system robust enough to remain stable in the presence of these 132 high frequency modes, realizing that degradation in LOS performance would occur. Our designs have not achieved that goal at this point in the experiment, but the results, discussed in the next section, are encouraging.

3.3 Controller Results

The results of the control system designs with four of the actuator/sensor selections described in Section 2 are summarized in Table 3-1. The diagonal elements of the Q matrices used in the LQ designs, and the resulting line-of-sight results for the full-state feedback case under the column headed by LQ are shown. Note that the LQ designs with translational actuators/sensors required much lower weighting of the controlled variables (line-of-sight displacements) in the performance index than did the design with axial members, while achieving approximately the same LOS performance.

Not reflected in the table are the design iterations on the Q matrix for each particular actuator/sensor selection that led to acceptable LOS performance. These iterations showed that each Z result was relatively insensitive to changes in its own weighting or the weighting of the other terms. However, an order of magnitude change in the weighting for LOSX or LOSY, namely q_1 or q_2 , from those shown in the table yielded approximately an order of magnitude change in the LOSX or LOSY value.

Recalling that actuator/sensor selection D-9A was a subset of selection D-14, one can note only a slight degradation in the LOS responses between these two for the LQ design.

The original 18 mode LQ design for selection D-9A encountered numerical difficulties when evaluating the poles of its state-feedback design. These numerical difficulties were alleviated when mode 19, which has extremely low control and output influences, was deleted from the design process. Mode 19 was of course included in the evaluation models.

Going to the final column of Table 3-1, one can see that actuator/sensor selection C yielded the largest number of modes in a stable evaluation. The addition of one mode beyond any of the stable evaluations shown in the last column gave an unstable system. Note that selection D-9A, which was a subset of selection D-14, had a much lower stable evaluation model than D-14. In general, taking into account the number of actuators/sensors in each selection, the translational members yielded control systems with superior stability properties compared to the design using axial members.

For the two designs giving the greatest envelope of stability, the LOS results were computed for the LQG compensator evaluated with the 18 mode design model and with a 30 mode evaluation model (modes 7-36). While slight degradation occurred in the LCSX and LOSY results for the LQG compensator evaluated with 18 modes compared to the full-state feedback results in the LQ column, significant degradation in LOS did occur when the LQG compensator was evaluated with modes 7-36.

3.4 Future Controller Designs

As part of the scientific experiment explained in Section 2, changes will be made in the control system design with an eye toward improving the stability results. Specifically, the choice of state and control weighting matrices in the LQ performance index could be altered to lower the multivariable bandwidth. In addition, other frequency shaping techniques may have to be used to ensure adequate high frequency attenuation in the LQ design. Hopefully, in addition, a reasonable disturbance rejection controller design can be found which relies less on explicit knowledge of the disturbances' structural locations and stochastic properties. If a linear quadratic regulator can be designed with some of the improved properties mentioned above, the estimator may have to be designed using "full-state recovery techniques" [Ref. 3-3] to preserve those good features, which otherwise are not guaranteed to hold when an estimator of general design is used in the compensator.

3.5 Conclusion

This section has illustrated the LQG disturbance rejection controller results for four actuator and sensor selections used on ACOSS Model No. 2. These selections were the variables under investigation in the experiment referred to in Section 2. The results indicated that translational actuators and sensors gave superior line-of-sight and stability results when compared to axial actuators and sensors. Changes in the controller design philosophy will be made to improve the stability results in the future part of this experiment.

References

- 3-1. "ACOSS-Eleven Second Semiannual Technical Report, Vol. 2: Active Controller Designs, Report CSDL-R-1583, Charles Stark Draper Laboratory, Cambridge, MA, August 1982.
- 3-2. Kwakernaak, H. and Sivan, R., Linear Optimal Control Systems, Wiley, New York, NY, 1972.
- 3-3. Doyle, J.C. and Stein G., "Multivariable Feedback Design: Concepts for a Classical/Modern Synthesis," IEEE Trans. Automatic Control, Vol. AC-26, No. 1, Feb. 1981, pp. 4-17.

Table 3-1. Controller design results.

Actuator/ Sensor Selection	Weights			LQ (modes 7-24)			LQ (modes 7-24)			LQ (modes 7-36)			Modes in Stable Eval- uation
	q_1	q_2	q_3	LOSX (μ r)	LOSSY (μ r)	Z (10^{-3} m)	LOSSX (μ r)	LOSSY (μ r)	Z (10^{-3} m)	LOSSX (μ r)	LOSSY (μ r)	Z (10^{-3} m)	
B (14 axial)	10^3	10^1	10^{-4}	0.01958	0.01146	0.0041							7-29
C (12 transl.)	10^0	10^{-1}	10^{-5}	0.00532	0.00851	0.00136	0.00644	0.05073	0.00136	31.44	19.16	0.03848	7-39
D-14 (14 transl.)	10^{-1}	10^{-2}	10^{-6}	0.02025	0.03204	0.00188	0.02124	0.06888	0.001883	15.84	9.2	0.01347	7-36
D-9A (9 transl.)	10^{-1}	10^{-2}	10^{-6}	0.0257	0.03317	0.00345							7-29

SECTION 4

SAMPLED DATA CONTROL OF FLEXIBLE STRUCTURES USING NON-COLOCATED VELOCITY FEEDBACK

4.1 Overview

A framework is developed for sampled data control of flexible structures, in terms of discrete time recursive equations in second order form. This framework is used to analyze the sampled data control scheme where the loop is closed using constant gain output velocity feedback. It is well known that the closed loop is stable if colocated velocity feedback with symmetric and positive definite feedback gain is used, so long as the sampling rate is sufficiently high. In this section it is shown that the closed loop can be stabilized using sampled data output velocity feedback for arbitrary sampling rate; our approach is to make use of appropriately defined non-colocated velocity feedback. This approach leads to explicit stability conditions in terms of the feedback gain and the sampling rate.

4.2 Models for Sampled Data Controlled Flexible Structures

A sampled data controlled flexible structure can be defined as a distributed parameter system, where the structure input is the output of an ideal zero order hold and the structure output is sampled. Although distributed parameter models typically involve infinite dimensional variables, our analysis is based on the finite dimensional model

$$M\ddot{q} + Kq = Bu \quad (4-1)$$

For simplicity in the subsequent development no structural damping is included. The structural displacement vector $q = (q_1, \dots, q_n)$ and the force input vector $u = (u_1, \dots, u_m)$. The mass matrix M and the structural stiffness matrix K are assumed symmetric and positive definite. Throughout, we consider velocity output of the form

$$y = Cq \quad (4-2)$$

where the velocity output vector $y = (y_1, \dots, y_m)$. The input influence matrix B and output influence matrix C are assumed to be dimensionless.

The structure input u is defined in terms of the input sequence u_k by the ideal zero order hold relation

$$u(t) = u_k, \quad kT \leq t < kT+T \quad (4-3)$$

The output sequence y_k is defined in terms of the structure output y by the ideal sampling relation

$$y_k = y(kT)$$

The fixed value $T > 0$ is the constant sampling time. This open loop sampled data controlled structure can be viewed as a discrete time system with input sequence u_k and output sequence y_k , where $k = 0, 1, \dots$.

Let ϕ be a $n \times n$ nonsingular modal matrix and let Ω^2 be a $n \times n$ diagonal modal frequency matrix [Ref. 4-1] satisfying

$$\phi^T M \phi = I, \quad \phi^T K \phi = \Omega^2 = \text{diag}(\omega_1^2, \dots, \omega_n^2)$$

Introduce the coordinate change

$$\mathbf{q} = \Phi \eta$$

so that Eqs. (4-1), (4-2) can be written as

$$\ddot{\eta} + \Omega^2 \eta = \Phi^T B u \quad (4-4)$$

$$y = C \Phi \dot{\eta}$$

It is an easy task to solve the vector equation Eq. (4-4), using Eq. (4-3), to obtain

$$\eta_{k+1} = (\cos \Omega T) \eta_k + \Omega^{-1} (\sin \Omega T) \dot{\eta}_k + \Omega^{-2} (I - \cos \Omega T) \Phi^T B u_k \quad (4-5)$$

$$\dot{\eta}_{k+1} = -\Omega (\sin \Omega T) \eta_k + (\cos \Omega T) \dot{\eta}_k + \Omega^{-1} (\sin \Omega T) \Phi^T B u_k \quad (4-6)$$

where $\eta_k = \eta(kT)$, $\dot{\eta}_k = \dot{\eta}(kT)$, and $\sin \Omega T = \text{diag}(\sin(\omega_1 T), \dots, \sin(\omega_n T))$, $\cos \Omega T = \text{diag}(\cos(\omega_1 T), \dots, \cos(\omega_n T))$ [Ref. 4-2].

Although the first order recursive equations Eqs. (4-5), (4-6) could be used, it is more convenient for our purposes to make use of a second order recursive equation in $\dot{\eta}_k$ alone

$$\dot{\eta}_{k+1} - 2(\cos \Omega T) \dot{\eta}_k + \dot{\eta}_{k-1} = \Omega^{-1} (\sin \Omega T) \Phi^T B (u_k - u_{k-1}) \quad (4-7)$$

$$y_k = C \Phi \dot{\eta}_k \quad (4-8)$$

The modal equations Eqs. (4-7), (4-8) form the basis for our subsequent analysis. It is natural to make use of the recursive equation for \dot{n}_k alone in considering velocity feedback systems.

It should be noted that relations Eqs. (4-7), (4-8) involve no numerical approximation; they are valid for any sampling time $T > 0$.

4.3 Constant Gain Velocity Feedback

Constant gain output velocity feedback has been studied extensively for analog controlled structures. Our interest is in use of constant gain output velocity feedback for sampled data controlled structures.

Consider the closed loop sampled data controlled structure defined by Eqs. (4-7) and (4-8), using the control input sequence

$$u_k = -Gy_k \quad (4-9)$$

where G is a constant $m \times m$ feedback gain matrix. Substituting Eq. (4-9) into Eqs. (4-7) and (4-8), a closed loop recursive equation is obtained

$$\begin{aligned} \dot{n}_{k+1} &= [2\cos\Omega T - \Omega^{-1}(\sin\Omega T)\phi^T BGC\phi] \dot{n}_k \\ &+ [I - \Omega^{-1}(\sin\Omega T)\phi^T BGC\phi] \dot{n}_{k-1} = 0 \end{aligned} \quad (4-10)$$

The closed loop characteristic equation can be written as

$$\begin{aligned} d(T, z) &= \det [I - (2\cos\Omega T - \Omega^{-1}(\sin\Omega T)\phi^T BGC\phi)z \\ &\quad \times (I - \Omega^{-1}(\sin\Omega T)\phi^T BGC\phi)] = 0 \end{aligned}$$

The objective of constant gain velocity feedback control is to make the closed loop as described by Eq. (4-10) geometrically stable, i.e., to make the closed loop characteristic zeros lie inside the unit disk.

We use Eq. (4-10) as the basis for our subsequent analysis of the closed loop. If $\sin\Omega T$ is nonsingular, the following implications hold: if $\dot{\eta}_k \rightarrow 0$ as $k \rightarrow \infty$, then necessarily $u_k \rightarrow 0$ as $k \rightarrow \infty$ and $\eta_k \rightarrow 0$ as $k \rightarrow \infty$; consequently $\dot{x}_k \rightarrow 0$ and $x_k \rightarrow 0$ as $k \rightarrow \infty$.

4.4 Colocated Velocity Feedback

Recall the following results for constant gain output velocity analog feedback control where $u = -Gy$. If colocated force actuators and velocity sensors are selected so that $C = B^T$, then the closed loop analog controlled structure is asymptotically stable if G is any symmetric, positive definite matrix, and if a certain controllability assumption is satisfied [Refs. 4-3, 4-4, 4-5]. Moreover, this result does not depend on the particular values of the modal frequencies and modal functions.

We first mention a rather obvious result that if the sampled data feedback control is chosen according to the analog feedback theory, then the closed loop is stable for sufficiently small sampling time. The brief proof is included for completeness; it also serves as an introduction to our subsequent development.

Theorem 4-1. Assume that

- (a) $C = B^T$,
- (b) the matrix pair $(\Omega^2, \phi^T B)$ is completely controllable, and
- (c) G is symmetric and positive definite.

Then the closed loop equation Eq. (4-10) is geometrically stable for sufficiently small sampling time $T > 0$.

Proof. Consider the associated polynomial

$$\begin{aligned} p(T, w) &= \det \left[2(I + \cos \Omega T - \Omega^{-1} (\sin \Omega T) \phi^T B G C \phi) \frac{T^2 w^2}{4} \right. \\ &\quad \left. + 2\Omega^{-1} (\sin \Omega T) \phi^T B G C \phi \frac{T w}{2} + 2(I - \cos \Omega T) \right] \end{aligned} \quad (4-11)$$

By assumption the polynomial defined by

$$\lim_{T \rightarrow 0} p(T, w) \frac{1}{T^2}$$

has all zeros in the left-half-plane; hence there is a number $\bar{T} > 0$ such that $p(T, w)$ has all its zeros in the left-half-plane for $0 < T < \bar{T}$.

Using the bilinear transformation

$$z = \frac{1 + \frac{T w}{2}}{1 - \frac{T w}{2}} \quad (4-12)$$

it follows that the zeros of $d(T, z)$ are necessarily inside the disk; hence Eq. (4-10) is stable. \square

This result has limited application since there is no indication of the range of values of the sampling times, relative to the feedback gain matrix, required for closed loop stability. In Reference 4-6, conditions are developed which, in principle, characterize a range of values of the sampling time for which the closed loop system is stable. Unfortunately, the conditions depend on an a priori computable bound on an exponential matrix; computation of such a bound, in analytical terms, is not considered in Reference 4-6. Of course one could perform a numerical search, based on the characteristic polynomial $d(T, z)$ (or equivalently $p(T, w)$) for a specific case, to determine a range of values

of the sampling time for which the closed loop is stable. However, for the case of colocated velocity feedback there are no known explicit conditions, in terms of the sampling time and feedback gain matrix, which guarantee stability of the closed loop sampled data system.

4.5 Non-colocated Velocity Feedback

We now present the main result of the paper: a set of explicit conditions on the sampling time and feedback gain matrix for which the closed loop sampled data controlled structure is stable. The key idea is to suitably modify the assumption of colocated force actuators and velocity sensors.

Theorem 4-2. Assume that $\sin\Omega T$ is nonsingular and

- (a) $C = B\phi(\sin\Omega T)^{-1}T^{-1}\phi^{-1}$,
- (b) the matrix pair $([I + \cos\Omega T]^{-1}[I - \cos\Omega T], \phi^T B)$ is completely controllable,
- (c) G is symmetric and positive definite, and
- (d) $I + \cos\Omega T - T\phi^T C^T G C \phi$ is positive definite.

Then the closed loop equation Eq. (4-10) is geometrically stable.

Proof. The assumptions can be shown to guarantee that the zeros of $p(T, w)$ defined in Eq. (4-11) are in the left-half-plane. The bilinear transformation defined in Eq. (4-12) guarantees that the zeros of $d(T, z)$ are necessarily inside the unit disk. Hence Eq. (4-10) is stable. \square

Informally, note that as the sampling time satisfies $T \rightarrow 0$ that from condition (a), $C \rightarrow B^T$, and that conditions (b), (c), (d) of Theorem 4-2 tend toward conditions (b), (c) of Theorem 4-1. But for $T > 0$ the extra requirement of condition (d) of Theorem 4-2 is imposed on the feedback gain; this imposes a limit on the "size" of the gain matrix. Condition (a) of Theorem 4-2 implies that the output velocity feedback given by Eq. (4-2) be selected in a specific way. Clearly the actuators and sensors would generally not be colocated.

Conditions (a) and (d) of Theorem 4-2 do depend on explicit knowledge of the modal frequencies and modal functions and they depend on the particular value of the sampling time. Unlike the corresponding analog case, the closed loop, with assumptions of Theorem 4-2 satisfied, is not robust to arbitrary uncertainties in the modal data and to modal truncation. However, an arbitrary structure can be stabilized using sampled data velocity feedback with arbitrary sampling time; the suggested approach depends on a proper choice of force actuator and velocity sensor locations so that condition (a) of Theorem 4-2 is satisfied.

4.6 An Example

As a simple example consider the scalar equations in modal coordinate form with one actuator input

$$\ddot{n}_1 + \omega_1^2 n_1 = u$$

$$\ddot{n}_2 + \omega_2^2 n_2 = u$$

where $\omega_1^2 \neq \omega_2^2$.

Based on Theorem 4-1, the sampled data feedback control

$$u(t) = -G[\dot{n}_1(kT) + \dot{n}_2(kT)], \quad kT \leq t < kT+T,$$

with $G > 0$ and $\omega_i T \neq n\pi$, $n=0,1,\dots$; $i=1,2$ stabilizes the closed loop for $T > 0$ sufficiently small. Even in this simple case analytical conditions on the range of values of the sampling time and the feedback gain for which the closed loop system is stable are exceedingly complicated. Evidently a proper choice of values for the feedback gain and the sampling time would require use of numerical search procedures.

Now consider the sampled data control

$$u(t) = -G \left[\left(\frac{\sin \omega_1 T}{\omega_1 T} \right) \dot{n}_1(kT) + \left(\frac{\sin \omega_2 T}{\omega_2 T} \right) \dot{n}_2(kT) \right], \quad kT \leq t < kT+T,$$

where the output is chosen so that condition (a) of Theorem 4-2 is satisfied; clearly such velocity sensors would not be colocated with the specified force actuators. On the basis of Theorem 4-2 the closed loop is guaranteed to be stable if $\omega_i T \neq n\pi$, $n=0,1,\dots$; $i=1,2$; and if the relatively simple analytical conditions

$$0 < GT < \frac{(\omega_i T)^2 (1 + \cos \omega_i T)}{(\sin \omega_i T)^2}, \quad i=1,2$$

$$0 < GT < \frac{(\omega_1 T)^2 (\omega_2 T)^2 (1 + \cos \omega_1 T) (1 + \cos \omega_2 T)}{(\omega_2 T)^2 (1 + \cos \omega_2 T) (\sin \omega_1 T)^2 + (\omega_1 T)^2 (1 + \cos \omega_1 T) (\sin \omega_2 T)^2}$$

are satisfied. Thus proper choice of values for the feedback gain and the sampling time is considerably simplified.

4.7 Conclusions

We have presented one approach where feedback gains and sampling time can be readily selected to guarantee that the sampled data controlled structure is stable. Our conditions imply that force actuators and velocity sensors be located to satisfy a specific analytical condition which, in fact, depends on the sampling time. These explicit results are in contrast to the lack of available explicit guidelines for choosing the feedback gains and a sampling time in the case where colocated actuators and sensors are used.

References

- 4-1 Bellman, R., Introduction to Matrix Analysis, McGraw-Hill, New York, NY, 1960.
- 4-2 Serbin, S.M., "Rational Approximations of Trigonometric Matrices with Application to Second-Order Systems of Differential Equations," Applied Math. and Computation, Vol. 5, No. 1, Feb. 1979, pp. 75-92.
- 4-3 Walker, J.A. and Schmitendorf, W.E., "A Simple Test for Asymptotic Stability in Partially Dissipative Symmetric Systems," J. Applied Mechanics, Vol. 40, No. 4, Dec. 1973, pp. 1120-1121.
- 4-4 Benhabib, R.J., Iwens, R.P., and Jackson, R.L., "Stability of Large Space Structure Control Systems Using Positivity Concepts," J. Guidance and Control, Vol. 4, No. 5, Sep.-Oct. 1981, pp. 487-494.
- 4-5 Balas, M.J., "Direct Velocity Feedback Control of Large Space Structures," J. Guidance and Control, Vol. 2, No. 3, May-Jun. 1979, pp. 252-253.
- 4-6 Balas, M.J., "Discrete-Time Stability of Continuous-Time Controller Designs for Large Space Structures," J. Guidance and Control, Vol. 5, No. 5, Sep.-Oct. 1982, pp. 541-543.

SECTION 5

OPTIMAL TRACKING AND TERMINAL TRACKING MANEUVERS FOR FLEXIBLE SPACECRAFT

5.1 Introduction

The problem of feedback control of flexible spacecraft undergoing large-angle maneuvers is a topic of continuing interest in the aerospace community. Two types of closed-loop slewing maneuvers are of particular interest. First, tracking maneuvers where the control is determined in such a way as to cause the state to track or follow a desired output state. Second, terminal tracking maneuvers where some elements of the state are required to exactly satisfy nonzero terminal constraints.

The necessary conditions defining the solutions for tracking and terminal tracking problems are well known. Nevertheless, the computational burden required to numerically integrate the resulting systems of coupled nonlinear Riccati-like differential equations has seriously hindered the common application of these control techniques.

To overcome the computational difficulties noted above, closed form solutions are presented for the necessary conditions defining the solutions for the following linear time-invariant control problems:

- (a) The linear tracking problem;
- (b) The terminal tracking problem;
- (c) The state trajectories for the conventional closed-loop system dynamics equation.

The remainder of the section is presented in three parts. Section 5.2 presents closed form solutions for the Riccati and prefilter

equations of the linear tracking problem. Maneuver simulations are presented for both conventional and control-rate-penalty control designs [Refs. 5-1, 5-2]. Section 5.3 presents closed form solutions for the three nonlinear coupled Riccati-like differential equations, defining the solution for the terminal control problem. Maneuver simulations are presented for both conventional and control-rate-penalty control designs. Section 5.4 presents a closed form solution for the state trajectories of a conventional feedback control system, when the plant and the state are assumed to be perfectly known. The solution for the state is presented in a simple recursive form.

5.2 Closed Form Solution for the Linear Tracking Problem

In this subsection the problem of maneuvering a flexible spacecraft through a large angle is considered, where the feedback control system is required to track a desired output state. The desired output state is assumed to be provided from an open-loop solution for the linear time invariant system model (see References 5-1 and 5-2 for examples of suitable open-loop solutions).

The optimal control problem of this section is formulated by defining a performance index which consists of an integral of quadratic forms in the state, control, and control-rate. The necessary conditions for this problem lead to two nonlinear Riccati-like differential equations [Ref. 5-6]. One equation is the standard Riccati equation, which possesses a well-known solution in terms of a steady-state plus transient term [Ref. 5-1]. The remaining vector equation is a prefilter equation which has foreknowledge of the desired output state, and is coupled to the standard Riccati equation. In Section 5.2.4, a new closed form solution is presented for the auxiliary Riccati-like vector equation.

5.2.1 Optimal Linear Tracking Problem

The optimal reference tracking problem is formulated by finding the control inputs $u(t)$ to minimize

$$J = \frac{1}{2} \|z^*(t_f) - z(t_f)\|_S^2 + \frac{1}{2} \int_{t_0}^{t_f} [\|z^*(t) - z(t)\|_Q^2 + \|u(t)\|_R^2] dt \quad (5-1)$$

for the system

$$\dot{x} = Ax + Bu, \quad x(t_0) = x_0 \quad (5-2)$$

$$z = Cx \quad (5-3)$$

where $\|p\|_W = p^T W p$, z^* is the desired output state, A is the system dynamics matrix, B is the control influence matrix, C is the measurement influence matrix, S is the terminal state weight matrix, Q is the state weight matrix, R is the control weight matrix, x is the state, and u is the control. (For maneuvers where the state is augmented by the control and control-rate penalties, the A and B matrices of Eq. (5-2) are modified as shown in Reference 5-1).

5.2.1.1 The Open-Loop Control Problem for the Desired Output State

The desired output state, $z^*(t)$, in Eq. (5-1) is assumed to be provided by the solution for the following open-loop control problem, where we seek the control inputs $u^*(t)$ to minimize

$$J^* = \frac{1}{2} \int_{t_0}^{t_f} [\|x^*(t)\|_{Q^*}^2 + \|u^*(t)\|_{R^*}^2] dt \quad (5-4)$$

for the system

$$\begin{aligned}\dot{x}^* &= Ax^* + Bu^*, & x^*(t_0) &= x_0^*, & x^*(t_f) &= x_f^* \\ z^* &= Cx^*\end{aligned}\quad (5-5)$$

As shown in Reference 5-2, the closed form solution for the open-loop problem defined by Eqs. (5-4) and (5-5) can be written as

$$\begin{Bmatrix} x^*(t) \\ \lambda^*(t) \end{Bmatrix} = e^{\Omega(t-t_0)} \begin{Bmatrix} x_0^* \\ \lambda_0^* \end{Bmatrix} \quad (5-6)$$

where

$$\Omega = \begin{bmatrix} A & -B(R^*)^{-1}B^T \\ -Q^* & -A^T \end{bmatrix}, \quad (5-7)$$

$$\lambda_0^* = \begin{pmatrix} \phi_{x^*x^*} \\ \phi_{x^*\lambda^*} \end{pmatrix}^{-1} \left\{ x_f^* - \phi_{x^*x^*} x_0^* \right\}, \quad (5-8)$$

$e^{(\cdot)}$ = the exponential matrix,

$\lambda^*(t)$ = the costate vector for the open-loop solution,

and $\phi_{x^*x^*}$, $\phi_{x^*\lambda^*}$ are partitions of $e^{(\cdot)}$ for $t=t_f$.

To obtain $x^*(t)$ from Eq. (5-6), the following mapping equation is defined:

$$x^*(t) = H e^{\Omega(t-t_0)} \begin{Bmatrix} x_0^* \\ \lambda_0^* \end{Bmatrix} \quad (5-9)$$

where $H = [I \ 0]$ is a $(n \times 2n)$ selection operator and x^* is $(n \times 1)$.

As shown in what follows, the explicit presence of $e^{(\cdot)}$ in Eq. (5-9) permits a closed form solution to be obtained for the prefilter equation of the linear tracking problem.

5.2.2 Necessary Conditions for the Linear Tracking Problem

The necessary conditions defining the optimal tracking problem for Eqs. (5-1), (5-2), and (5-3) are given by the following Riccati-like differential equations [Ref. (5-3), pp. 100-102]:

$$\dot{P} = -PA - A^T P + PBR^{-1}B^T P - C^T Q C \quad ; \quad P(t_f) = C^T S C \quad (5-10)$$

$$\dot{\xi} = -[A - BR^{-1}B^T P]^T \xi - C^T Q C x^* \quad ; \quad \xi(t_f) = C^T S C x^*(t_f) \quad (5-11)$$

where the optimal control is given by

$$u = -R^{-1}B^T[Px - \xi] \quad (5-12)$$

5.2.3 Closed Form Solution for the Time-Varying Riccati Equation

The solution for Eq. (5-10) has been previously obtained in References 5-2 and 5-4, and can be written as

$$P(t) = P_{ss} + \Theta^{-1}(t) \quad (5-13)$$

where P_{ss} is the solution for the algebraic Riccati equation

$$-P_{ss}A - A^TP_{ss} + P_{ss}B R^{-1} B^T P_{ss} - C^T Q C = 0 \quad (5-14)$$

and the closed form solution for $\theta(t)$ can be shown to be

$$\theta(t) = \theta_{ss} + e^{\tilde{A}(t-t_f)} [\theta_f - \theta_{ss}] e^{\tilde{A}^T(t-t_f)} \quad (5-15)$$

where $\tilde{A} = A - B R^{-1} B^T P_{ss}$, $\theta_f = (C^T S C - P_{ss})^{-1}$, and θ_{ss} satisfies the algebraic Lyapunov equation

$$\tilde{A}\theta_{ss} + \theta_{ss}\tilde{A}^T = B R^{-1} B^T \quad (5-16)$$

5.2.4 Closed Form Solution for the Prefilter Equation

The solution for ξ in Eq. (5-11), follows on assuming the product form solution

$$\xi(t) = \theta^{-1}(t) r(t) \quad (5-17)$$

where θ is defined by Eq. (5-15) and the linear constant coefficient vector differential equation for r can be shown to be

$$\dot{r} - \tilde{A}r = -\theta C^T Q C x^* \quad , \quad r(t_f) = \theta_f C^T S C x^*(t_f) \quad (5-18)$$

(To derive Eq. (5-18) one requires the differential equation for θ given by: $\dot{\theta} = \tilde{A}\theta + \theta \tilde{A}^T - B R^{-1} B^T$).

The solution for r in Eq. (5-18) can be shown to be

$$r(t) = e^{\tilde{A}t} [r_0 - \int_0^t e^{-\tilde{A}\tau} \theta(\tau) C^T Q C x^*(\tau) d\tau] \quad (5-19)$$

where the initial condition for the vector r is given by

$$r_o = e^{-\bar{A}t_f} \theta_f C^T S C x^*(t_f) + \int_0^{t_f} e^{-\bar{A}\tau} \theta(\tau) C^T Q C x^*(\tau) d\tau \quad (5-20)$$

The solution for the integral expression in Eq. (5-19) follows on introducing $\theta(t)$ from Eq. (5-15) and $x^*(t)$ from Eq. (5-9) into Eq. (5-19), leading to

$$\int_0^t e^{-\bar{A}\tau} \theta(\tau) C^T Q C x^*(\tau) d\tau = \left[\begin{array}{l} \int_0^t e^{-\bar{A}\tau} D_1 e^{\Omega\tau} d\tau \\ D_2 \int_0^t e^{-\bar{A}\tau} D_3 e^{\Omega\tau} d\tau \end{array} \right] \left\{ \begin{array}{l} x_o^* \\ \lambda_o^* \end{array} \right\} \quad (5-21)$$

where

$$D_1 = \theta_{ss} C^T Q C H \quad (5-22)$$

$$D_2 = e^{-\bar{A}t_f} [\theta_f - \theta_{ss}] e^{-\bar{A}^T t_f} \quad (5-23)$$

$$D_3 = C^T Q C H \quad (5-24)$$

As shown in Reference 5-5, the integrals involving the matrix exponentials in Eq. (5-21) can be easily evaluated by defining the constant matrices

$$C_1 = \begin{bmatrix} \bar{A} & D_1 \\ 0 & \Omega \end{bmatrix}, \quad C_2 = \begin{bmatrix} -\bar{A}^T & D_3 \\ 0 & \Omega \end{bmatrix}$$

and computing the matrix exponentials

$$e^{C_1 t} = \begin{bmatrix} F_1(t) & G_1(t) \\ 0 & F_2(t) \end{bmatrix}, \quad e^{C_2 t} = \begin{bmatrix} F_3(t) & G_2(t) \\ 0 & F_4(t) \end{bmatrix}$$

where

$$F_1(t) = e^{\tilde{A}t}, \quad F_2(t) = F_4(t) = e^{\Omega t}, \quad F_3(t) = e^{-\tilde{A}^T t}$$

$$G_1(t) = e^{\tilde{A}t} \int_0^t e^{-\tilde{A}\tau} D_1 e^{\Omega\tau} d\tau, \quad G_2(t) = e^{-\tilde{A}^T t} \int_0^t e^{\tilde{A}^T \tau} D_3 e^{\Omega\tau} d\tau$$

As a result, it follows that the integrals in Eq. (5-21) are given by

$$\int_0^t e^{-\tilde{A}\tau} D_1 e^{\Omega\tau} d\tau = F_3^T(t) G_1(t) \quad (5-25)$$

$$\int_0^t e^{\tilde{A}^T \tau} D_3 e^{\Omega\tau} d\tau = F_1^T(t) G_2(t) \quad (5-26)$$

5.2.4.1 Recursion Relationships for the Integrals of Exponential Matrices

In order to evaluate Eqs. (5-25) and (5-26) at discrete time steps, the semi-group properties of exponential matrices are now exploited; yielding the following recursion relationships for the matrix partitions of $e^{C_1(n+1)\Delta t}$ and $e^{C_2(n+1)\Delta t}$:

$$F_j [(n+1)\Delta t] = F_j(\Delta t) F_j(n\Delta t) , \quad F_j(0) = I , \quad j = 1, 2, 3, 4$$

$$G_1 [(n+1)\Delta t] = F_1(\Delta t) G_1(n\Delta t) + G_1(\Delta t) F_2(n\Delta t) , \quad G_1(0) = 0$$

$$G_2 [(n+1)\Delta t] = F_3(\Delta t) G_2(n\Delta t) + G_2(\Delta t) F_2(n\Delta t) , \quad G_2(0) = 0$$

from which the integrals of Eq. (5-25) and (5-26) follow as

$$\int_0^{(n+1)\Delta t} e^{-\tilde{A}\tau} D_1 e^{\tilde{Q}\tau} d\tau = F_3^T [(n+1)\Delta t] G_1 [(n+1)\Delta t] \quad (5-27)$$

$$\int_0^{(n+1)\Delta t} e^{-\tilde{A}^T \tau} D_3 e^{\tilde{Q}\tau} d\tau = F_1^T [(n+1)\Delta t] G_2 [(n+1)\Delta t] \quad (5-28)$$

where $\Delta t = (t_f - t_0)/m$ and m is the total number of discrete time steps.

5.2.4.2 Vector Recursion Relationships for $x[(n+1)\Delta t]$

Substituting Eq. (5-27) and (5-28) into Eq. (5-21), yields

$$\int_0^{(n+1)\Delta t} e^{-\tilde{A}\tau} \Theta(\tau) C^T Q C x^*(\tau) d\tau =$$

$$= F_3^T [(n+1)\Delta t] G_1 [(n+1)\Delta t] s_0$$

$$+ D_2 F_1^T [(n+1)\Delta t] G_2 [(n+1)\Delta t] s_0$$

or

$$= F_3^T[(n+1)\Delta t] \{F_1(\Delta t)G_1(n\Delta t) + G_1(\Delta t)F_2(n\Delta t)\} s_o$$

$$+ D_3 F_1^T[(n+1)\Delta t] \{F_3(\Delta t)G_2(n\Delta t) + G_2(\Delta t)F_2(n\Delta t)\} s_o$$

$$\text{where } s_o^T = [(x_o^*)^T \ (\lambda_o^*)^T]$$

The number of mathematical operations required in the equation above can be minimized by defining the following three vector functions and associated recursion relationships:

$$x_1[(n+1)\Delta t] = G_1[(n+1)\Delta t] s_o = F_1(\Delta t)x_1(n\Delta t) + G_1(\Delta t)x_3(n\Delta t); x_1(0) = 0$$

$$x_2[(n+1)\Delta t] = G_2[(n+1)\Delta t] s_o = F_3(\Delta t)x_2(n\Delta t) + G_2(\Delta t)x_3(n\Delta t); x_2(0) = 0$$

$$x_3[(n+1)\Delta t] = F_2[(n+1)\Delta t] s_o = F_2(\Delta t)x_3(n\Delta t); x_3(0) = s_o$$

As a result, the recursive expression for the integral in Eq. (5-19), can be written as

$$\int_0^{(n+1)\Delta t} e^{-\tilde{A}\tau} \theta(\tau) C^T Q C x^*(\tau) d\tau = F_3^T[(n+1)\Delta t] x_1[(n+1)\Delta t]$$

$$+ D_3 F_1^T[(n+1)\Delta t] x_2[(n+1)\Delta t]$$

where the recursion relationships for the matrix partitions $G_1[(n+1)\Delta t]$ and $G_2[(n+1)\Delta t]$ have been replaced by the vector recursion relationships for $x_1[(n+1)\Delta t]$, $x_2[(n+1)\Delta t]$, and $x_3[(n+1)\Delta t]$.

5.2.4.3 Recursion Relationship for $\Theta[(n+1)\Delta t]$

Subject to the recursion relationships above, the time histories for P and ξ in Eq. (5-12) easily follow, where $\Theta[(n+1)\Delta t]$ in Eq. (5-15) is given by

$$\Theta[(n+1)\Delta t] = \Theta_{ss} + F_1(\Delta t) [\Theta(n\Delta t) - \Theta_{ss}] F_1^T(\Delta t)$$

and

$$\Theta(0) = \Theta_{ss} + F_3^T(t_f) [\Theta_f - \Theta_{ss}] F_3(t_f)$$

5.2.5 Illustrative Examples

The specific model considered in this section (see Figs. 5-1 and 5-2) consists of a rigid hub with four identical elastic appendages attached symmetrically about the central hub. In particular, the following idealizations are considered: (i) single-axis maneuvers; (ii) in-plane motion; (iii) anti-symmetric deformations; (iv) small linear flexural deformations; (v) only the linear time-invariant form of the equation of motion is considered; and (vi) the control actuators are modelled as concentrated torque generating devices. The distributed control system for the vehicle consists of: (i) a single controller in the rigid part of the structure, and (ii) a single controller in each elastic appendage. In the optimal control performance index, however, the control weighting matrices are adjusted in order to have the rigid body control provide the primary torque for maneuvering the vehicle, while the appendage controllers act principally as vibrational suppressors.

For all cases, the following configuration parameters are assumed: the moment of inertia of the undeformed structure about the spin axis, I , is 6764 kg-m^2 ; the mass/length ratio of the four identical elastic appendages, ρ , is 0.04096 kg/m ; the length of each cantilevered appendage, L , is 35 m ; the flexural rigidity of each cantilevered

appendage, EI , is $1500 \text{ kg-m}^3/\text{s}^2$; and the radius of the rigid hub, r , is 1 m. For simplicity, each appendage is assumed to have one controller located half-way along its span. In the integrations over the mass and stiffness distributions, the radius of the hub is not neglected in comparison to the appendage length. In the structural modeling equations, the following comparison functions have been adopted as "assumed modes"

$$\phi_p(x-r) = 1 - \cos[p\pi(x-r)/L] + 0.5(-1)^{p+1} [p\pi(x-r)/L]^2 \quad (p = 1, 2, \dots, n) \quad (5-29)$$

which satisfy the geometric and physical boundary conditions.

$$\phi_p|_{x=r} = \phi'_p|_{x=r} = \phi''_p|_{x=r+L} = \phi'''_p|_{x=r+L} = 0 \quad (5-30)$$

of a clamped free appendage, where $(*)' = d(*)/dx$. In addition, full state feedback is assumed for the results of this section.

The output vector is assumed to be given by

$$y = \{y_1 \ y_2^T \ y_3 \ y_4 \ y_5^T\}^T \quad (5-31)$$

where

y_1 = central hub angular velocity

y_2 = four times the angular velocity at each appendage controller location relative to the central hub

y_3 = hub angular position

y_4 = four times the tip deflection of each appendage

y_5 = controls and control-rates

The number of elements in y_2 is given by the number of controllers on each of the four appendages. The output sub-vector y_5 exists when control-rates are penalized. The elements of y_5 correspond to the additionally augmented states.

Referring to Tables 5-1a and 5-2, the graphical summaries of the states and controls are discussed qualitatively in what follows.

Case 1 (Fig. 5-3) presents a terminal controller example maneuver in which two flexible modes are controlled in addition to the rigid body rotation. There are six states in this problem, all of which are specified at the final time. The time histories for this case are virtually identical to the results obtained from an open-loop controller using the same weight matrices in the performance index. The jump discontinuities in the control torques at the initial and final times are characteristic of controllers with no penalties on the control-rates in the performance index. As shown in Reference 5-1, the presence of these discontinuities tends to excite both modeled and unmodeled high frequency structural modes.

Case 2 (Fig. 5-4) presents the same maneuver as in Case 1, except that the performance index now includes penalties on the first and second time derivatives of the control torques [Ref. 5-2]. Including these penalties allows the control torques and torque-rates to be specified at the initial and final times, thereby eliminating the terminal jump discontinuities in the control profiles. For this particular control problem, the states are augmented to include the control and first time-derivative of the control, while the second time-derivative of the control becomes the commanded input to the augmented system. On comparing with the results of Case 1, one finds much smoother modal amplitude and control torque time histories, although the peak torques and tip deflection are somewhat higher than those in Case 1.

Case 3 (Fig. 5-5) presents the results of a spin-to-rest maneuver in which the weight matrices and final conditions are identical with those of Case 2. The initial conditions are different from those in Case 2, but the time-varying feedback gains are identical. As the plots in Figure 5-7 show, the terminal controller has little difficulty in bringing the system to the required final conditions.

Case 4 (Fig. 5-6) presents the results of a spin-to-rest maneuver where off-nominal plant parameters are used. In particular, the moment of inertias for the hub and appendages are increased by 10% and the appendage mass per unit length is decreased by 10%, while the time-varying feedback gains are computed using the nominal structural parameters. Although the structural parameters are changed by only 10%, the overall effect on the entire structure is quite large. Specifically, the first and second mode eigenvalues, ω^2 , are increased by 16% and 22% respectively, while the ratio of the hub moment of inertia to appendage moment of inertia is increased by 22%. Nevertheless, the plots show that most of the state variables reach their prescribed terminal boundary conditions.

In Cases 1 through 4 the results have been compared with the corresponding open-loop maneuvers, and have been found to be identical within plotting accuracy, as expected. Furthermore, the closed form solutions for $P(t)$ and $\xi(t)$ have also been compared with the backward integrated solutions of Eqs. (5-10) and (5-11) for verification.

5.3 Closed Form Solution for the Terminal Tracking Problem

In this subsection the problem of maneuvering a flexible spacecraft through a large angle is considered, where the terminal state is subject to constraints. The basic approach differs from the standard linear quadratic regulator design, in that a quadratic penalty term on

the final value of the state is not included in the performance index. As a result, the numerical difficulties associated with handling large terminal penalty matrices are not encountered.

The optimal control problem of this section is specified by defining a performance index which consists of an integral of quadratic forms in the state, control, and control-rates, where the terminal state is subject to constraints. In particular, the terminal constraints replace the conventional weighted quadratic form in the terminal states. The necessary conditions for this problem lead to three nonlinear Riccati-like differential equations [Ref. 5-6]. One equation is the standard Riccati equation, which possesses a well-known solution in terms of a steady-state plus transient term (see Eq. (5-13)). On the other hand, the remaining two equations are coupled to the standard Riccati equation. In Sections 5.3.3 and 5.3.4, new closed form solutions are presented for the two auxiliary Riccati-like equations.

5.3.1 Optimal Terminal Controller

The optimal terminal control problem is formulated by finding the control inputs $u(t)$ to minimize

$$J = \frac{1}{2} \int_{t_0}^{t_f} (x^T F^T Q F x + u^T R u) dt \quad (5-32)$$

for the system

$$\dot{x} = Ax + Bu, \quad \text{given } x(t_0) \quad (5-33)$$

with outputs

$$y = Fx$$

$$(5-34)$$

where x , u , A , B , Q , and R are defined following Eq. (5-3), F is the measurement influence matrix, and the state is subject to the specified terminal constraints

$$x_i(t_f) = \bar{x}_i, \quad i = 1, \dots, q \quad (q \leq n) \quad (5-35)$$

Of particular interest is the fact that the performance index of Eq. (5-32) does not contain a terminal weight matrix which penalizes the final values of the state.

5.3.1.1 Necessary Conditions for the Terminal Tracking Problem

As shown in Reference 5-6, the necessary conditions defining the optimal solution are given by the following coupled Riccati-like matrix differential equations

$$\dot{P} + PA + A^T P - PBR^{-1}B^T P + F^T QF = 0; \quad P(t_f) = 0 \quad (5-36)$$

$$\dot{S} + (A^T - PBR^{-1}B^T)S = 0; \quad S^T(t_f) = (\partial\psi/\partial x) \Big|_{t_f} \quad (5-37)$$

$$\dot{G} = S^T B R^{-1} B^T S; \quad G(t_f) = 0 \quad (5-38)$$

where $\psi^T = [\bar{x}_1, \bar{x}_2, \dots, \bar{x}_q]$ and the optimal continuous feedback law is given by

$$u(t) = -C(t)x(t) - D(t)\psi \quad (5-39)$$

where

$$C = R^{-1} B^T (P - S G^{-1} S^T) \quad (5-40)$$

$$D = R^{-1} B^T S G^{-1} \quad (5-41)$$

The control vector u of Eq. (5-39) takes the state vector from $x(t_0)$ at time t_0 to ψ at time t_f , while minimizing the cost function of Eq. (5-32).

In the next section closed form solutions are presented for Eqs. (5-36), (5-37), and (5-38), thus reducing the solution for the feedback gains to the direct computation of algebraic equations without numerical integration.

5.3.2 Closed Form Solution for the Time-Varying Riccati Equation

$$P(t) = P_{ss} + \Theta^{-1}(t) \quad (5-42)$$

where P_{ss} is the solution for the algebraic Riccati equation

$$-A^T P_{ss} - P_{ss} A + P_{ss} B R^{-1} B^T P_{ss} - F^T Q F = 0 \quad (5-43)$$

and the solution for $\Theta(t)$ follows as

$$\Theta(t) = \Theta_{ss} - e^{\bar{A}(t-t_f)} (\Theta_{ss} + P_{ss}^{-1}) e^{\bar{A}^T(t-t_f)} \quad (5-44)$$

where $e^{(\cdot)}$ is the exponential matrix, $\bar{A} = A - B R^{-1} B^T P_{ss}$, and the solution for Θ_{ss} is defined by Eq. (5-16).

5.3.3 Closed Form Solution for S(t)

The new solution for $S(t)$ in Eq. (5-37) follows on assuming the product form solution

$$s(t) = \theta^{-1}(t)s_c(t) \quad (5-45)$$

where θ is defined by Eq. (5-44) and s_c is to be determined.

Substitution of Eq. (5-45) into Eq. (5-37) leads to the following linear constant coefficient matrix differential equation for $s_c(t)$:

$$\dot{s}_c(t) - \bar{A}s_c(t) = 0; \quad s_c(t_f) = -P_{ss}^{-1}s(t_f) \quad (5-46)$$

from which it follows that the solution for $s(t)$ in Eq. (5-45) can be written as:

$$s(t) = -\theta^{-1}(t)e^{\bar{A}(t-t_f)}P_{ss}^{-1}s(t_f)$$

where the differential equation for θ is given by: $\dot{\theta} = \bar{A}\theta + Q\bar{A}^T - BR^{-1}B^T$. The solution for $s_c(t)$ in Eq. (5-46) can be shown to be

$$s_c(t) = -e^{\bar{A}(t-t_f)}P_{ss}^{-1}s(t_f) \quad (5-47)$$

5.3.4 Closed Form Solution for G(t)

The solution for $G(t)$ in Eq. (5-38) can be shown to be:

$$G(t) = s^T(t)\theta(t)s(t) + s^T(t_f)P_{ss}^{-1}s(t_f) \quad (5-48)$$

which can be easily verified by direct differentiation.

5.3.5 Calculation of the Optimal Control

The control is computed by writing Eq. (5-39) in the form

$$\begin{aligned}
 u(t) &= -C(t)x(t) - D(t)\psi \\
 &= -R^{-1}B^T[P_{ss}x(t) + \theta^{-1}(t)x(t) + S(t)x_1(t)]
 \end{aligned} \tag{5-49}$$

where $x_1(t)$ is obtained by solving the following linear equation:

$$G(t)x_1(t) = \psi - S(t)x(t)$$

5.3.6 Example Maneuvers

The vehicle configuration and system parameters of Section 5.2.5 are assumed for the example maneuvers of this section. Furthermore, full state feedback is assumed for the results of this section and the output vector is assumed to be defined by Eq. (5-31).

Referring to Tables 5-1b and 5-3, the graphical summaries of the states and controls are discussed qualitatively in what follows.

Case 1 (Fig. 5-7) presents a terminal controller example maneuver in which two flexible modes are controlled in addition to the rigid body rotation. There are six states in this problem, all of which are specified at the final time. As a result, P , S , and G in Eqs. (5-42), (5-45), and (5-48) are 6×6 matrices. The time histories for this case are virtually identical to the time histories obtained from the corresponding open-loop controller, using the same weight matrices in the performance index. The observed jump discontinuities in the control torques at the initial and final times are characteristic of this type of control design.

Case 2 (Fig. 5-8) presents a spin-up maneuver with two flexible modes controlled, in which the final angle is free to be determined by the controller. As a result, the P , S , and G matrices have the following dimensions: $P(6 \times 6)$, $S(6 \times 5)$, and $G(5 \times 5)$. In particular, the final angle

selected is exactly the angle selected by the analogous open-loop free final angle transversality conditions [Ref. 5-1].

Case 3 (Fig. 5-9) presents the same maneuver as in Case 1, except that the performance index now includes penalties on the first and second time derivatives of the control torques [Ref. 5-2]. Including these penalties allows the control torques and torque-rates to be specified at the initial and final times, thereby eliminating the terminal jump discontinuities in the control profiles. For this particular control problem, the states are augmented to include the control and first time-derivative of the control, while the second time-derivative of the control becomes the commanded input to the augmented system. On comparing with the results of Case 1, one finds a much smoother modal amplitude and control torque time history, although the peak torques and tip deflection are somewhat higher than those in Case 1. The dimensions of the P, S, and G matrices are all 10x10 for Case 3.

Case 4 (Fig. 5-10) presents the same maneuver as in Case 2, with the additional penalty on the control-rates. As in Case 2, all the states, controls, and control-rates are specified at the final time for the terminal controller, except for the maneuver angle, which is not specified at the final time. As a result, the P, S, and G matrices have the following dimensions: P(10x10), S(10x9), and G(9x9). On comparing the results with Case 2, the modal amplitude and control torque time histories are found to be much smoother, although the peak values are higher. Moreover, the terminal jump discontinuities in the control torque shown in Case 2 are eliminated in Case 4, thus making it less susceptible to control spillover.

Case 5 (Fig. 5-11) presents the results of a maneuver in which the weight matrices and final conditions are identical with those of Case 3. The initial conditions are different from those in Case 3, but the time-varying feedback gains are identical. As the plots in Figure 5-10 show, the terminal controller has little difficulty in bringing the system to the required final conditions.

Case 6 (Fig. 5-12) presents the results of a maneuver in which the moment of inertias of the hub and appendages are increased by 10% and the appendage mass per unit length is decreased by 10%, while the time-varying feedback gains are computed using the nominal structural parameters. Although the structural parameters are changed by only 10%, the overall effect on the entire structure is quite large. Specifically, the first and second mode eigenvalues, ω^2 , are increased by 16% and 22%, respectively, while the ratio of the hub moment of inertia to appendage moment of inertia is increased by 22%. However, the plots show that with the terminal controller, most of the state variables reach their prescribed terminal boundary conditions.

The results of in Cases 1 through 5 have been compared with the corresponding open-loop maneuvers, and have been found to be identical within plotting accuracy, as expected. Furthermore, the closed form solutions for $P(t)$, $S(t)$, and $G(t)$ have also been compared with the backward integrated solutions for verification.

5.4 An Analytic Solution for the State Trajectories of a Feedback Control System

As part of the normal process of a control system design, the analyst typically is interested in determining the state trajectories for the controlled system. In practice, this process is straightforward, since the feedback form of the control can be introduced in the equation of motion and numerically integrated. Nevertheless, this process can be computationally intensive if either time-varying control gains are used or small integration step sizes are required by the presence of high frequency system dynamics.

In an effort to overcome the computational difficulties listed above, a change of variables is presented in this subsection for the

standard closed-loop system dynamics equation, which permits a closed form expression to be obtained for the state trajectories.

5.4.1 Optimal Control Problem

The fixed time linear optimal control problem is formulated by finding the control inputs $u(t)$ to minimize

$$J = \frac{1}{2} x_f^T S F x_f + \frac{1}{2} \int_{t_0}^{t_f} (x^T Q x + u^T R u) dt \quad (5-50)$$

for the system

$$\dot{x} = Ax + Bu, \quad \text{given } x(t_0) \quad (5-51)$$

$$y = Fx \quad (5-52)$$

where x , u , A , B , F , Q , R , and S are defined following Eq. (5-3).

As shown in Reference 5-6, the optimal control is given by

$$u(t) = -R^{-1} B^T P(t) x(t) \quad (5-53)$$

where P is the solution for the differential matrix Riccati equation

$$\dot{P} = -AP - PA^T + PBR^{-1}B^T P - Q ; \quad P(t_f) = S \quad (5-54)$$

Upon introducing Eq. (5-53) into Eq. (5-51), the standard closed-loop system dynamics equation follows as

$$\dot{x}(t) = [A - BR^{-1}B^T P(t)]x(t) ; \quad x_0 = x(t_0) \quad (5-55)$$

(It should be observed that the equation above is the adjoint to the homogeneous part of Eq. (5-11).)

To obtain the solution for Eq. (5-55), the following closed form solution for $P(t)$ [Refs. 5-1, 5-3] is introduced in Eq. (5-55):

$$P(t) = P_{ss} + \theta^{-1}(t) \quad (5-56)$$

where P_{ss} is defined by Eq. (5-43). The variable $\theta(t)$ is given by

$$\theta(t) = \theta_{ss} + e^{\bar{A}(t-t_f)} \left[(F^T S F - P_{ss})^{-1} - \theta_{ss} \right] e^{\bar{A}^T(t-t_f)} \quad (5-57)$$

where $\bar{A} = A - BR^{-1}B^T P_{ss}$, $e^{(\cdot)}$ is the exponential matrix, and the solution for θ_{ss} is defined by Eq. (5-16).

Substituting Eq. (5-56) into Eq. (5-55), yields the modified form of the closed-loop system dynamics equation

$$\dot{x}(t) = [\bar{A} - BR^{-1}B^T \theta^{-1}(t)]x(t) ; \quad x_0 = x(t_0) \quad (5-58)$$

where it follows that the equation above is nonautonomous.

5.4.2 Change of Variables for $x(t)$

To simplify Eq. (5-58) the following coordinate transformation for the dependent variable $x(t)$ is introduced:

$$x(t) = \theta(t)r(t) \quad (5-59)$$

where $\theta(t)$ is given by Eq. (5-57) and $r(t)$ is a vector function which is to be determined.

Upon differentiating Eq. (5-59) we find

$$\dot{x} = \dot{\theta}r + \theta\dot{r} \quad (5-60)$$

or

$$\dot{x} = (\bar{A}\theta + \theta\bar{A}^T - BR^{-1}B^T)r + \theta\dot{r} \quad (5-61)$$

where $\dot{\theta}$ in Eq. (5-60) has been replaced by: $\dot{\theta} = \bar{A}\theta + \theta\bar{A}^T - BR^{-1}B$.

The differential equation for r is obtained by introducing Eqs. (5-59) and (5-61) into Eq. (5-58), leading to

$$\theta(\dot{r} + \bar{A}^T r) = 0 \quad (5-62)$$

from which it follows that the linear constant coefficient vector differential equation for r is given by

$$\dot{r} = -\bar{A}^T r ; \quad r_0 = \theta^{-1}(t_0)x_0 \quad (5-63)$$

The solution for r follows as

$$r(t) = e^{-\bar{A}^T(t-t_0)}r_0 \quad (5-64)$$

Substituting Eq. (5-64) into Eq. (5-59) produces the desired solution for the state trajectories as

$$x(t) = \theta(t)e^{-\bar{A}^T(t-t_o)} r_o \quad (5-65)$$

5.4.3 Recursion Relationship for Evaluating the State at Discrete Times

If the solution for $x(t)$ is required at the discrete times $t_k = t_o + k\Delta t$ ($k = 1, \dots, N$) for $\Delta t = (t_f - t_o)/N$, then Eq. (5-65) can be written as

$$x(t_k) = A_k r_o + b_k, \quad k = 0, \dots, N \quad (5-66)$$

where

$$A_o = \theta_{ss} e^{-\bar{A}^T t_o}, \quad b_o = e^{-\bar{A} t_f} [(F^T S F - P_{ss})^{-1} - \theta_{ss}] e^{-\bar{A}^T (t_o - t_f)} r_o$$

$$A_k = A_{k-1} e^{-\bar{A} \Delta t}, \quad b_k = e^{-\bar{A} \Delta t} b_{k-1}; \quad k=1, \dots, N$$

5.4.4 Conclusions

Closed form solutions for the feedback gains required by an optimal linear tracking controller and an optimal terminal controller have been developed. Results of example maneuvers have been shown which demonstrate the efficiency and validity of the formulations described. The use of control-rate penalties in each case have been shown to improve the overall system response.

In addition, a straightforward algorithm has been presented for generating the state trajectories for a feedback control system. The algorithm is computationally efficient in that no numerical integration is required and simple recursion relationships generate the desired solution at discrete times. Furthermore, this algorithm has significant potential if used in conjunction with algorithms which attempt to enhance system robustness, by iteratively refining the weighting matrices appearing in Eq. (5-50).

References

- 5-1 Turner, J. D., "Large Angle Spacecraft Slewing Maneuvers," ACOSS Eleven Second Semiannual Technical Report, Vol. 2: Active Controller Designs, Report CSDL-R-1583, Charles Stark Draper Laboratory, Cambridge, MA, August 1982; Section 7.
- 5-2 Turner, J. D., "Large-Angle Spacecraft Slewing Maneuvers," ACOSS Eleven Semiannual Technical Report, Vol. 2, Report CSDL-R-1536, Charles Stark Draper Laboratory, Cambridge, MA, February 1982; Section 8.
- 5-3 Sage, A. P., and C. C. White, Optimum System Control, Second Edition, Prentice-Hall, Englewood Cliffs, NJ, 1977.
- 5-4 Potter, J. E., and W. E. Vander Velde, "Optimum Mixing of Gyroscope and Star Tracker Data," J. Spacecraft Rockets, Vol. 5, No. 5, May 1968, pp. 536-540.
- 5-5 Van Loan, C. F., "Computing Integrals Involving the Matrix Exponential," IEEE Trans. Automatic Control, Vol. AC-23, No. 3, June 1978, pp. 395-404.
- 5-6 Bryson, A. and Ho, Y. C., Applied Optimal Control, Wiley, New York, NY, 1975.

Table 5-1a. Test case maneuver descriptions:
linear tracking problem.

Case No.	No. of Modes	$t_f - t_o$ (sec)	$k^{(1)}$	θ_o (rad)	$\dot{\theta}_o$ (rad/s)	θ_f (rad)	$\dot{\theta}_f$ (rad/s)	CPU ⁽²⁾ (sec)
1	2	15	0	0	0	0.4	0	27
2	2	15	2	0	0	0.4	0	59
3	2	15	2	0.15	-0.02	0.4	0	58
4	2	1.5	2	0	0	0.4	0	58

Table 5-1b. Test case maneuver descriptions:
terminal tracking problem.

Case No.	No. of Modes	$t_f - t_o$ (sec)	$k^{(1)}$	θ_o (rad)	$\dot{\theta}_o$ (rad/s)	θ_f (rad)	$\dot{\theta}_f$ (rad/s)	CPU ⁽²⁾ (sec)
1	2	15	0	0	0	0.4	0	34
2	2	15	0	0	0	(free)	0.04	32
3	2	15	2	0	0	0.4	0	83
4	2	15	2	0	0	(free)	0.04	77
5	2	15	2	0.15	-0.02	0.4	0	83
6	2	15	2	0	0	0.4	0	83

Notes:

1. k denotes the order of the highest time derivative of the control which is penalized in the performance index.
2. The CPU time is obtained using an Amdahl 470-V/8 with 150 time-steps for each integration.

Table 5-2. Weighting matrices for example maneuvers:
linear tracking problem.

Case No.	Open-Loop Weighting Matrices ^(1,2)
1	$Q^* = \text{diag} [1(-5) \ 1(-3) \ 1(-3) \ 1(-3) \ 1(-3) \ 1(-3)]$ $R^* = \text{diag} [1(-3) \ 1(0)]$
2,3,4	$Q^* = W_{\Sigma\Sigma} \otimes W_{\text{oo}} \otimes W_{11}$ $W_{\Sigma\Sigma} = \text{diag} [1(-5) \ 1(-3) \ 1(-3) \ 1(-3) \ 1(-3) \ 1(-3)]$ $W_{\text{oo}} = \text{diag} [1(-9) \ 1(-9)]$ $W_{11} = \text{diag} [1(-9) \ 1(-9)]$ $R^* = \text{diag} [1(-3) \ 1(1)]$
Closed-Loop Weighting Matrices	
1	$Q = \text{diag} [1(-3) \ 1(-2) \ 1(-3) \ 1(-5)]$ $R = \text{diag} [1(-3) \ 1(0)]$
2,3,4	$Q = \text{diag} [1(-3) \ 1(-2) \ 1(-3) \ 1(-5) \ 1(-9) \ 1(-9) \ 1(-9) \ 1(-9)]$ $R = \text{diag} [1(-3) \ 1(1)]$

Notes:

1. $b(a)$ denotes $b \times 10^a$
2. \otimes denotes direct sum

Table 5-2. Weighting matrices for example maneuvers:
linear tracking problem (continued).

Case No.	Terminal Output Weighting Matrix(1)
1	$S = \begin{bmatrix} 2.3(7) & & \\ 2.7(6) & 4.9(5) & \\ 4.0(5) & 5.4(4) & 7.5(7) \\ 1.0(3) & 1.7(2) & 3.6(5) \\ & & 2.0(3) \end{bmatrix}$ Symmetric
2,3,4	$S = \begin{bmatrix} 3.9(7) & & \\ -3.3(6) & 4.9(7) & \\ 2.5(6) & -9.0(4) & 2.2(5) \\ 7.6(2) & 7.4(4) & 1.3(2) \\ 2.6(4) & -7.0(3) & 1.4(3) \\ 1.7(5) & 2.0(4) & 6.6(3) \\ 1.4(2) & -3.2(1) & 7.2(0) \\ 9.9(2) & -1.2(2) & 3.3(1) \end{bmatrix}$ $\begin{bmatrix} & & \\ & & \\ & & \\ 7.8(1) & & \\ 2.0(5) & 7.2(1) & \\ 1.3(2) & -1.8(4) & 7.0(2) \\ 1.4(3) & 4.0(-1) & 3.8(-1) \\ 6.6(3) & -6.7(2) & 1.6(4) \\ 7.2(0) & -3.3(0) & 1.0(-1) \\ 3.3(1) & -3.2(0) & 1.1(2) \\ -9.1(1) & -1.2(0) & -1.6(-2) \end{bmatrix}$ Symmetric

Note:

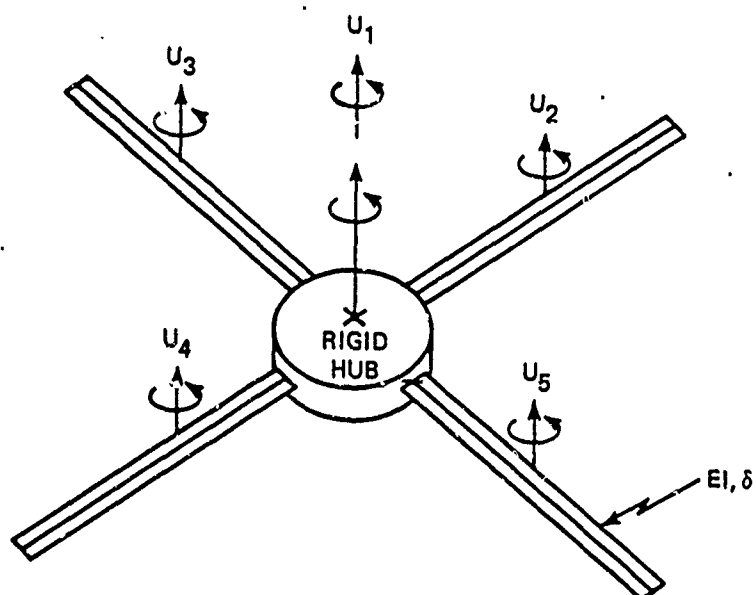
1. $b(a)$ denotes $b \times 10^a$

Table 5-3. Weighting matrices for example maneuvers:
terminal tracking problem.

Case No.	Weighting Matrices(1)
1,2	$Q = \text{diag}[1(-3), 1(-2), 1(-3), 1(-5)]$ $R = \text{diag}[1(-3), 1(0)]$
3,5,6	$Q = \text{diag}[1(-3), 1(-2), 1(-3), 1(-5), 1(-9), 1(-9), 1(-9), 1(-9)]$ $R = \text{diag}[1(-3), 1(1)]$
4	$Q = \text{diag}[1(-3), 1(-2), 1(-3), 1(-5), 1(-9), 1(-9), 1(-9), 1(-9)]$ $R = \text{diag}[1(-3), 1(0)]$

Note:

1. $b(a)$ denotes $b \times 10^a$



$\{U_1, U_2, \dots, U_5\}$ = SET OF DISTRIBUTED CONTROL TORQUES

Figure 5-1. Undeformed structure.

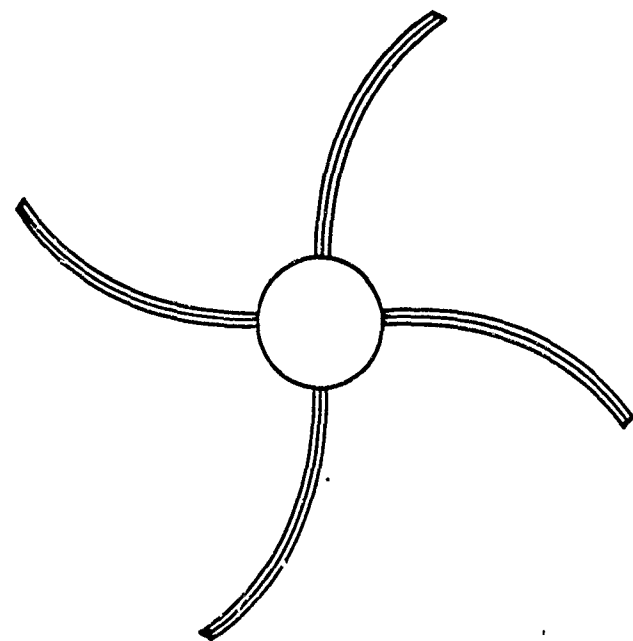


Figure 5-2. Antisymmetric deformation.

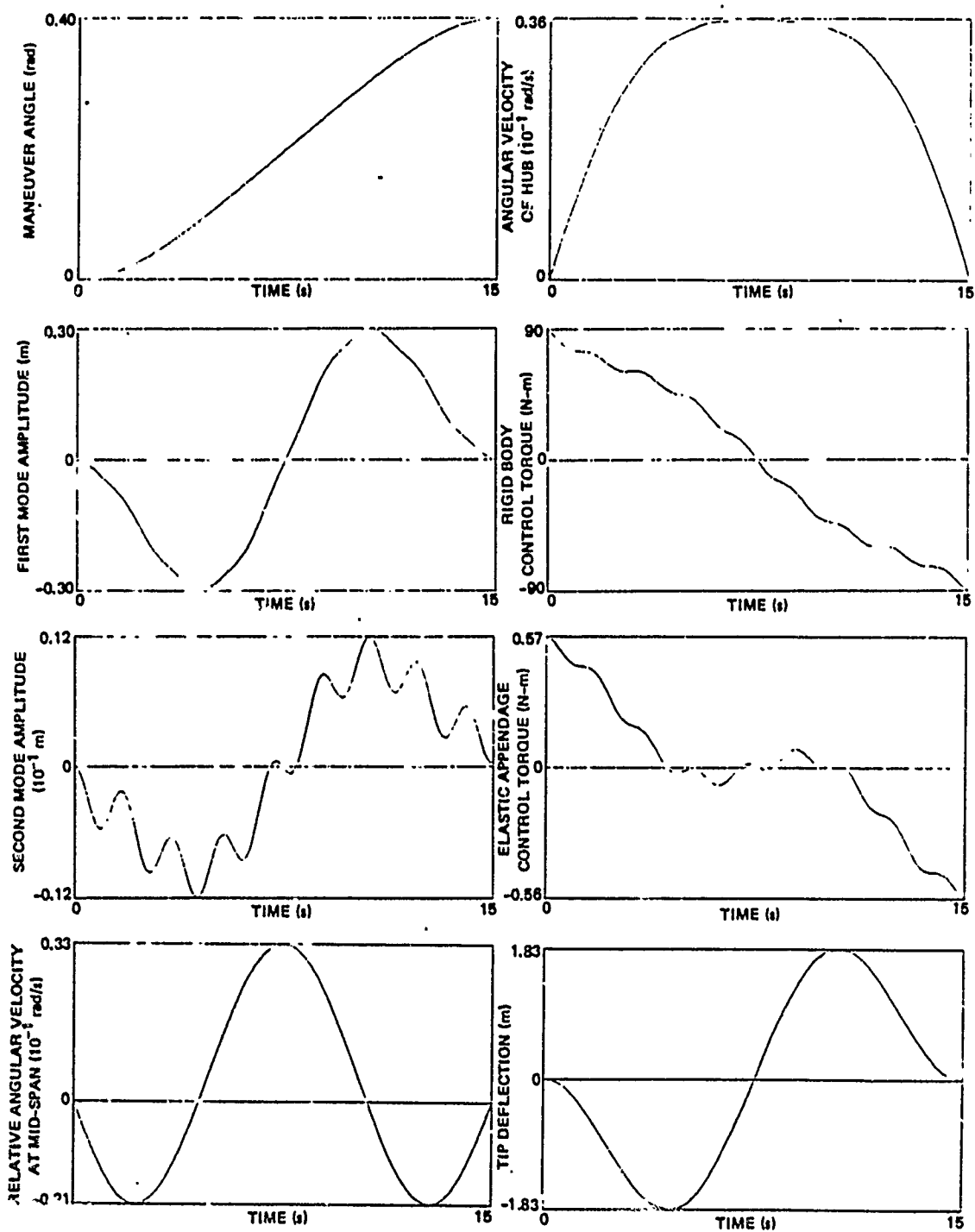


Figure 5-3. Case 1, rest-to-rest maneuver, 2 modes, 5 controls.

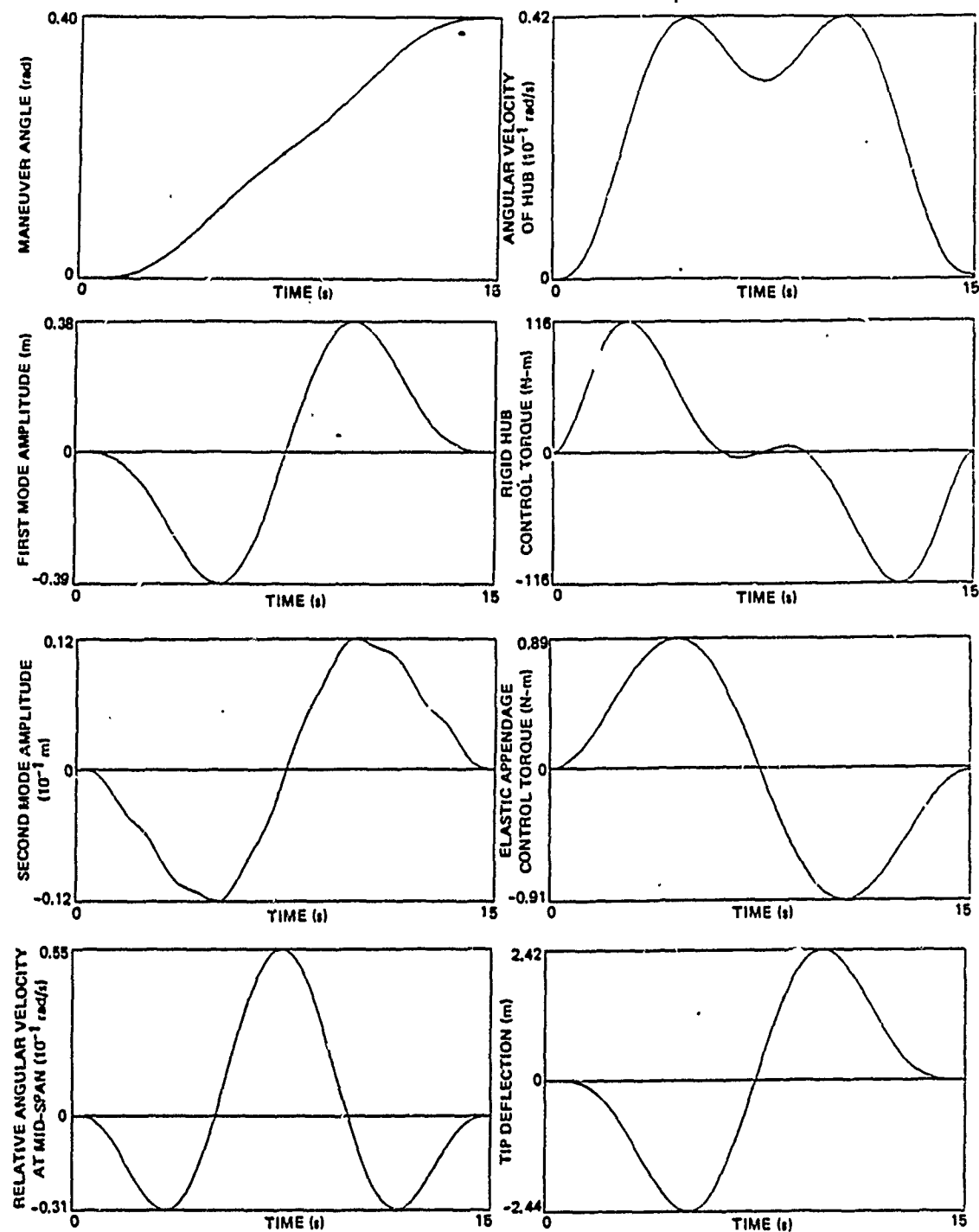


Figure 5-4. Case 2, rest-to-rest maneuver, 2 modes, 5 controls, control-rate penalty with $k = 2$.

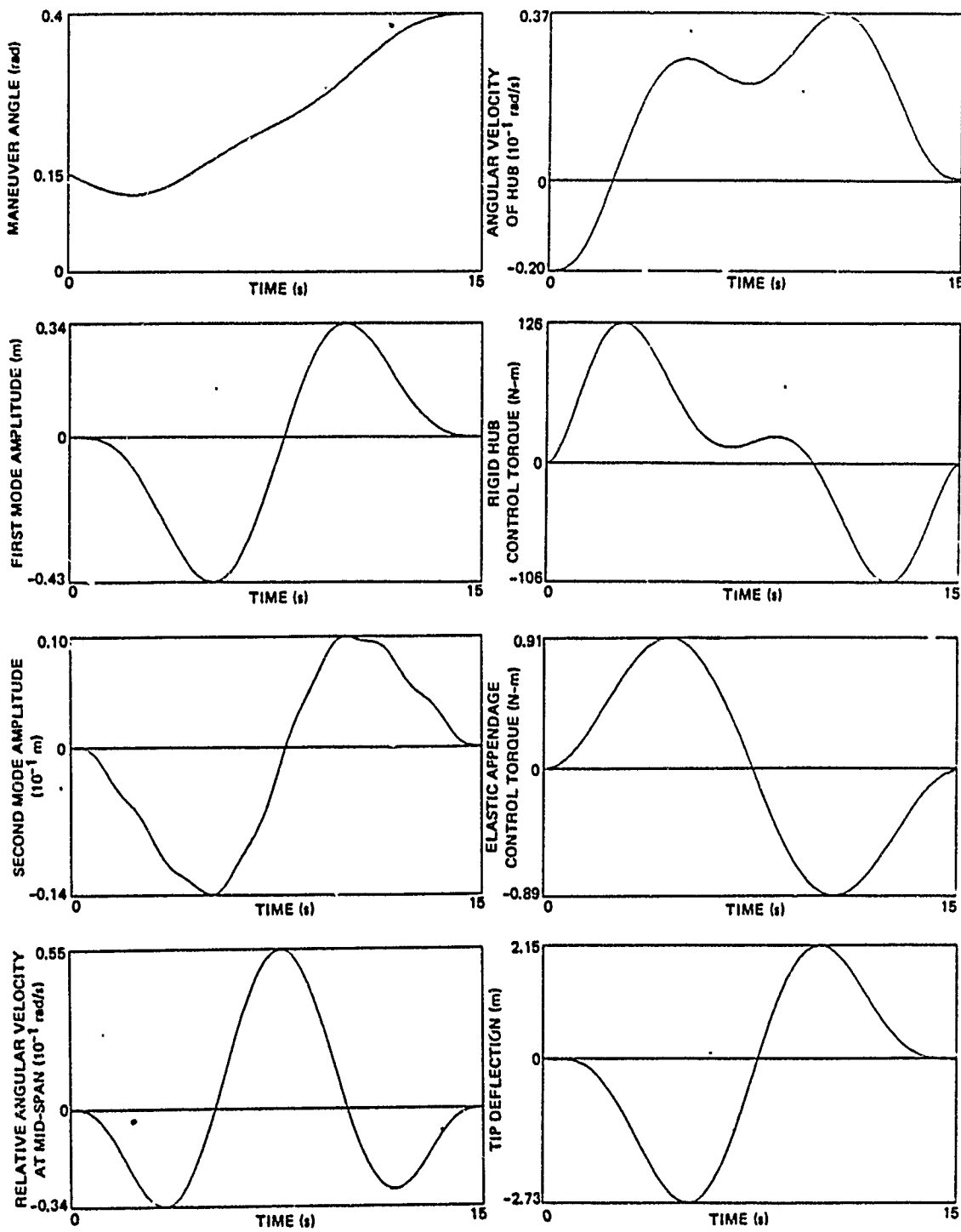


Figure 5-5. Case 3, spin-to-rest maneuver, 2 modes, 5 controls, control-rate penalty with $k = 2$.

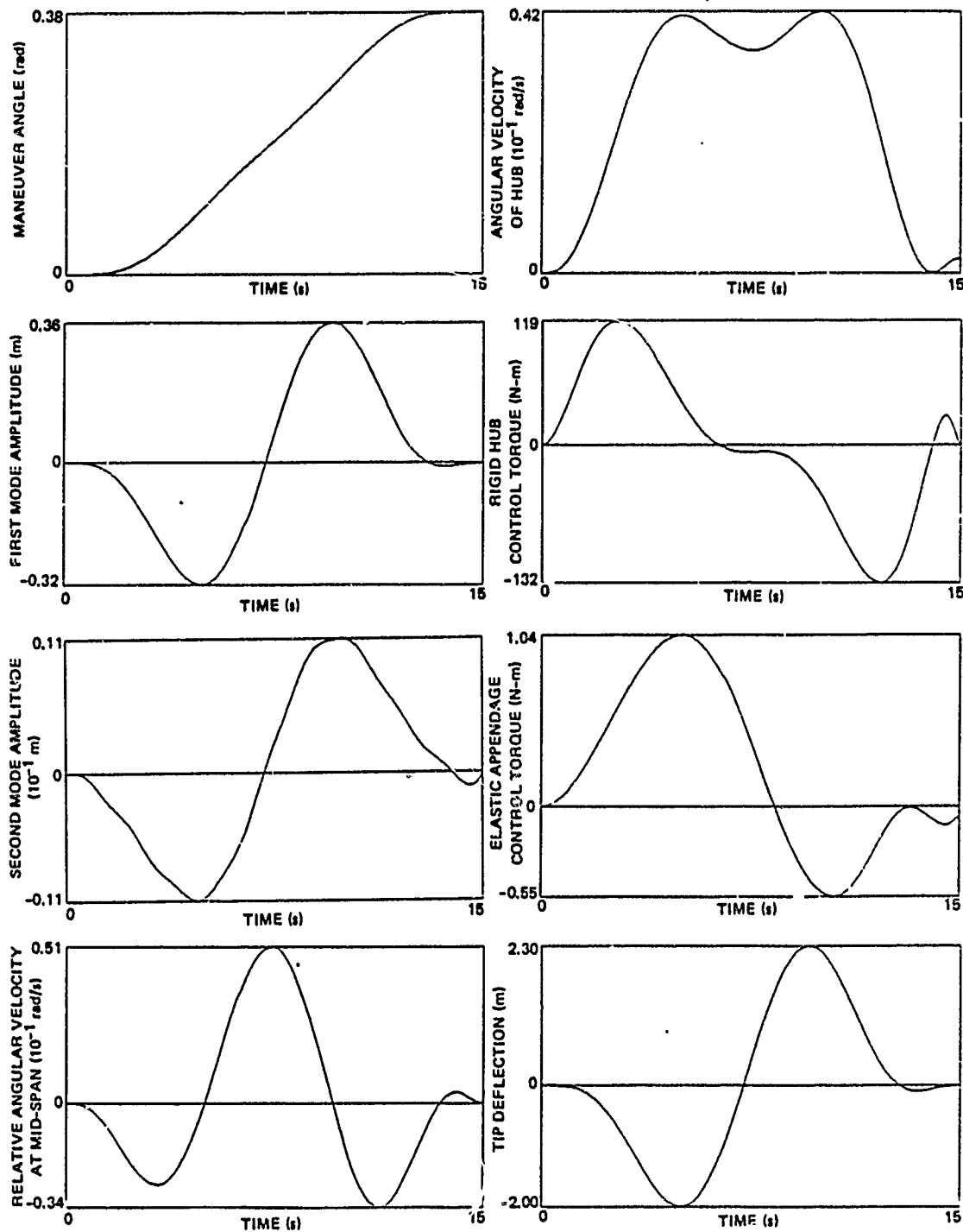


Figure 5-6. Case 4, rest-to-rest maneuver, off-nominal structural parameters, 2 modes, 5 controls, $k = 2$.

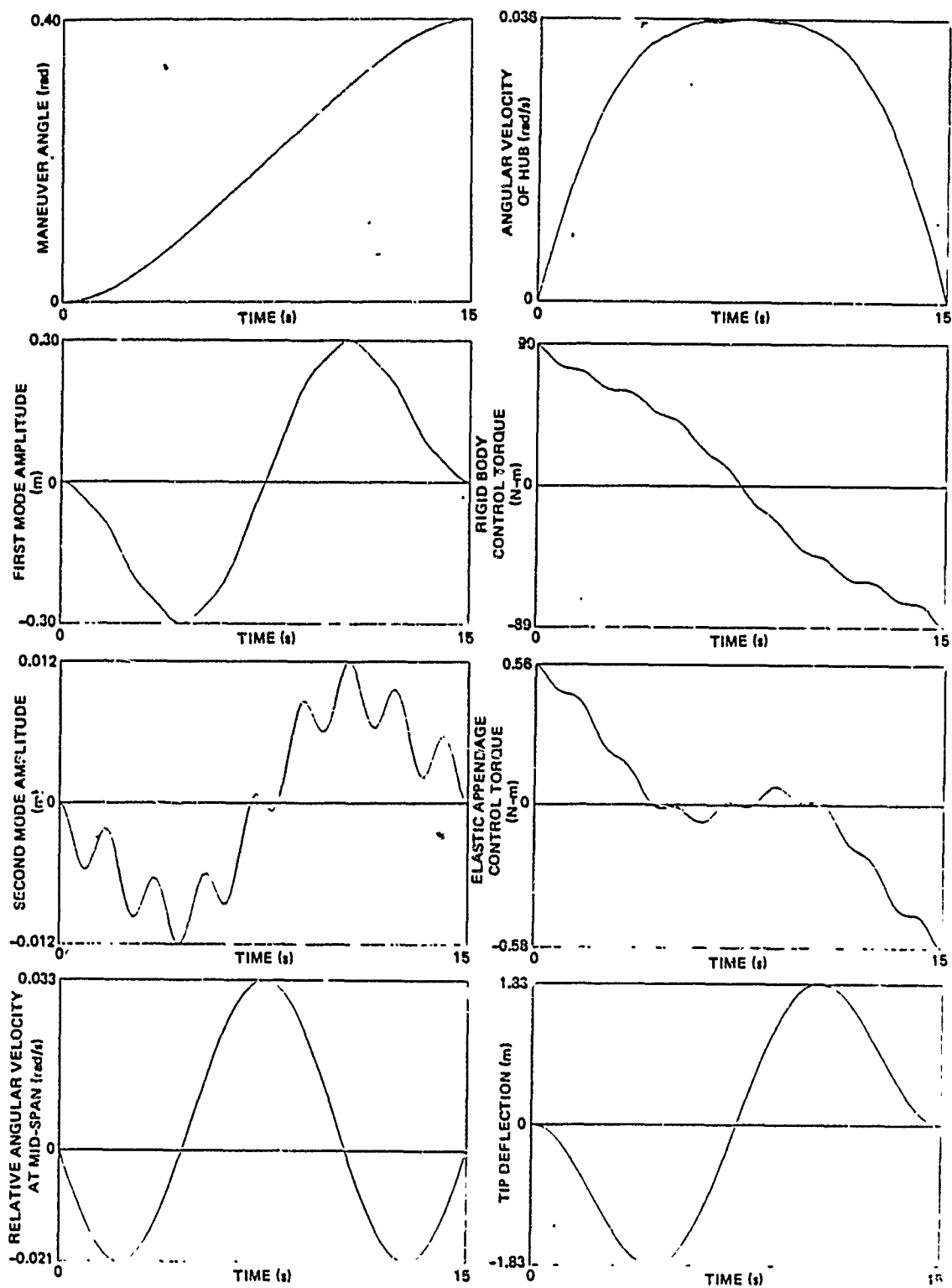


Figure 5-7. Case 1, rest-to-rest maneuver, 2 modes, 5 controls.

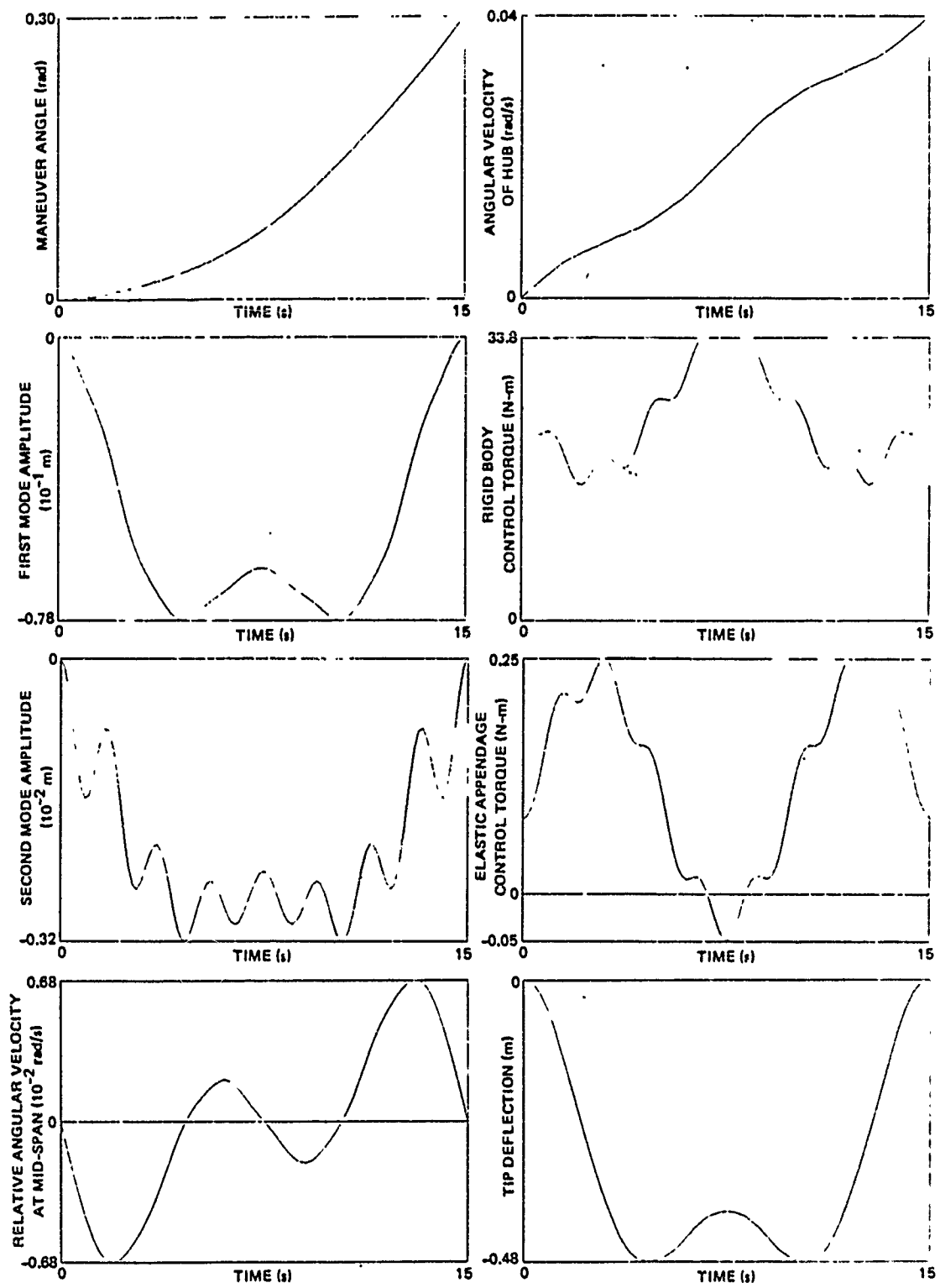


Figure 5-8. Case 2, free final angle spin-up maneuver, 2 modes, 5 controls.

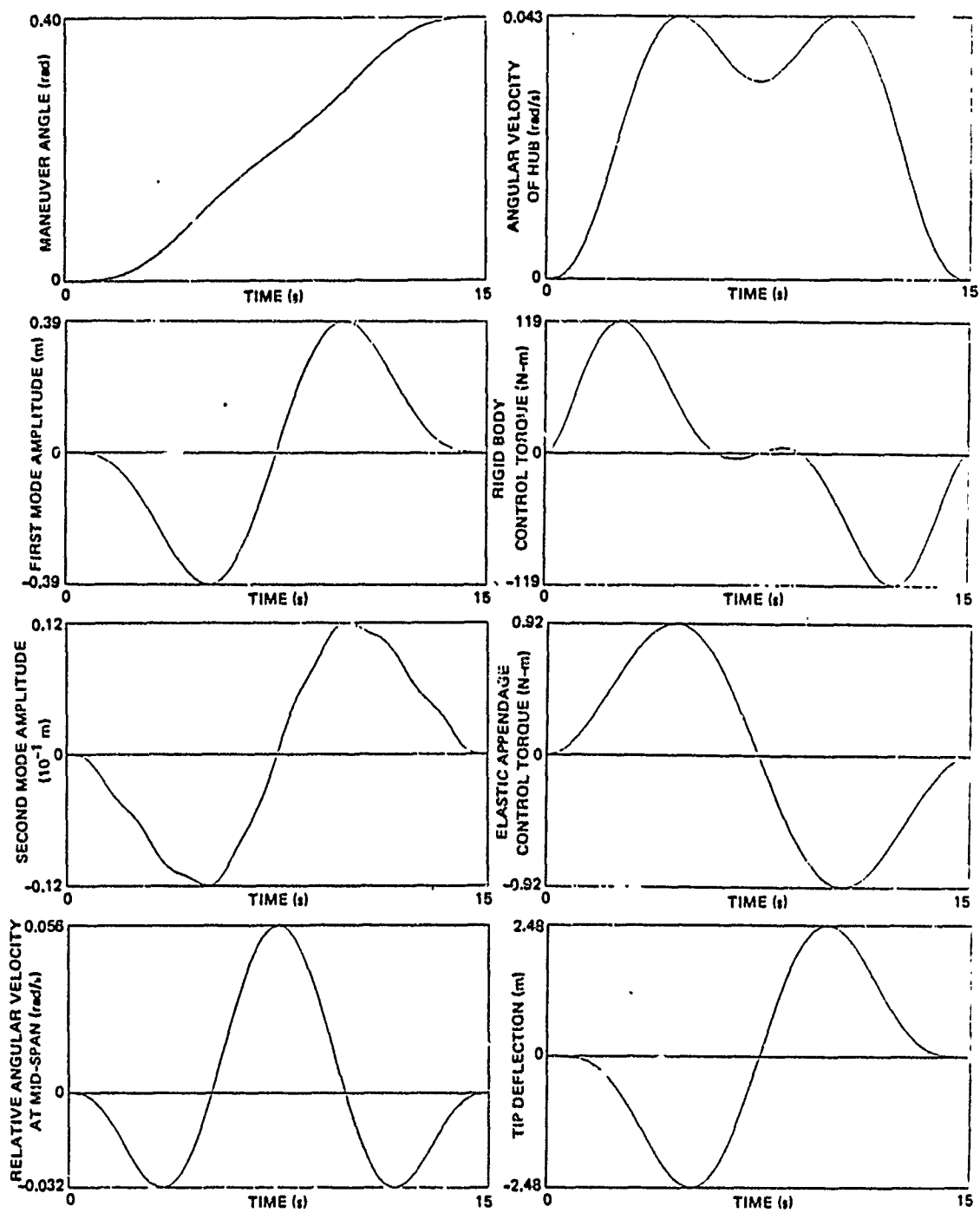


Figure 5-9. Case 3, rest-to-rest maneuver, 2 modes, 5 controls, control-rate penalty with $k = 2$.

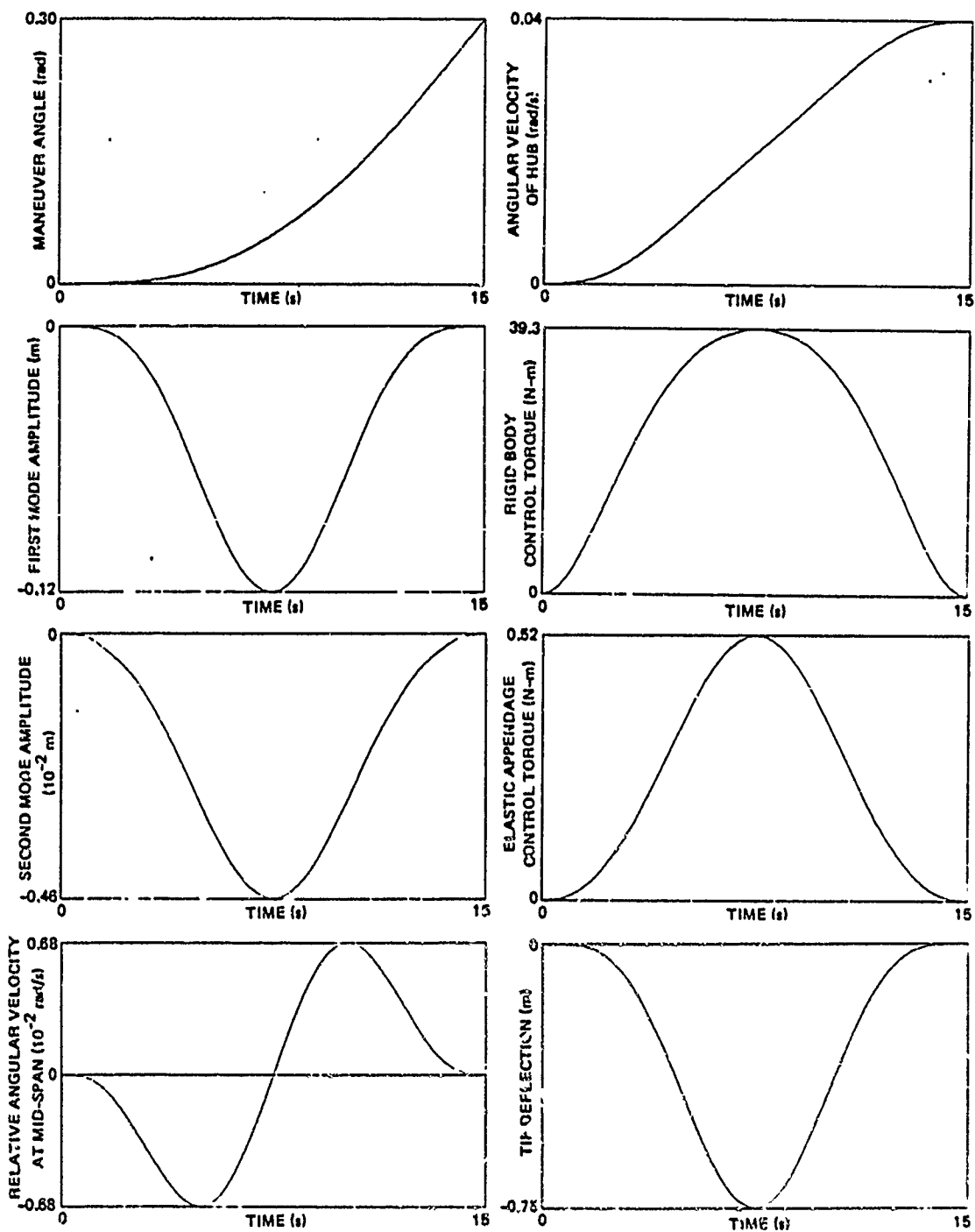


Figure 5-10. Case 4, free final angle spin-up maneuver, 2 modes, 5 controls, control-rate penalty with $k = 2$.

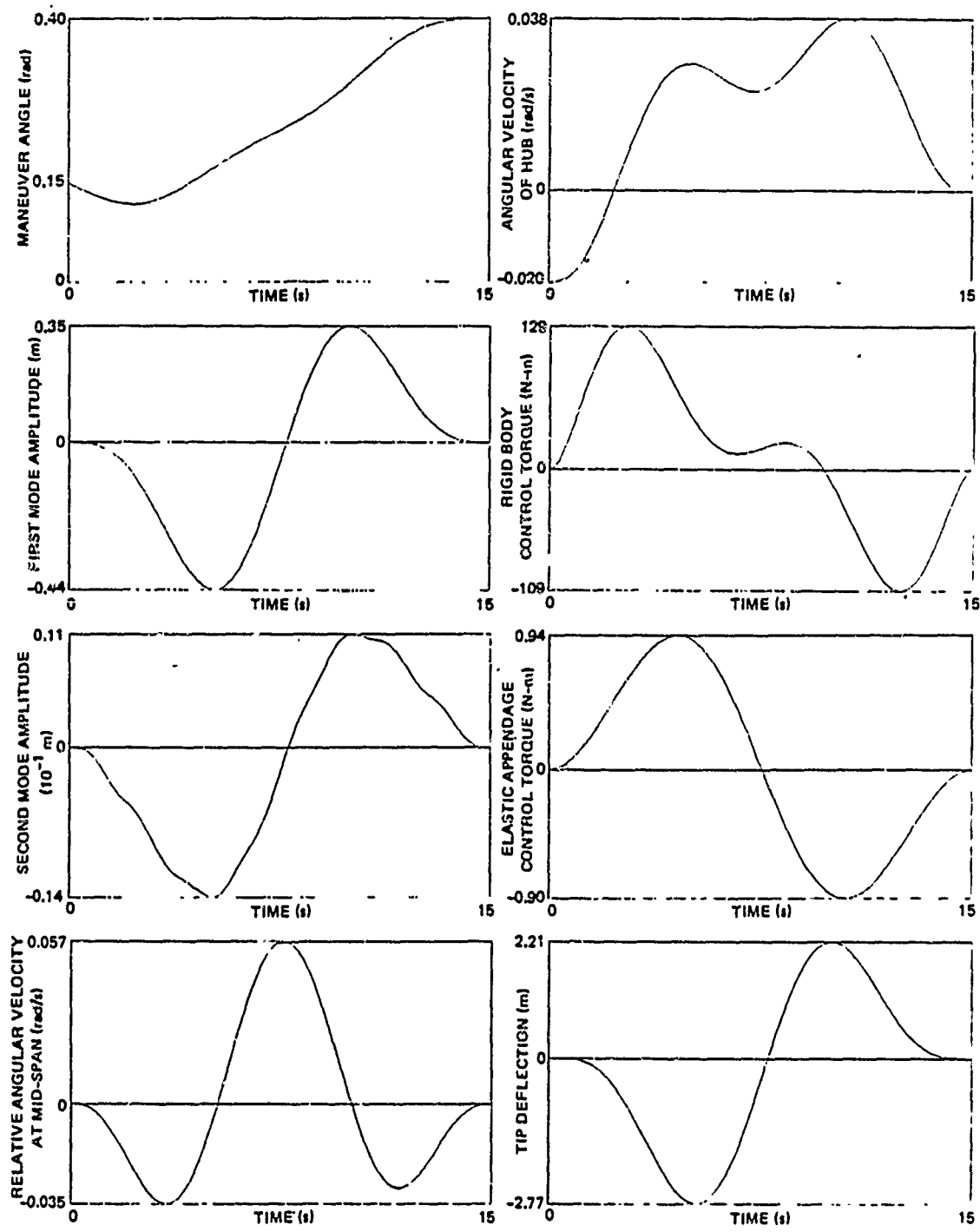


Figure 5-11. Case 5, spin-to-rest maneuver, 2 modes, 5 controls, control-rate penalty with $k = 2$.

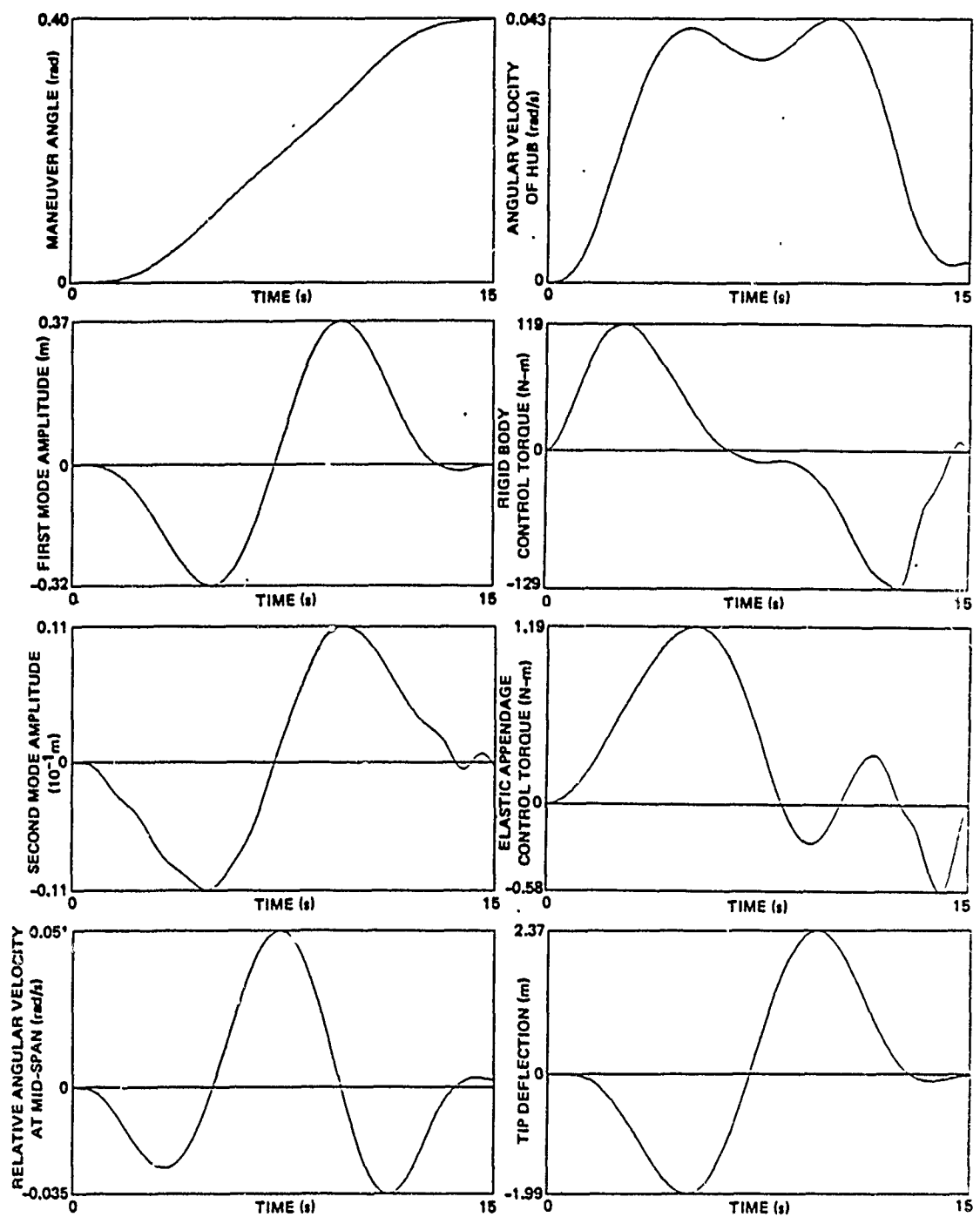


Figure 5-12. Case 6, rest-to-rest maneuver, off-nominal structural parameters, 2 modes, 5 controls, $k = 2$.

MISSION
of
Rome Air Development Center

RADC plans and executes research, development, test and selected acquisition programs in support of Command, Control Communications and Intelligence (C³I) activities. Technical and engineering support within areas of technical competence is provided to ESD Program Offices (POs) and other ESD-elements. The principal technical mission areas are communications, electromagnetic guidance and control, surveillance of ground and aerospace objects, intelligence data collection and handling, information system technology, ionospheric propagation, solid state sciences, microwave physics and electronic reliability, maintainability and compatibility.